National Library of Canada

Acquisitions and Bibliographic Services Branch

395 Wellington Street
Ottawa, Ontario
K1A 0N4

Bibliothèque nationale du Canada

Direction des acquisitions et des services bibliographiques

395, rue Wellington
Ottawa (Ontario)
K1A 0N4

Your file Votre référence

Our file Notre référence

NOTICE

The quality of this microform is heavily dependent upon the quality of the original thesis submitted for microfilming. Every effort has been made to ensure the highest quality of reproduction possible.

If pages are missing, contact the university which granted the degree.

Some pages may have indistinct print especially if the original pages were typed with a poor typewriter ribbon or if the university sent us an inferior photocopy.

Reproduction in full or in part of this microform is governed by the Canadian Copyright Act, R.S.C. 1970, c. C-30, and subsequent amendments.

AVIS

La qualité de cette microforme dépend grandement de la qualité de la thèse soumise au microfilmage. Nous avons tout fait pour assurer une qualité supérieure de reproduction.

S'il manque des pages, veuillez communiquer avec l'université qui a conféré le grade.

La qualité d'impression de certaines pages peut laisser à désirer, surtout si les pages originales ont été dactylographiées à l'aide d'un ruban usé ou si l'université nous a fait parvenir une photocopie de qualité inférieure.

La reproduction, même partielle, de cette microforme est soumise à la Loi canadienne sur le droit d'auteur, SRC 1970, c. C-30, et ses amendements subséquents.

Canada

UNIVERSITY OF ALBERTA

RIBOZYME-MEDIATED GENE REGULATION: POTENTIAL FOR CONTROLLING GENE EXPRESSION IN HIGHER PLANTS

B

BRIAN GORDON AYRE

A thesis submitted to the Faculty of Graduate Studies and Research in partial fulfilment of the requirements for the degree of DOCTOR OF PHILOSOPHY

in

PLANT MOLECULAR BIOLOGY AND BIOTECHNOLOGY

DEPARTMENT OF PLANT SCIENCE

EDMONTON, ALBERTA

Fall 1995

ISBN 0-612-06179-5

Canada

UNIVERSITY OF ALBERTA

LIBRARY RELEASE FORM

Name of Author: **Brian Gordon Ayre**

Title of Thesis: **Ribozyme-Mediated Gene Regulation: Potential for Controlling Gene Expression in Higher Plants**

Degree: **Doctor of Philosophy**

Year this Degree Granted: **1995**

Brian Ayre

4875 Maxine Lane
Victoria, BC.
Canada

Date: August 29, 1995

University of Alberta

Faculty of Graduate Studies and Research

The undersigned certify that they have read, and recommend to the Faculty of Graduate Studies and Research for acceptance, a thesis entitled Ribozyme Mediated Gene Regulation: Potential for Controlling Gene Expression in Higher Plants submitted by Brian Gordon Ayre in partial fulfillment of the requirements for the degree of Doctor of Philosophy in Plant Molecular Biology and Biotechnology.

Dr. A. A. Szalay (Supervisor)

Dr. J. Weiner

Dr. W. Dixon

Dr. L-J. Chang

Dr. G. Bruening (External)

Date: August 22, 1995

Dedicated to My Parents

ABSTRACT

The recent discovery that short ribonucleic acid motifs can cleave RNA in a catalytic fashion present ial for regulating gene expression via sequence specific, RNA mediated transcript ation. In this study, hammerhead catalytic RNAs (ribozymes) were designed to target, and cleave, specific sites in transcripts derived from the bacterial luciferase reporter gene. Ribozyme activity against the luciferase target RNA was analysed *in vitro*, and *in vivo* in an *E. coli* model system, transiently transfected plant protoplasts, and stably transformed plant tissues, with the aim of establishing the efficacy of using hammerhead ribozymes to control gene expression in higher plants. Kinetic parameters for the reaction catalysed by the ribozymes were measured, and are comparable to those established for similar systems. The rate limiting step in single turn-over reactions was determined to be the product association rate, and the rate limiting step for multiple turn-over reactions was determined to be the rate of product dissociation. HeLa cell nuclear extracts were added to the *in vitro* reaction mixtures to study potential enhancement of the reaction rates by RNA binding proteins. For *in vivo* analysis, ribozymes were expressed in *E. coli* cells from a bacteriophage T7 promoter, in conjunction with the luciferase target. Ribozymes were estimated to be present in a 100 fold excess over luciferase mRNA, and are demonstrated to be active against related substrate transcripts. In plant cells, ribozyme effects on target mRNA abundance was studied in transiently transfected alfalfa protoplasts, transgenic *Nicotiana tabacum*, and transgenic *Arabidopsis thaliana*. For indirect, *in vivo* analysis of catalytic activity, levels of luciferase enzyme activity in experimental, and control cultures, or tissues, were compared. Ribozyme activity *in vivo* was measured directly by way of ribonuclease protection assay analysis of transcript structure, and quantity. The results obtained from this work *in vitro* suggest a role for ribozyme technologies in complementing current mechanisms of engineered gene repression, but the *in vivo* results emphasise the challenges encountered in applying novel technologies to the complex cellular environment. The universal application of ribozymes for regulating gene expression in differentiated organisms will require a deeper understanding of the fundamental processes which affect RNA interactions in living cells.

ACKNOWLEDGEMENTS

I would like to express my appreciation to the individuals who made this work possible. First, I extend my gratitude to my supervisor, Dr. A. Szalay, for his patience, guidance and support throughout the course of my graduate program. I would like to thank the members of my supervisory committee, especially Dr. J. Weiner for his encouragement and help from start to finish; Dr. W. Addison, and Dr. F. Miller, for support and helpful discussions throughout most of this work; and Dr. W. Dixon for joining the committee on short notice. I would also like to thank my examiners, Dr. I.J. Chang, and Dr. G. Bruening, University of California, Davis, for reviewing the thesis, and for sharing their expertise in the field of ribozyme-mediated gene regulation.

I thank the members of the Plant Molecular Genetics and Biotechnology Laboratories, particularly Dr. W. Langridge for his expertise and constant generosity; Dr. M. Baga for tolerating a young, naive student; Dr. A. Escher for advice and several plasmids; Dr. Stolarz for sharing his knowledge of plant tissue culture; and Dr. L. Bogre for supplying me with the alfalfa suspension culture on several occasions. For introducing me to a diverse array of interests, personalities, and many of the techniques used in this research, I also thank Dr. R. Mayerhofer, Dr. G. Wang, Dr. C. Jiang, Dr. A. Melnikov, Dr. I. Meskiene, Dr. H. Ray, Dr. M. Aguilar, Dr. G. Bagi, C. Pruski, P. Dale, P. Ceranic, A. Szenthe, K. Illes, A. Miok, L. Giacomin, D. Shkolny, S. Katzeff, and R. M^{c}Burney.

Sincere thanks to Dr. J. J. Rossi, Loma Linda University, for the close collaboration and needed encouragement. I would also like to thank Dr. D. Black, UCLA, for the HeLa cell nuclear extract; Dr. A. Horak, Dr. W. Bridger, and Dr. B. Malcolm for help with the kinetic studies; Dr. D. Glimm for advice on RNA isolation and characterisation; and Dr. A. Good for a bunch of little things.

I extend my appreciation to Karl, Cory, Chris, and Scott for keeping me sane, "Leo" and B. Alexander for help in the greenhouse, and R. M^{c}Garry for support during the preparation of the thesis.

I would like to acknowledge my funding sources, NSERC, and the Canadian Wheat Board.

Finally, I would like to thank my parents for their unconditional support and encouragement.

TABLE OF CONTENTS

LIST OF TABLES

LIST OF FIGURES

ABBREVIATIONS

2,4-D	2,4-dichlorophenoxyacetic acid
Ap	Ampicillin
ATP	Adenosine 5'-triphosphate
BAP	Benzyl amino purine
bp	Base pair
BSA	Bovine serum albumin
Ca-PEG	Calcium polyethylene glycol
CaMV	Cauliflower mosaic virus
CAT	Chloramphenicol acetyltransferase
Cb	Carbenicillin
CIP	Calf intestinal alkaline phosphatase
Cl	Claforan (cefotaxim)
CTD	Carboxy terminal domain
CTP	Cytidine 5'-triphosphate
dATP	2'-Deoxyadenosine 5'-triphosphate
dCTP	2'-Deoxycytidine 5'-triphosphate
ddH2O	Deionised, distilled water
DEPC	Diethyl pyrocarbonate
dGTP	2'-Deoxyguanosine 5'-triphosphate
dsDNA	Double stranded DNA
DTT	Dithiothreitol
dTTP	2'-Deoxythymidine 5'-triphosphate
EDTA	Ethylenediaminetetraacetic acid
EtBr	Ethidium bromide
GIT	Guanidinium *iso*-thiocyanate
Gm	Gentamycin
GTP	Guanosine 5'-triphosphate
GUS	β-Glucuronidase
HEPES	N-[2-hydroxyethyl] piperazine-N'-[2-ethanesulfonic acid]
HH16	Hammerhead 16
HIV	Human immunodeficiency virus
Hm	Hygromycin

hnRNP	heterogeneous nuclear ribonucleoprotein
IPTG	Isopropyl-β-D-thiogalactopyranoside
kcal	Kilocalorie
Km	Kanamycin
LB	Luria-Bertani
LMP	Low melting point
*lux*A	Bacterial luciferase α subunit encoding gene
*lux*B	cterial luciferase β subunit encoding gene
*lux*F	Bacterial luciferase fusion gene
mas	Mannopine synthase
MCS	Multiple cloning site
MES	Morpholinoethane sulfonic acid
MS	Murashige Skoog
NAA	Naphthalene acetic acid
NCp7	HIV nucleocapsid protein
nos	Nopaline synthase
nt	Nucleotide
O.D.	Optical density
oligos	Oligonucleotide
PAGE	Polyacrylamide gel electrophoresis
PCR	Polymerase chain reaction
PEG	Polyethylene glycol
pol	polymerase
polyA	Poly-adenylation
Rif	Rifampicin
RNase	Ribonuclease
RPA	Ribonuclease protection assay
rRNA	ribosomal RNA
SDS	Sodium dodecyl sulfate
TBE	Tris borate EDTA
TEMED	N, N, N', N'-Tetramethylethylenediamine
Tris-HCl	Tri (hydroxy methyl) amino methane - hydrochloric acid
UTP	Uridine 5'-triphosphate
UV	Ultraviolet

1. INTRODUCTION

1.1 RNA Catalysis

Prior to 1982, a molecular biologist's view of the cell was relatively simple: DNA was an information-storing molecule, proteins were the catalytic, or structural result of that information, and RNA acted as an intermediate in moving the information from the DNA to the sites of protein synthesis.

The 1989 Nobel Prize for Chemistry was awarded to Thomas Cech of the University of Colorado, and Sidney Altman of Yale University for their independent discoveries that RNA molecules can act as enzymes. Thomas Cech was studing the excision of a 413 nucleotide intron from *Tetrahymena* ribosomal RNA precursors, and discovered that the intron itself is responsible for its own splicing, via two site-specific, consecutive phosphoester transesterfications, in the presence of magnesium or manganese cations, and a guanosine or guanosine nucleotide co-factor (Kruger *et al.*, 1982). Such self-splicing introns are classified as Group I introns. Sidney Altman was studying Ribonuclease P (RNase P), a small ribonucleoprotein responsible for cleaving the 5' end of transfer RNA precursors, and discovered that the catalytic activity of this molecule resides in the RNA portion, which is stabilised by the small protein subunit (Guerrier-Takada, *et al.*, 1982).

Since these two landmark discoveries, numerous other biological reactions were found to be, or are speculated to be, carried out by RNA. A number of small plant pathogenic RNAs (viroids, virusoids, and satellite RNAs, discussed below), and the Hepatitis delta virus undergo autocatalytic cleavage (Wu, *et al.*, 1989), as do RNA transcripts from satellite II DNA of the newt (Forster, *et al.*, 1988), and from a *Neurospora* mitochondrial DNA plasmid (Saville and Collins, 1990). Group II intron sequences, like the Group I intron sequences discussed above, undergo autocatalysed splicing, but with a lariat intermediate very similar to that seen for spliceosome mediated mRNA splicing (Jacquier, 1990). Indeed, the splicing activity of the spliceosome is suspected to be found in the RNA components, with protein modulation (Jacquier, 1990).

Convincing evidence that the RNA component of the 50S ribosomal subunit from *Thermus aquaticus* can perform the peptidyl transferase reaction in the absence of protein (Noller, *et al.*, 1992) suggests that rRNA is responsible for at least some of the ribosomes translation processes - speculation that is supported by the demonstration that the group I intron of *Tetrahymena* can perform the aminoacyl esterase reaction of the ribosome (Piccirilli, *et al.*, 1992).

With the exception of the RNA component of RNase P, all naturally occurring RNA catalysts discovered to date are self-cleaving or self-splicing. However, each of the sequences can be manipulated to act against specific target transcripts. The catalytic sequences derived from viroids and virusoids, termed the hammerhead motif (see below), are the most versatile RNA catalysts for modulating gene expression due to their small size, and minimal substrate sequence requirements. The hammerhead motif, or ribozyme, was utilised in this study to alter gene expression in higher plants, and is therefore the only motif discussed further.

1.2 The Hammerhead Motif of Plant Pathogenic RNAs

Viroids are small (246-375 nucleotides), single stranded, circular RNAs pathogenic to higher plants that are capable of independent replication and infection without encapsulation. Virusoids are very similar to viroids, except that virusoids rely on a helper virus for replication, and encapsulation. Virusoids are frequently referred to as virus satellite RNAs as they are encapsulated with the helper virus genome, and can make up as much as 90% of the RNA in the viral paticle (Riesner, 1985).

Neither type of molecule encodes proteins, and the pathogenesis of these molecules are poorly understood, but are probably different. Some virusoids are associated with symptom reduction of the host virus, and are therefore considered to be parasites of the virus (Gerlach, *et al.*, 1987). Several viroids have either sequence homology, or sequences complementary to small nuclear RNAs, particularly U1 RNA (involved in splicing), U3B (located in the nucleolus) (Riesner, 1985), and 7S RNA (the

RNA component of the eucaryotic signal recognition particle), and are speculated to be pathogenic through an antisense effect (Haas, *et al.*, 1988; Symons, 1989a).

Viroids and virusoids are believed to replicate in plant cells by a rolling circle mechanism to produce longer than unit length transcripts. Two models for this form of replication have been presented, depending on whether or not the concatemer transcribed from the infectious strand is, or is not, cleaved to a monomeric form (Symons, 1989b; 1992). The rolling circle pathway of replication requires highly specific cleavage within the concatemeric RNAs, and would require a host enzyme, if a protein was involved. Involvement of a host ribonuclease is unlikely, however, since no known plant ribonuclease has the high specificity required. Further, the wide host range of some viroids would require a universally present enzyme with the appropriate specificity. Alternatively, these RNA's could usurp specific components of the complexes involved in intron splicing. A third possibility is self cleavage, which is demonstrated for some, but not all, small plant pathogenic RNAs.

The first indication that a satellite RNA of a plant virus could self cleave came in 1986 from the lab of Bruening and colleagues, when dimeric genomes of the satellite RNA of tobacco ring spot virus formed monomeric genomes when subjected to repeated freeze thaw cycles. These monomers had 2',3' cyclic phosphate and 5' hydroxyl termini, rather than the "normal" 5' phosphate and 3' hydroxyl termini (Prody, *et al.*, 1986). It was subsequently discovered that the plus and minus strand of one viroid (Hutchins, *et al.*, 1986), and several virusoids also undergo site-specific cleavage, and that they all had segments of sequence homology surrounding the cleavage site. Based on these conserved sequences, a conserved secondary structure model was developed, consisting of three helices and thirteen conserved nucleotides precisely positioned with respect to the site of cleavage. The structure resembles the head of a carpenter's hammer, and is thus referred to as the hammerhead motif (Figure 1.1a) (Forster and Symons, 1987a). Deletion analysis and transcription *in vitro* of cDNA derived from virusoid sequences revealed that the 55 nucleotide hammerhead structure is sufficient for self-cleavage (Forster and Symons, 1987b). A standardised numbering system for the nucleotides within the hammerhead

motif was recently proposed (Hertel, *et al.*, 1992), and is utilised throughout this thesis (Figure 1.1c).

1.3 The Hammerhead Ribozyme as a Trans-cleaving Catalyst

Using the consensus secondary structure, Uhlenbeck (1987), at the University of Colorado transcribed *in vitro* two short oligonucleotides which could form the hammerhead structure *in trans* via base pairing. One oligomer consisted of 24 nucleotides and contained stem/loop structure III (according to the Forster and Symons numbering (1987b)) from the minus strand of the avocado sunblotch viroid, 7 of the 13 conserved nucleotides, and the cleavage site, such that this molecule acted as the substrate in the cleavage reaction. The second oligomer consisted of 16 nucleotides, no secondary structure, and the remaining 6 conserved nucleotides. This oligomer remained unaltered during cleavage, and therefore was the catalyst. Stems I and II were formed by base pairing between the two oligos, using complementary sequences not found in naturally occurring hammerhead structures (Figure 1.1b).

When mixed under appropriate conditions, rapid cleavage of the substrate strand was observed, showing that the hammerhead structure is necessary and sufficient for cleavage. On average, each catalyst oligomer acted on approximately 20 substrate molecules, showing that a portion of the hammerhead could act as a true RNA enzyme. More significantly, the experiment demonstrated that hammerhead ribozymes could potentially cleave any target RNA possessing the sequences necessary to complete the hammerhead domain. However, the ribozyme constructed by Uhlenbeck is of limited use for cleaving RNA in general because the substrate must contain numerous conserved sequences as well as conserved secondary structure. Such sequences would appear very rarely in most natural transcripts.

In order to improve the potential of ribozymes, Haseloff and Gerlach (1988) designed a ribozyme which greatly increased the number of possible target sites, but maintained sequence specificity. The substrate contained only those conserved sequences immediately 5' to the cleavage site, which in naturally occurring self-cleavage reactions is

GUC. In a random sequence, GUC is expected to appear on average every 64 nucleotides. However, *in vitro*, the G may be replaced by C, A or U, and the C may be altered to A or U, thus creating a virtually limitless target selection, albeit with reduced activity (Symons, 1992). The remaining conserved nucleotides, stem loop structure II, and the flanking guide sequences required for duplex formation with the target, constitutes the ribozyme strand (Figure 1.1c). The extent of base pairing between the target and the ribozyme affects the specificity, affinity, and the turnover of the ribozyme (Chapter 2).

1.4 Hammerhead Tertiary Structure

Because the products of cleavage via a hammerhead structure produce 2',3' cyclic phosphate and 5' hydroxyl termini, and because no guanosine cofactor is required, the cleavage mechanism for these molecules must be different from the mechanism of group I intron splicing. It is well established that RNA cleavage by base hydrolysis occurs by in-line nucleophilic attack on the scissile phosphate, resulting in 2',3' cyclic phosphate with stereo isomer inversion. The same mechanism is believed to occur in the hammerhead cleavage reaction. It is established that cleavage by the hammerhead proceeds with inversion of configuration of the sessile phosphate to form a 2',3' cyclic phosphate: probably via in-line attack by the essential 2' hydroxyl of the ribose on the phosphodiester bond at the cleavage site (Pley, *et al.*, 1994). The unique structure of the hammerhead is believed to bring the 2' hydroxyl into position for the reaction (Mei, *et al.*, 1989; Pley, *et al.*, 1994).

Structural studies carried out confirm the secondary structure (Figure 1.1), and predict the tertiary structure of the hammerhead motif. The secondary structure of several individual hammerhead/substrate complexes, or potential competing conformations, were predicted using standard RNA folding algorithms (Denman, 1993; Steinecke, *et al.*, 1994), and experimentally confirmed by RNase digestion and UV crosslinking. RNase digestion profiles of both *cis*- and *trans*-acting hammerhead structures were nearly identical, indicating that the structural interactions leading to cleavage are similar for both systems. The presence or absence of Mg^{2+}, which is absolutely required for activity, did not affect

the RNase digestion profiles, suggesting that Mg^{2+} does not modify the base pairing interactions in the hammerhead structure to induce cleavage, *i.e.*, Mg^{2+} is catalytic, not structural (Hodgson, *et al.*, 1994). Cross-linking studies suggest that the tertiary structure is not rigid, and that several inactive confirmations form, which are in equilibrium with the active structure. The cross-linking patterns differed between an RNA/RNA complex, and a RNA/DNA complex (DNA as an inactive substrate, due to the absence of the 2' hydroxyl group necessary for nucleophilic attack), raising the question as to whether folding is the same between the two (Woisard, *et al.*, 1994). It was also demonstrated that the active hammerhead structure does not preform in the catalytic strand, but forms only in the presence of the proper target (Homann, *et al.*, 1993).

The earliest three dimensional, self-cleaving hammerhead structure was computer generated (Mei, *et al.*, 1989), based on the secondary structure proposed by Forster and Symons (1987a). This model predicts that the ribose sugar moieties are in 3' *endo* conformations in standard A-type, Watson-Crick helices, as expected for RNA (Sainger, 1984). However, the ribose phosphate backbone is forced to take an abrupt turn between stems I and III (*i. e.*, at the cleavage site), and since the cytosine base does not interact with another base, it is free to move, allowing the ribose to enter the 2' *endo* conformation. This places the attacking hydroxyl in close proximity to the susceptible phosphate, and positions the leaving 5' oxygen for a direct in-line attack, such that the structure of the hammerhead leads to self-cleavage. The magnesium divalent cation is predicted to serve as a catalyst by stabilising the penta co-ordinate phosphate intermediate, and facilitating hydrogen transfer.

Fluorescence resonance energy transfer (FRET) analysis confirms the presence of Watson-Crick base pair interactions in A-type helices in the stems of helices I, II, and III. However, this study suggests a Y, or wishbone conformation, in which helices I and II are in close proximity, and helix III is pointing away. This study also suggests a number of non-Watson-Crick nucleotide interactions among the conserved nucleotides in the catalytic core. The study does not demonstrate the co-ordination of Mg^{2+} into the structure, but the authors speculate on a Mg^{2+} binding site involving U4, G5, A6, and C17 (the cleavage site), at the base of stem I (Tuschl, *et al.*, 1994).

X-ray crystallography with a substrate strand made entirely of deoxyribonucleotides, also confirms the presence of A-type helices, and supports the wishbone conformation, but differs on the localisation of the Mg^{2+} (Pley, *et al.*, 1994). The authors report 1) a sharp turn between stems I and II (nucleotides C3- A6), whereas stem II and III are nearly co-linear (*i. e.*, Y-shaped), 2) a non-Watson-Crick duplex between U7 -> A9 and G12 -> A14 (*i. e.*, at the base of the Watson-Crick helix of stem II), and 3) that the DNA substrate strand is splayed out between nucleotides dT16.1 and dC17 (*i. e.*, the cleavage site). The Mg^{2+} is however, situated at the base of stem II, isolated from the cleavage site, and presumably has a stabilising function rather than a catalytic function.

The Y shaped structure is also supported by transient electric birefringence - and by a pseudoknot between helix I and II in at least one functional ribozyme, consistent with helices I and II being in proximity (Cech and Uhlenbeck, 1994).

These experimental determinations of the tertiary structure contrast with the computer model presented by Mei, *et al.*, (1989). However, it should be noted that the wishbone structure does not present a structure which would allow the required in-line nucleophilic attack to produce the 2',3' cyclic phosphate, and, in the structure determined by crystallography, there is not a divalent cation bound at the active site. As explained by Pley, *et al.*, (1994), in-line attack could occur if the phosphate of the scissile bond could twist inward, or the nucleotide could flip out. The catalytic core would therefore destabilise, or flex the substrate strand to allow the scissile phosphodiester linkage to twist into a confirmation that would allow cleavage, without major disruption of the stems or the tertiary structure of the core, and it would position the divalent cation, but it is not known how.

1.5 Ribozymes May Potentially Limit Gene Expression

The ability of hammerhead ribozymes to cleave specific target sequences presents the potential to control the expression of endogenous genes, or to artificially immunise organisms against viral pathogens. Ribozymes have therefore received a great deal of

attention in many diverse organisms. In medicine, ribozymes are being studied extensively as anti-viral agents, particularly against HIV and Hepatitis B (Sarver, *et al.*, 1990; Chen, *et al.*, 1992; Yu, *et al.*, 1993; Dropulic, *et al.*, 1993). Ribozymes *in vivo* have also been demonstrated to be effective against endogenous deleterious genes, such as oncogene transcripts (Pachuk, *et al.*, 1994), and drug resistance gene transcripts (Kiehntopf, *et al.*, 1994). In these experiments, ribozymes were delivered transiently, either as RNA, or as genes inserted into expression cassettes. Ribozymes permanently incorporated into the genome of transgenic mice have also been effective (Larson, *et al.*, 1994).

In agriculture, several reports exist for the *in vivo* activity of ribozymes in higher plant tissues, which are discussed in detail in Chapters 4 and 5. Advances in ribozyme technology in medicine can be applied directly to the Animal Sciences, and indeed, ribozymes were demonstrated to inhibit Bovine Leukaemia Virus *in vivo* (Cantor, *et al.*, 1993).

Ribozymes are also useful in basic molecular biology, such as studies involving mRNA 3'-end maturation, and export, (Eckner, *et al.*, 1991; Egli and Gruss, 1994), spliceosome-mediated splicing (Rossi, *et al.*, personal communication), and trimming RNAs into desired structures unattainable with expression cassettes (Leiser, *et al.*, 1992).

1.6 Utility of Ribozymes in Plant Biology

It would be highly beneficial to both agricultural applications, and basic science to establish plant lines with reduced or eliminated expression of specific genes. Basic research would benefit by facilitating the study of gene function through the creation of specific somatic mutations (reverse genetics). In agriculture, the value and utility of many crop species would be increased by reducing or eliminating undesirable compounds in seeds, or by generating immunity against intracellular pathogens.

At present, a reliable and effective method for reducing, or preventing the expression of a specific gene is not available for higher plants. Random mutagenesis by chemical or physical means often results in multiple mutation events, and requires screening a large number of plants to identify the mutation of interest. In prokaryotic

organisms and lower eukaryotes (including some plants) homologous recombination is frequently employed to disrupt the gene of interest by inserting a selectable marker gene. Homologous recombination is reported in higher plants, but the efficiency is low, and non-homologous recombination occurs more frequently than homologous recombination (Offringa, *et al.*, 1990; Offringa, *et al.*, 1993). Antisense RNA technologies have emerged as the method of choice for down regulating specific genes in transgenic plants (Oeller, *et al.*, 1991; Murata, *et al.*, 1992; Knutzon, *et al.*, 1992). The antisense transcript, however must be present in the cell at levels equal to, or exceeding the amount of transcript from the gene of interest for efficient repression (Rothstein, *et al.*, 1987). This prevents the application of antisense RNA for repression of a gene in a particular organ at a particular stage of development, where a promoter with the strength and specificity required to drive transcription at the required level is not available.

1.7 Research Objectives

The goal of this research is to analyse the potential of catalytic RNA for controlling the expression of specific genes at the post-transcriptional level. Research into the use of catalytic RNA for controlling gene expression is worthwhile due to the advantages over the other discussed systems. 1) Unlike induced mutagenesis, catalytic RNA can be targeted to a specific gene of interest. 2) The catalytic RNA gene can be placed downstream of a promoter of known function, thereby repressing the gene of interest in specific organs at specific stages of development - unlike homologous recombination. 3) In contrast to antisense technologies, the catalytic properties of the RNA could potentially inhibit the expression of genes which are transcribed to levels higher than those of the catalytic RNA.

The luciferase reporter gene system (*lux*) from the bioluminescent marine bacterium, *Vibrio harveyi*, was chosen as a target gene for analyzing ribozyme-mediated transcript elimination. This reporter system is advantageous because it allows rapid quantitative analysis of enzyme levels, and in additon, the system is well established in our laboratory (Langridge, *et al.*, 1994). Wild type bacterial luciferase [alkanal

monooxygenase (FMN-linked); alkanal, reduced-FMN: oxygen oxidoreductase (1-hydroxylating, luminescing), EC 1.14.14.3] is a heterodimeric enzyme composed of one α (40kDa) and one β (36kDa) subunit, that catalyzes the following reaction: $FMNH_2 + O_2 + RCHO \rightarrow FMN + RCOOH + H_2O + 1\ h\nu_{490nm}$. However, except where noted, the luciferase reporter gene used in these studies consists of a *lux*A and *lux*B gene fused into a single open reading frame encoding a new bacterial luciferase active as a monomer (*lux*-F), with a specific activity and emission spectrum comparable to the wild type heterodimeric enzyme (Escher, *et al.*, 1989).

Since the purpose of this project was to analyse the efficacy of using hammerhead ribozymes to control gene expression in higher plants, the ribozyme and target sequences used are derived from the versatile plant cloning vector, pPCV701-*lux*-FP1. The luciferase gene on pPCV701-*lux*-FP1 is driven by the P1 promoter of the auxin-, and wounding-regulated, 500 nt, mannopine synthase (*mas*) dual promoter, isolated from the mannopine synthase operon of the *Agrobacterium tumefaciens* Ti plasmid (Figure 1.2) (Velten, *et al.*, 1984; Koncz, *et al.*, 1987; Langridge, *et al.*, 1989). Three ribozymes of the Haseloff and Gerlach design were constructed in collaboration with Dr. John Rossi, Beckman Research Center, City of Hope, California. The sequence of each catalytic domain is identical to that found in the satellite RNAs of the tobacco ring spot virus. Flanking each catalytic domain on the 5' and 3' sides is 7 to 10 nucleotides complementary to sequences found in the target transcript. One ribozyme, ribo, is targeted to the untranslated leader region of the P1 promoter, immediately upstream of the *lux* ATG initiation codon. The second and third ribozyme, ribo1 and ribo4, are targeted to sequences in the luciferase structural gene, approximately 100 nucleotides downstream of the ATG start codon. Ribo4 is a dual ribozyme which incorporates most of the sequences of ribo1, plus additional sequences required to cleave the target at a second location eight nucleotides downstream of the first cleavage site (Figure 1.2). For each ribozyme, a corresponding control ribozyme was constructed in order to differentiate between gene repression due to a cleavage event and the intrinsic antisense RNA properties of ribozymes. These control ribozymes contain a single A to T transversion at position 14 of

the hammerhead domain (Figure 1.1c), designated A14T, which is inactive, but should still form the essential secondary structure.

Within this thesis, four areas of investigation are addressed. Chapter 2 deals with hammerhead ribozyme activity *in vitro*. In Chapter 3, ribozyme activity *in vivo* is discussed with respect to an *E. coli* model system. Ribozyme activity is analysed by way of transient expression in alfalfa protoplasts in Chapter 4, and ribozymes are investigated in stably transformed plant tissues in Chapter 5. Chapter 6 presents a discussion concerning the use of hammerhead ribozymes to control gene expression, and mechanisms for improved design and activity.

Figure 1.1

The Hammerhead motif

A. The self-cleaving hammerhead domain of the satellite RNA of tobacco ring spot virus (sTRSV). 5' and 3' orientations are indicated, and nucleotide numbering is relative to the sTRSV genome. Stem-loop structures are labelled with Roman numerals, and the cleavage site is marked with an arrow. Conserved sequences are boxed.

B. *Trans*-cleaving ribozyme as designed by Uhlenbeck, (1987). S = substrate strand, R = ribozyme strand, other markings are as in **A**.

C. Versatile hammerhead ribozyme designed by Haseloff and Gerlach, (1988). Standardised nucleotide numbering is as per Hertel, *et al.*, (1992).

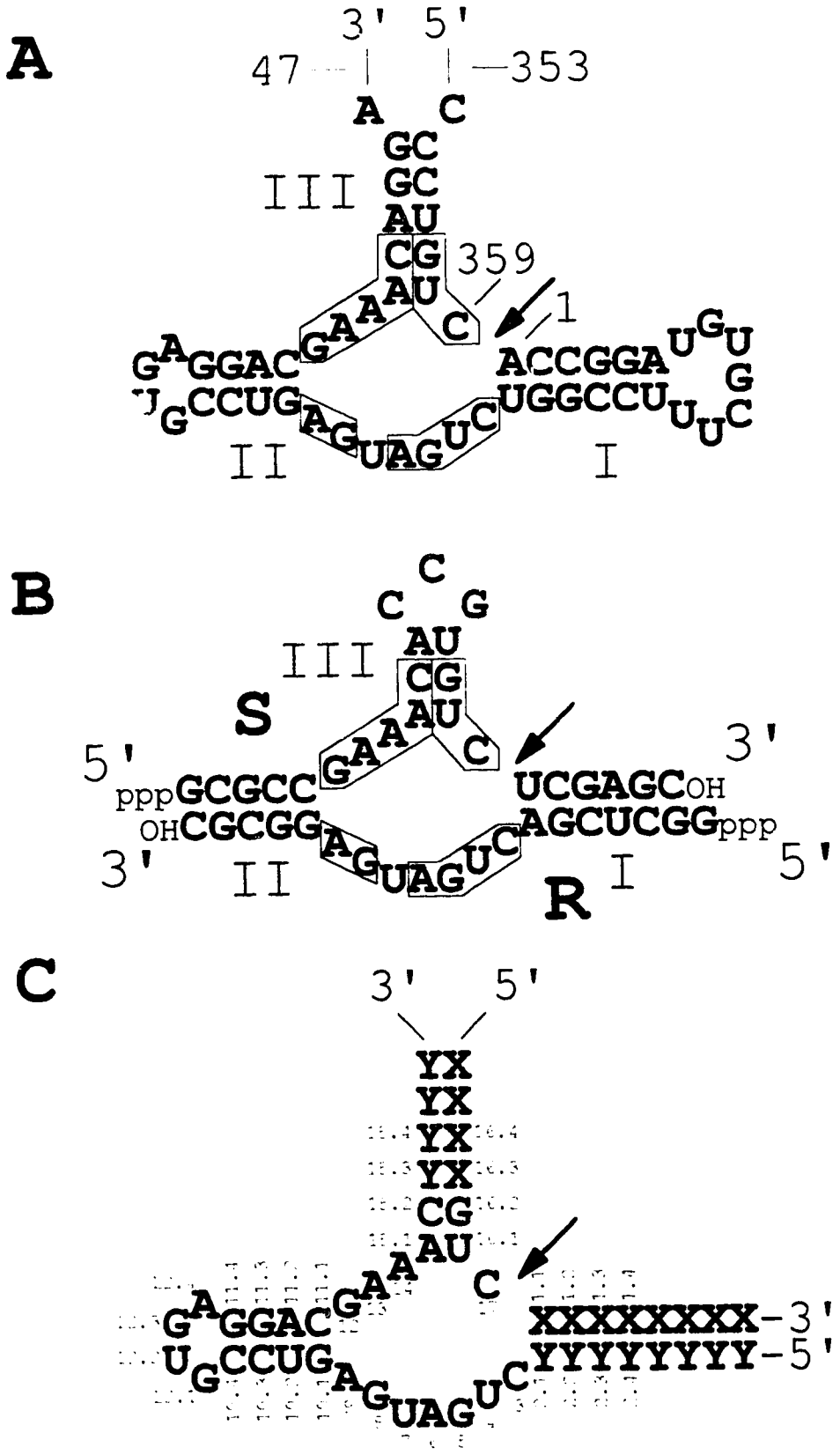
A
3' 5'
47
353
III
359
1
II
I
B
S
5'
3'
R
C
3' 5'
XXXXXXXX-3'
YYYYYYYY-5'

Figure 1.2

Ribozymes targeted against sequences in the bacterial luciferase gene transcript.

A. Sequence of the ribozyme catalytic core derived from the catalytic domain of the satellite RNA of the tobacco ring spot virus, and the control core with an A to T transversion at position 14.

B. Linear map of the region between the left and right T-DNA borders of pPCV701-*lux*-FP1 (details in Chapter 4, and 5): BL, left T-DNA border; pA, poly-adenylation signal; *npt*II, coding sequence of neomycin phosphotransferase from Tn5 (conferring kanamycin resistance); P*nos*, promoter element from the nopaline synthase gene; *lux-F*, coding sequence of the bacterial luciferase fusion protein; *mas*, mannopine synthase dual promoter; P1, P1 promoter of the mannopine synthase dual promoter; P2, P2 promoter of the mannopine synthase dual promoter; *amp*R, gene encoding ampicillin resistance (β-lactamase); pBR, origin of replication from pBR322; Pg5, promoter element of gene 5 from the *Agrobacterium tumefaciens* Ti plasmid; BR, right T-DNA border. Restriction sites: H, HindIII; S, SalI; E, EcoRI; P, PstI; B, BamHI.

C. Enlarged view of pPCV701-*lux*-FP1 showing the ribozyme cleavage sites, and complementary sequences. Nucleotides are numbered relative to the luciferase ATG start codon, ribozymes are as labelled, P, PstI restriction site. The sequence, and structure of the three ribozymes used in this study, ribo, ribo1, and rib4 are also indicated.

A.

Catalytic core: 5'-CTGATGAGTCCGTGAGGACGAA-3'

Control core: 5'-CTGATGAGTCCGTGAGGACGAT-3'

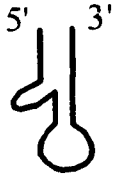

B.

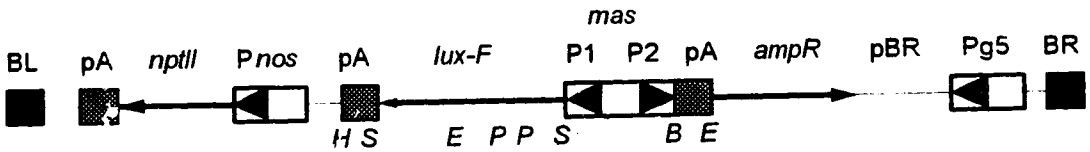

C.

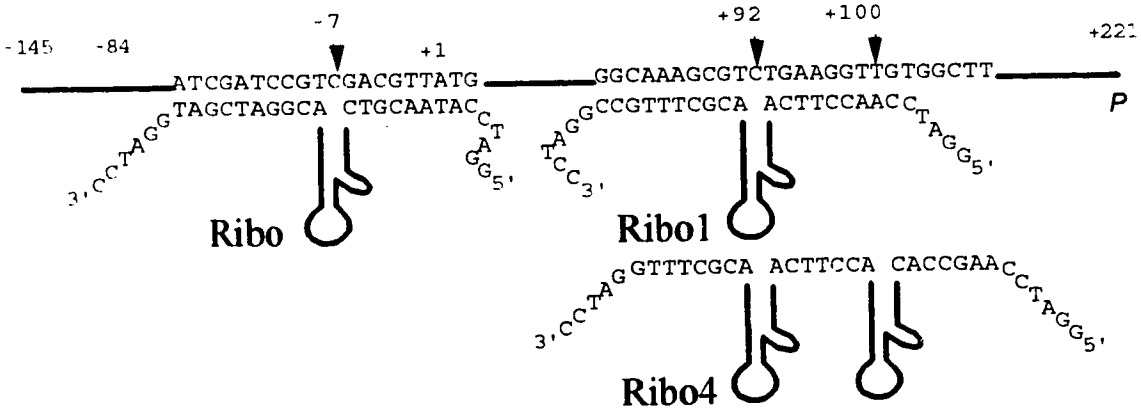

1.8 Bibliography

Buzayan, J. M., Gerlach, W. L., Bruening, G. (1986). Non-enzymatic cleavage and ligation of RNAs with sequences that are complementary to a plant virus satellite RNA. *Nature* **323**, 349-353.

Cantor, G. H., McElwain, T. F., Birkebak, T. A., and Palmer, G. H. (1993). Ribozyme cleaves *rex/tax* mRNA and inhibits bovine leukaemia virus expression. *Proc. Natl. Acad. Sci. USA* **90**, 10932-10936.

Cech, T. R., and Uhlenbeck, O. C. (1994). Hammerhead nailed down. *Nature* **372**, 39-40.

Chen, C., Banerjea, A. C., Harmison, G. G., Haglund, K., and Schubert, M. (1992). Multitarget-ribozyme directed to cleave up to nine highly conserved HIV-1 *env* RNA regions inhibits HIV-1 replication - potential effectiveness against most presently sequenced HIV-1 isolates. *Nucleic Acids Res.* **20**, 4581-4589.

Denman, R. (1993). Using RNAFOLD to predict the activity of small catalytic RNAs. *Biotechniques* **15**, 1090-1094.

Dropulic, B., Elkins, D. A., Rossi, J. J., and Sarver, N. (1993). Meeting Report - Ribozymes: Use as anti-HIV therapeutic molecules. *Antisense Research and Development* **3**, 87-94.

Eckner, R., Ellmeier, W., and Birnstiel, M. L. (1991). Mature mRNA 3' end formation stimulates RNA export from the nucleus. *EMBO J.* **10**, 3513-3522.

Egli, C. M., and Braus, G. H. (1994). Uncoupling of mRNA 3' cleavage and polyadenylation by expression of a hammerhead ribozyme in yeast. *J. Biol. Chem.* **269**, 27378-27382.

Escher, A., O'Kane, D. J., Lee, J., Szalay, A. A. (1989). Bacterial luciferase αβ fusion protein is fully active as a monomer and highly sensitive *in vivo* to elevated temperature. *Proc. Natl. Acad. Sci. USA.* **86**, 6528-6532.

Forster, A. C., Davies, C., Sheldon, C. C., Jeffries, A. C., and Symons, R. H. (1988). Self-cleaving viroid and newt RNAs may only be active as dimers. *Nature* **334**, 265-267.

Forster, A. C., and Symons, R. H. (1987a). Self-cleavage of plus and minus RNAs of a virusoid and a structural model for the active sites. *Cell* **49**, 211-220.

Forster, A. C., and Symons, R. H. (1987b). Self-cleavage of virusoid RNA is performed by the proposed 55-nucleotide active site. *Cell* **50**, 9-16.

Gerlach, W. L., Llewellyn, D., and Haseloff, J. (1987). Construction of a plant disease resistance gene from the satellite RNA of tobacco ring spot virus. *Nature* **328**, 802-805.

Guerrier-Takada, C., Gardiner, K., Marsh, T., Pace, N., and Altman, S. (1982). The RNA moiety of ribonuclease P is the catalytic subunit of the enzyme. *Cell* **35**, 849.

Haas, B., Klanner, A., Ramm, K., and Sanger, H. L. (1988). The 7S RNA from tomato leaf tissue resembles a signal recognition particle RNA and exhibits a remarkable sequence complementary to viroid. *EMBO* **7**, 4063-4074.

Haseloff, J., and Gerlach, W. L. (1988). Simple RNA enzymes with new and highly specific endoribonuclease activities. *Nature* **334**, 585-591.

Hertel, K. J., Pardi, A., Uhlenbeck, O. C., Koizumi, M., Ohtsuka, E., Uesugi, S., Cedergren, R., Eckstein, F., Gerlach, W. L., Hodgson, R., and Symons R. H. (1992). Numbering system for the hammerhead. *Nucleic Acids Res.* **20**, 2352.

Heus, H. A., and Pardi, A. (1991). Nuclear magnetic resonance studies of the hammerhead ribozyme domain: secondary structure formation and magnessium ion dependence. *J. Mol. Biol.* **217**, 113-124.

Hodgson, R. A. J., Shirley, N. J., Symons, R. H. (1994). Probing the hammerhead ribozyme structure with ribonucleases. *Nucleic Acids Res.* **22**, 1620-1625.

Homann, M., Tzortzakaki, S., Rittner, K., Sczakiel, G., and Tabler, M. (1993). Incorporation of the catalytic domain of a hammerhead ribozyme into antisense RNA enhances its inhibitory effect on the replication of human immunodeficiency virus type 1. *Nucleic Acids Res.* **21**, 2809-2814.

Hutchins, C. J., Rathjen, P. D., Forster, A. C., and Symons, R. H. (1986). Self-cleavage of plus and minus RNA transcripts of avocado sunblotch viroid. *Nucleic Acids Res.* **14**, 3627-3640.

Jacquier, A. (1990). Self-splicing group II and nuclear pre-mRNA introns: how similar are they? *Trends Biochem. Sci.* **15**,351-354.

Kienhntopf, M., Brach, M. A., Licht, T., Petschauer, S., Karawajew, L., Kirschning, C., and Herrmann, F. (1994). Ribozyme-mediated cleavage of the MDR-1 transcript restores chemosensitivity in previously resistant cancer cells. *EMBO J.* **13**, 4645-4652.

Koncz, C., Olsson, O., Langridge, W. H. R., Schell, J., Szalay, A. A. (1987) Expression and assembly of functional bacterial luciferase in plants. *Proc. Natl. Acad. Sci. USA*. **84**, 131-135.

Knutzon, D. S., Thompson, G. A., Radke, S, E., Johnson, W. B., Knauf, V. C., Kridl, J. C. (1992). Modification of *Brassica* seed oil by antisense expression of a stearoyl-acyl carrier protein desaturase gene. *Proc. Natl. Acad. Sci. USA* **89**, 2624-2628.

Kruger, K., Grabowski, P.J., Zaug, A. J., Sands, J., Gottschling, D. E., and Cech, T. R. (1982). Self-splicing RNA: autoexcision and autocyclisation of the ribosomal RNA intervening sequence of *Tetrahymena*. *Cell* **31**, 147.

Larson, S., Hotchkiss, G., Andang, M., Nyholm, T., Inzunza, J., Jansson, I., and Ahrlund-Richter, L. (1994). Reduced β2-*microglobulin* mRNA levels in transgenic mice expressing a designed hammerhead ribozyme. *Nucleic Acids Res.* **22**, 2242-2248.

Langridge, W. H. R., Fitzgerald, K. J., Koncz, C., Schell, J., Szalay, A. A. (1989). Dual promoter of *Agrobacterium tumefaciens* mannopine synthase genes is regulated by plant growth hormones. *Proc. Natl. Acad. Sci. USA*. **86**, 3219-3223.

Langridge, W. H. R., Escher, A., Wang, G., Ayre B., Fodor, I., Szalay, A. A. (1994). Low-light image analysis of transgenic organisms using bacterial luciferase as a marker. *J. Biolumin Chemilumin.* **9**, 185-200.

Leiser, R. M., Ziegler-Graff, V., Reutenauer, E., Herrbach, E., Lemaire, O., Guilley, H., Richards, K., Jonard, G. (1992). Agroinfection as an alternative to insects for infecting plants with beet western yellows luteovirus. *Proc. Natl. Acad. Sci. USA*. **89**, 9136-9140.

Mei, H., Kaaret, T. W., Thomas, C. B. (1989) A computational approach to the mechanism of self-cleavage of hammerhead RNA. *Proc. Natl. Acad. Sci. USA* **86**, 9727-9731.

Murata, N., Ishizaki-Nishizawa, O., Higashi, S., Hayashi, H., Tasaka, Y., Nishida, I. (1992). Genetically engineered alteration in the chilling sensitivity of plants. *Nature* **356**, 710-713.

Noller, H. F., Hoffarth, V., and Zimniak, L. (1992). Unusual resistance of peptidyl transferase to protein extraction procedures. *Science* **256**, 1416-1419.

Oeller, P. W., Min-Wong, L., Taylor, L. P., Pike, D. A., Theologis, A. (1991). Reversible inhibition of tomato fruit senescence by antisense RNA. *Science* **254**, 437-439.

Pachuk, C. J., Yoon, K., Moelling, K., and Coney, L. R. (1994). Selective cleavage of *bcr-abl* chimeric RNAs by a ribozyme targeted to non-contiguous sequences. *Nucleic Acids. Res.* **22**, 301-307.

Piccirilli, J. A., McConnell, T. S., Zaug, A. J., Noller, H. F., and Cech, T. R. (1992). Aminoacyl esterase activity of the *Tetrahymena* ribozyme. *Science* **256**, 1420-1424.

Pley, H. W., Flaherty, K. M., and McKay, D. B. (1994). Three dimensional structure of a hammerhead ribozyme. *Nature* **372**, 68-74.

Prody, G. A., Bakos, J. T., Buzayan, J. M., Schneider, I. R., and Bruening, G. (1986). Autolytic processing of dimeric plant virus satellite RNA. *Science* **231**, 1577-1580.

Riesner, D. (1985). The Viroids. *Ann. Rev. Biochem.* **54**, 531-564.

Rothstein, S. J., DiMaio, J., Strand, M., Rice, D. (1987). Stable and heritable inhibition of the expression of nopaline synthase in tobacco expressing antisense RNA. *Proc. Natl. Acad. Sci. USA* **84**, 8439-8443.

Saenger W. (1984). In: *Principles of Nucleic Acid Structure*. Springer Verlag, New York.

Sarver, N., Cantin, E. M., Chang, P. S., Zaia, J. A., Ladne, P. A., Stephens, D. A., and Rossi, J. J. (1990). Ribozymes as potential anti-HIV-1 therapeutic agents. *Science* **247**, 1222-1225.

Saville, B. J., and Collins, R. A. (1990). A site-specific self-cleavage reaction performed by a novel RNA in *Neurospora* mitochondria . *Cell* **61**, 685-696.

Steinecke, P., Steger, G., and Schreier, P. H. (1994). A stable hammerhead structure is not required for endonucleolytic activity of a ribozyme *in vivo*. *Gene* **149**, 47-54.

Symons, R. H. (1989a). Pathogenesis by antisense. *Nature* **338**, 542-543.

Symons, R. H. (1989b). Self-cleavage of RNA in the replication of small pathogens of plants and animals. *Trends in Biochem.* **14**, 445-450.

Tuschl, T., Gohlke, C., Jovin, T. M., Westhof, E., and Eckstein, F. (1994). A three-dimensional model for the hammerhead ribozyme based on fluorescence measurements. *Science* **266**, 785-789.

Uhlenbeck, O. C. (1987). A small catalytic oligoribonucleotide. *Nature* **328**, 596-600.

Velten, J., Velten, R., Hain, R., Schell. J. Isolation of a dual plant promoter fragment from the Ti plasmid of *Agrobacterium tumefaciens*. *EMBO J.* **3**, 2723-2730.

Woisard, A., Fourrey, J. L., Favre, A. (1994). Multiple folded conformations of a hammerhead ribozyme domain under cleavage conditions. *J. Mol. Biol.* **239**, 366-370.

Wu, H., Lin, Y., Lin, F., Makino, S., Chang, M., Lai, M. M. C. (1989). Human hepatitis D virus RNA subfragments contain an autocleavage activity. *Proc. Natl. Acad. Sci. USA* **86**, 1831-1835.

Yu, M., Ojwang, J., Yamada, O., Hampel, A., Rapapport, J., Looney, D., and Wong-Staal, F. (1993) A hairpin ribozyme inhibits expression of diverse strains of human immunodeficiency virus type 1. *Proc. Natl. Acad. Sci. USA* **90**, 6340-6344.

2. RIBOZYME ANALYSIS *IN VITRO*

2.1 Introduction

The ribozymes utilised in this study were tested *in vitro* to characterise elements of the ribozyme-mediated cleavage reaction which may affect the activity observed *in vivo*, with the aim of generating improved designs. Kinetic parameters were measured to define the rate-limiting step of the reaction, and to compare the activity of these ribozymes with those established earlier in the literature. In addition, the ribozymes were tested in the presence of nuclear extracts to determine if nuclear proteins, which are associated with RNA *in vivo*, alter the kinetic parameters obtained *in vitro*.

2.1.1 Minimal kinetic mechanism

Despite the versatility of the Haseloff and Gerlach design (Figure 1.1c), *in vitro* analysis of ribozyme function reveals variable levels of activity, including slow multiple turnover rates, and incomplete cleavage of target molecules. The steady state, multiple turnover reaction rate, k_{cat}, varies 100 fold among tested catalyst/substrate pairs (Fedor and Uhlenbeck, 1992; Hertel *et al.*, 1994). The K_M for different intermolecular reactions vary 1000 fold, such that equal molar concentrations of substrate and ribozyme result in one half of the substrate being cleaved in times ranging from less than one minute, to greater than five hours (Ruffner *et al.*, 1989).

The minimal kinetic mechanism for intermolecular hammerhead catalysis involves substrate annealing (k_1), cleavage (k_2), and product dissociation (Figure 2.1). A detailed determination of the individual rate constants for a well characterised, 38 nt ribozyme (Figure 2.1b) targeted to a 17 nt target through 8 base pairs on each guide arm is presented in Figure 2.1c (Hertel, *et al.*, 1994).

The chemical cleavage reaction rate, k_2, was determined for several hammerhead ribozymes and their respective targets, and in most cases is in the range of 1-2 min^{-1}. Values of k_{cat} in the range of 1 min^{-1}, and K_M values in the nanomolar range, are characteristic of most RNA endonucleases, including group I intervening sequences,

hairpin ribozymes, and RNase P (Fedor and Uhlenbeck, 1992). Values of k_{cat} less than k_2 imply another step in the reaction outlined is rate-limiting. Factors affecting catalytic activity could include non-conserved sequences in the helix regions imparting subtle changes on the environment in the region of the cleavage domain (affecting k_2), the rate of substrate association (k_1), or the rate of product dissociation (k_3, k_4, k_5, and k_6).

2.1.2 Non-conserved sequences can alter k_2

Rates of 1 min^{-1} for hammerheads previously analysed, despite differences in the non-conserved helix I and III regions, argue against these sequences having a significant effect on the chemical cleavage rate (Fedor and Uhlenbeck, 1990). Altering, or removing the non-conserved sequences, or the tetraloop of stem/loop II have a minimal effect on the cleavage rate, providing helix stability is maintained. However, the semi-conserved purine:pyrimidine base pair at positions 10.1 and 11.1 shows a strong preference for G:C, presumably due to a nearest neighbor effect on the highly conserved single stranded bases at positions 9 and 12 (Tuschl and Eckstein, 1993; Long and Uhlenbeck, 1994). Altering these sequences results in decreased catalytic efficiency.

2.1.3 Non-conserved sequences affect k_1

The formation of intermolecular helices (the association rate constant, k_1) is expected to be relatively fast between the catalyst and the substrate under saturating conditions. Early studies estimated substrate association to be less than one second, based on the rate of formation of RNA duplexes of similar length and strand concentrations (Ruffner, *et al.*, 1989). Subsequent, more detailed analysis demonstrated that trace concentrations of substrate were saturated with excess ribozyme within 20 seconds of mixing, and determined k_1 values to be at least ten fold higher than (k_2 + k_{-1}) values for ribozyme/substrate pairs with greater than five nucleotides duplexed in helices I and III (Figure 2.1c) (Fedor and Uhlenbeck, 1992; Hertel *et al.*, 1994).

However, non-reactive intramolecular secondary structures in the substrate or ribozyme, substrate or ribozyme aggregates, and the effects imparted by distal,

non-complementary sequences flanking the hammerhead structure can retard formation of the intermolecular secondary structure required for cleavage, and have a significant effect on the overall rate of reaction (Taylor and Rossi, 1991; Denman, 1993; Bertrand, *et al.*, 1993). Substrates shown to form aggregates, as determined by non-denaturing gel electrophoresis, are virtually non-reactive, and have high K_M values (Fedor and Unlenbeck, 1990). Consequently, target (or ribozyme) concentrations required for saturating levels and maximum cleavage rates may be difficult, or impossible to obtain.

The rate-limiting step under these non-saturating conditions shifts from chemical cleavage to substrate association (k_1). The rate constant becomes dependent on the rate of helix-coil transition since inactive structures must melt before active complexes can be formed. Helix-coil transitions which are concentration independent are the result of intramolecular structures (Ruffner, *et al.*, 1989) whereas concentration dependent structures, which are rapidly resolved (relative to the dissociation constant of the particular structure) upon dilution, are the result of intermolecular interactions (*i. e.*, aggregates) (Fedor and Uhlenbeck, 1990).

2.1.4 Non-conserved sequences affect product dissociation

Under saturated conditions, ribozymes with five nucleotides or less, base paired in each of helices I and III demonstrate overall reaction rates equivalent to the k_2 values, such that the cleavage step is rate-limiting. However, with increasing helix length, and/or stability, product dissociation becomes rate-limiting as a function of the free energy required to melt the duplex. Multiple turnover kinetic experiments with excess substrate to ribozyme are characterised by initial bursts of product formation, followed by a reduction in the steady state reaction rate. The amount of product produced during the initial activity burst is stoichiometric with ribozyme concentrations, and is the result of free ribozyme binding to free target after initiating the reaction. The subsequent reduced steady state is dependent on the rate of product dissociation, since the products must dissociate before the ribozyme can anneal with another substrate. Longer or more stable helices increase this effect (Fedor and Uhlenbeck, 1990; 1992).

2.1.5 Non-conserved sequences affect ribozyme specificity

The guide arms flanking the catalytic domain of a hammerhead ribozyme determine the specificity of the reaction: approximately 15 nt of complementary sequence is required to uniquely identify an mRNA in a higher eukaryote. Increasing the length of duplex formation between a ribozyme and a target can decrease the specificity, if the ribozyme binds to a mismatched target with free energy greater than that required for cleavage. Herschlag (1991) presents an intriguing theoretical argument on this issue, and experimental evidence was presented for the well characterised hammerhead, HH16 (Figure 2.1b). HH16 does not efficiently differentiate between a target annealed through 13 nucleotides of duplex, and the same target with a single nucleotide mismatch seven nucleotides 5' of the cleavage site (G16.6U), at 25°C (Tsuchihashi, *et al.*, 1993). However, another ribozyme is reported to efficiently differentiate between homologous targets sharing 18 out of 22 nucleotides in the duplex region (Bennett and Cullimore, 1992), at 50°C, but the increased temperature probably reduces the free energy barrier of the mismatched ES complex sufficiently to favour substrate dissociation over cleavage. Bertrand *et al.*, (1994) performed a detailed analysis of ribozyme activity *in vitro* with respect to duplex length and specificity. The authors report a maximal k_{cat}/K_M with up to 7 bp of duplex per guide arm, with specificty determined by 12 bp of total duplex, at 37°C.

2.1.6 Hammerhead ribozyme catalytic activity is enhanced by proteins

When the recognition sequence of a ribozyme is extended beyond a certain length, turnover is slowed by product dissociation, and specificity is decreased if binding to mismatched targets is strong enough to enable cleavage. The approximately 15 nt required to identify a unique mRNA in a cell binds with sufficient free energy to slow product release and limit specificity. However, several single-stranded RNA-binding proteins enhance kinetic rate constants and specificity by either RNA chaperone, or matchmaker activities (Portman and Dreyfuss, 1994).

Matchmakers are proteins which bind specifically, or non-specifically to RNA. They are believed to function via protein-protein interactions which bring two ribonucleprotein complexes together (either intra- or intermolecularly), thereby increasing

the localised concentration of RNA, and prolonging the necessary RNA-RNA associations for the formation of stable base pair interactions and annealing. Matchmakers are characterised by flexible, repeating domains (glycine-rich domains, for example) for stabilising the transient complex formed when two ribonucleoproteins collide, and co-operative binding to facilitate protein-protein interaction. The heterogeneous nuclear ribonucleoprotein (hnRNP) A1 is proposed to operate in this manner (Pontius, 1993; Portman and Dreyfuss, 1994).

RNA chaperones, on the other hand, are believed to modulate RNA conformation directly by maintaining the unstructured conformation of nascent polynucleotides to prevent misfolding and inappropriate interactions. Chaperones are also believed to have unwinding characteristics, whereby the free energy required to disrupt inappropriate, or transient structures is reduced. RNA annealing is stimulated both by increasing the likelihood that collisions will be productive, and by reducing the amount of structure which must be undone during the "zipping" process. Chaperones may also reduce intermolecular repulsion by shielding the charge of the phosphate backbone.

The HIV nucleocapsid protein (NCp7) (Tsuchihashi, *et al.*, 1993; Muller, *et al.* 1994), *E. coli* ribosomal protein S12 (Coetzee, *et al.*, 1994), and hnRNP A1 (Herschlag, *et al.*, 1994; Bertrand and Rossi, 1994), affect both helix associations and helix dissociation, increasing both the rate of substrate association, and product dissociation. Bovine serum albumin, gene 32 of T4 bacteriophage (gp32), and *E. coli* single-stranded binding protein have no effect.

Facilitation by NCp7, the carboxy terminal domain (CTD) of hnRNP A1, and S12 was tested on the well characterised ribozyme, HH16. The enhancement of substrate annealing, product dissociation, and substrate discrimination by NCp7 was analysed in detail, and compared to the results reported for the same variables in the absence of protein (Tsuchihashi, *et al.*, 1993; Herschlag, *et al.*, 1994). NCp7 at concentrations sufficient to coat the RNA increased ribozyme/substrate annealing under subsaturating conditions 20 fold, but had no effect in saturating conditions, and no effect on k_{cat} if the ribozyme and substrate were pre-annealed. Thus NCp7 enhances the apparent second order rate constant k_{cat}/K_M (subsaturating conditions), but does not enhance the chemical

cleavage rate (k_2). The addition of CTD hnRNP A1, or S12 increased the reaction rates 20 fold, and 4-10 fold respectively. Rate constants (k_{cat}) for dissociation of P1 and P2 of 0.2 - 0.3 min^{-1} in the presence of 400-1600 nM NCp7 were similar to k_2 values in the absence of proteins (0.3 min^{-1}), an increase of 20-30 fold over the multiple turnover rate in the absence of NCp7. This increase therefore represents a shift of the rate-limiting step from product dissociation to chemical cleavage, and not necessarily the maximal enhancement by NCp7. The overall reaction rate was enhanced 5-10 fold by the carboxy terminal domain of hnRNP A1, and 2 fold by S12. NCp7 also resolves misfolded structures which are "trapped" in inactive confirmations, allowing the reaction to go to completion. NCp7 imparts these affects by binding and destabilising the duplex - effectively lowering the activation barrier for dissociation (chaperone functions).

HH16 does not differentiate between closely related substrates since the overall free energy of binding is greater than the free energy of cleavage. Addition of NCp7, under subsaturating conditions resulted in dramatic changes in reactivity between a 13 mer target, and 13 mer target with a single mismatch: cleavage of the 13 mer was increased while the cleavage of the mutant was decreased, with 20 fold discrimination. The effects of hnRNP A1 and S12 on HH16 specifity were not reported.

The above studies were carried out on a single hammerhead complex (HH16), which involved a minimal substrate and ribozyme. The kinetic behaviour of more complex ribozymes and substrates, in which the RNA sequences of both molecules extend beyond the duplex regions were reported for NCp7 (Bertrand and Rossi, 1994; and Muller *et al.*, 1994), and hnRNP A1 (Bertrand and Rossi, 1994). The results of Muller and colleagues, like those of Herschlag and co-workers, showed that NCp7 enhanced cleavage activity under subsaturating conditions: cleavage proceded up to 43% whereas without NCp7 cleavage was less than 2%. Bertrand and Rossi, however, report that neither NCp7, nor hnRNP A1, increased the reaction rate under subsaturating, single turnover conditions, relative to a bovine serum albumin control. Indeed, NCp7, but not hnRNP A1, inhibited substrate association for individual duplexes greater than 8 nucleotides in length. Under multiple turnover conditions, NCp7 and hnRNP A1 increased product dissociation in reactions with 6 or 7 nt duplexed (and to a lesser extent, 8 nt for NCp7), but had no effect

on longer duplexes. No other report has analysed the effect of proteins on duplex lengths greater than 8 nucleotides per helix.

Reports concur that k_{cat} of reactions with duplexes of 5 or less nucleotides are not enhanced, and even slightly reduced by NCp7 (Bertrand and Rossi report the same effect for hnRNP A1). It is expected that these reactions would not be stimulated, since product dissociation is not rate-limiting for helices of this size (Fedor and Uhlenbeck, 1990; 1992). The inhibitory effect of NCp7 could be explained if the free energy barrier of substrate dissociation is reduced sufficiently such that k_{-1} is more thermodynamically favourable than k_2.

For full length transcripts corresponding to naturally occurring mRNA (950 nt) under non-saturating conditions, cleavage was 10 fold less efficient than for a truncated transcript (60 nt) with an identical target sequence. This was attributed to increased intramolecular folding in the longer transcript (Bertrand, *et al.*, 1994). Addition of either NCp7 or hnRNP A1, increased the rate of cleavage 4 fold - indicating that substrate association is enhanced for mRNA length transcript (Bertrand and Rossi, 1994).

The genes for three ribozymes designed to cleave at specific sites in the luciferase transcript resulting from the luciferase gene harboured by pPCV701-*lux*-FP1, and the corresponding controls, were constructed in conjunction with Dr. John Rossi (section 1.7). Each gene was inserted into two different vectors suitable for *in vitro* transcription in order synthesise ribozyme and control RNA. Likewise, suitable DNA fragments were isolated from pPCV701-*lux*-FP1, and subcloned into pBluescript KS+ for the *in vitro* transcription of luciferase target RNA. The activity of each ribozyme, and the inactivity of each control, was tested in detail against one of the substrate transcripts, with respect to optimal temperature, and catalytic rate relative to time. Kinetic parameters of the active ribozymes were determined for single turnover reactions as a crude estimation of the activity which might be expected *in vivo*. Since RNA inside a cell is closely associated with proteins, (Dreyfuss, *et al.*, 1993), ribozyme activity was also tested in the presence of HeLa cell nuclear extracts.

2.2 Materials and Methods

2.2.1 Suppliers, plasmids, and common techniques:

Restriction endonucleases, and DNA modifying enzymes were obtained from Boehringer Mannheim (Laval, Quebec), or Gibco/BRL (Burlington, Ontario), unless otherwise stated. Nucleotides, unless supplied with a kit, were obtained from Boehringer Mannheim. Chemicals were obtained from Sigma (St. Louis, Missouri), BDH Inc. (Toronto, Ontario), or Fisher Scientific (Ottawa, Ontario). Bacterial media preparations were obtained from Gibco/BRL. pBluescript KS+ was obtained from Stratagene (La Jolla, California). PCFOLD version 4, and HYPERBOLIC REGRESSION ANALYSIS were obtained by anonymous file transfer protocol (ftp) from the Indiania State University Biology Server (ftp.bio.indiana.edu). NEWTEMP was supplied with PCFOLD. MOLECULE was obtained from the European Molecular Biology Laboratory (EMBL), via the Genome Database Organisation (http\\www.gdb.org\).

E. coli strain DH5α (*sup*E44 Δ*lac*U169 (ϕ80 Δ*lac*ZM15) *hsd*R17 *rec*A1 *end*A1 *gyr*A96 *thi-rel*A1) was used for all plasmid manipulation. Media for DH5α was either Luria-Bertani (LB) media (10 g/L tryptone, 5 g/L yeast extract, 10 g/L NaCl), or 2xYT media (16 g/L tryptone, 10 g/L yeast extract, 5 g/L NaCl). Where appropriate, media was supplemented with ampicillin (Ap), 100mg/L. Solid media contained 1.5% agar.

Techniques common to molecular biology, unless otherwise stated, were carried out as described in Sambrook *et al.*, (1992), or Ausubel *et al.*, (editors, 1994). *E. coli* transformations were performed as described by Chung, *et al.*, (1989), or by electroporation in a Bio-Rad (Hercules, California) Gene Pulser, as described by the manufacturer.

2.2.2 Oligonucleotide preparation:

Oligonucleotides were synthesised on an Applied Biosystems (ABI, Foster City, California) 380B DNA synthesiser by Anna Szenthe, deprotected, and desalted as described by the equipment manufacturer. If further purification was required (*i. e.*, if pellets appeared yellow in colour), oligonucleotides were passed through a G-50

Sephadex NAP-10 column (Pharmacia, Uppsala, Sweden), followed by ethanol precipitation. Deprotected oligonucleotides were resuspended in 50 µl double distilled H_2O, and the concentration was determined by spectrophotometry at 260 nM, assuming an extinction coefficient of 1 O.D. = 33 µg/ml single stranded DNA.

Full length oligonucleotides for gene synthesis were resolved in, and isolated from 0.75 mm 15% denaturing polyacrylamide gels (25 ml of 15% acrylamide:bis-acrylamide (19:1), 8 M urea, 1 x TBE buffer, and polymerised with 150 µl of 10% ammonium persulfate and 10 µl of TEMED). Electrophoresis was carried out in 1 x TBE buffer with a constant voltage of 400 volts for 1 hour, with 10 µg of oligonucleotide per well. Bands were detected by EtBr staining and UV illumination, or UV shadowing, and subsequently cut from the gel with a razor blade. Oligonucleotides were eluted from the excised polyacrylamide slabs into polyacrylamide gel electrophoresis elution buffer (0.1% SDS, 0.5 M ammonium acetate, 10 mM $MgCl_2$) for a minimum of two hours. Eluted oligonucleotides were precipitated and resuspended in ddH_2O.

2.2.3 Ribozyme gene synthesis

Each synthetic ribozyme gene was constructed from two oligonucleotides with 10 or 11 complementary nucleotides at the 3' ends, and BamHI restriction sites at the 5' ends. Ribozyme *ribo1* was constructed from oligos Ribo1-A, and Ribo1-B; control ribozyme *ribo1C* was constructed from oligos Ribo1-A, and Ribo1-BC; *ribo4* was constructed from oligos Ribo4-A, and Ribo4-B; and *ribo4C* was constructed from oligos Ribo4-A, and Ribo4-BC. The oligonucleotide sequences, and the respective complementary 3' ends are given below.

```
Ribo1-A  5'-CCGGATCCAACCTTCACTGATGAGTCCGTGAGG-3'
Ribo1-B                              3'-CAGGCACTCCTGCTTTGCGAAACGGCCTAGGCC-5'
Ribo1-BC                             3'-CAGGCACTCCTGCTATGCGAAACGGCCTAGGCC-5'

Ribo4-A  5'-CCGGATCCAAGCC
           -ACCTGATGAGTCCGTGAGGACGAAACCTTCAC-3'
Ribo4-B                            3'-CTTTGGAAGTGACTACTCAGGCACTCCTGCTTT-
                                                          GCGAAACCTAGGCC-5'
Ribo4-BC                           3'-CTATGGAAGTGACTACTCAGGCACTCCTGCTAT-
                                                          GCGAAACCTAGGCC-5'
```

Oligonucleotide pairs were subjected to eight rounds of annealing and elongation with Taq DNA polymerase (Perkin Elmer Cetus, BRL, or Boehringer Mannheim) in a Perkin Elmer Cetus (Norwalk, Conneticut) 480 Thermal Cycler: 4 μg of each oligo were combined in a 100 μl final volume of 100 μM of each of the four deoxynucleotide triphosphates, 1x commercial Taq polymerase buffer, 25 mM Mg^{2+}, and 2.5 units of Taq DNA polymerase . The cycling program consisted of an initial denaturation at 94°C for 5 minutes, 8 cycles of 1) denaturation at 94°C for 30 second , 2) annealling at 45°C for 60 second, and 3) extension at 72°C for 60 second, followed by a final extension at 72°C for 7 minutes.

Double stranded DNA products were isolated on a 15% (w/v) non-denaturing polyacrylamide gel (15% acrylamide:*bis*-acrylamide 29:1) and eluted from the gel pieces as described for oligonucleotides. Isolated dsDNA was quantitated and digested with BamHI in preparation for subcloning. Alternatively, dsPCR products were precipitated, resuspended, and digested directly with BamHI for subcloning without prior gel purification. BamHI-digested synthetic genes were gel purified as described to remove the 5' and 3' BamHI digestion products.

2.2.4 Construction of ribozyme vectors for in vitro transcription

Vector p*ribo*BS was obtained from Dr. Alan Escher. The *riboC* synthetic gene fragment was obtained by digestion of pPCV701FP$_1$R$_1$C (obtained from Dr. Alan Escher) with BamHI, followed by gel purification of the 50 nt fragment. The *riboC* gene was identified as serendipitous A to T transversion at position 14 (Figure 1.1c) in the *ribo* sequence.

For construction of p*riboC*BS, p*ribo1*BS, p*ribo1*CBS, p*ribo4*BS, and p*ribo4C*BS, a large molar excess of each synthetic ribozyme, and ribozyme control gene was ligated with pBluescript KS+ linearised with BamHI, and dephosphorylated with calf intestinal alkaline phosphotase (CIP) to prevent self ligation. Ligation products were transformed into *E. coli* strain DH5α. Colonies harbouring recombinant vectors were selected by alpha-complementation, and plasmids were isolated by alkaline lysis miniprep. The

number of ribozyme inserts was detemined by digestion with PvuII, and plasmids carrying a single insert were sequenced by either the Sequenase sequencing procedure (United States Biochemical (USB), Cleveland, Ohio) using ^{35}S as label, or by Taq cycle sequencing using ABI flourescent dye primers or dye terminators, according to the respective manufacturer's instructions. Plasmid isolations for Taq cycle sequencing with flourescent labels were carried out as described in the manual supplied with the sequencing kit (ABI part number 901497). Clones with the correct sequence, and an orientation such that transcription from the T3 promoter would produce a functional ribozyme were selected for large scale plasmid isolations (Figure 2.2).

Ribozyme, and ribozyme control genes were inserted into the vector pCTDel by a similar procedure (Materials and Methods, Chapter 3).

Ribozyme and control genes inserted into pBluescript KS+ are referred to collectively as the BS series, and individually are p*ribo*BS, p*ribo*CBS, p*ribo1*BS, p*ribo1C*BS, p*ribo4*BS, and p*ribo4C*BS. Likewise, ribozymes and controls inserted into pCTDel are referred to collectively as the CT series, and individually are pCT*ribo*, pCT*riboC*, pCT*ribo1*, pCT*ribo1C*, pCT*ribo4*, and pCT*ribo4C*.

2.2.5 Construction of Target vectors for <u>in vitro</u> transctription

Plasmid pluxtarBS was constructed for *in vitro* transcription of a truncated *lux* RNA target. The plant cloning vector pPCV701-*lux*-FP1 was transformed into the *E. coli* strain GM48 (*leu, thi, lac*Y, *gal*K, *gal*T, *ara, ton*A, *tsx, dam, dcm, sup*E-44), and isolated by large scale alkaline lysis/PEG precipitation in order to prevent *dam* methylation at ClaI sites. A 237 nt ClaI-PstI fragment, corresponding to 221 nt of *lux* structural gene and 16 nt of untranslated *mas* P1 promoter sequence, was isolated from an 8% non-denaturing polyacrylamide gel by elution into PAGE elution buffer, and ligated into dephosphorylated pBluescript KS+ digested with ClaI and PstI (Figure 2.3).

Recombinant plasmids were detected by β-galactosidase alpha complementation, and PvuII was used to identify plasmids carrying the expected size insert. Based on insert size, one colony was selected for large scale plasmid isolation, and sequenced. The

orientation of the *lux* insert was such that transcription with T3 RNA polymerase would produce a coding strand luciferase transcript (target for *in vitro* cleavage assays).

A second vector, pP1luxBS, was constructed for *in vitro* transcription of a truncated *lux* RNA target, consisting of 221 nt of luciferase coding sequence, and 145 nt of P1 promoter sequence upstream of the *lux* ATG sequence (61 nt upstream, and 84 nt downstream of the P1 transcription initiation site). A 1190 nt fragment consisting of 145 nt of the P1 promoter fused to the *luxA* structural gene was isolated from pPCV701-*lux*-FP1 by PCR amplification: 64 pmoles of gel purified 5' sense strand primer (P1start = CGT CAC GTC TTG CGC ATC G) was mixed with 50 pmoles of 3' antisense strand primer (*luxA*end = GGC ATC ACA TCA GAC TGG AAT AGC) and 10 ng of pPCV701-*lux*-FP1 in a standard 50 µl PCR reaction with 30 cycles of 94°C denaturation for 45 sec, annealing at 55°C for 1 minute, and elongation at 72°C for 2 minutes.

The PCR product was extracted with phenol/chloroform, precipitated, and resuspended in 30 µl of ddH_2O. A 1.67 µg aliquot of the PCR product was blunt ended by treatment with 1 unit of T4 DNA polymerase, and digested with PstI. 30 ng of the PstI digestion products were ligated with 100 ng of pBluescript KS+ digested with EcoRV and PstI, and recombinant vectors were selected by alpha-complementation. Isolated plasmids were digested with PvuII to select for inserts of the correct size, and several potential clones were sequenced. One clone was selected for large scale plasmid purification. The orientation of the insert was such that transcription with T3 RNA polymerase would produce a coding strand luciferase transcript (Figure 2.3).

pP1lux125 was constructed in order to remove potential secondary structure surrounding the ribo cleavage site of the truncated *lux* fragments in pluxtarBS and pP1luxBS (refer to section 2.3.1). 10 µg of pP1luxBS was digested with KpnI. The restriction enzyme was heat inactivated, and the vector precipitated with ethanol. After resuspension, the linearised plasmid was digested with HindIII, the mixture was extracted with phenol/chloroform, and precipitated. The resuspended vector was then treated with T4 DNA polymerase to produce blunt ends, and circularised by ligation (Figure 2.3). Isolated recombinant plasmids were digested with XhoI, which is in the deleted region such that correct plasmids would remain circular. Appropriate plasmids were digested

with BamHI and PvuII to accurately identify clones with the 30 nt deletion. Several clones were sequenced and one was selected for large scale amplification.

2.2.6 *In vitro transcription and purification of transcripts*

The ribozymes riboBS, ribo1BS, and ribo4BS were synthesised by *in vitro* transcription with T3 RNA polymerase from the vectors p*ribo*BS, p*ribo1*BS, and p*ribo4*BS linearised at the XbaI restriction endonuclease site of the pBluescript KS+ multiple cloning site. The corresponding control ribozymes were likewise transcribed from the respectiv control vectors. The ribozymes CTribo, CTribo1, and CTribo4 were synthesised by *in vitro* transcription with T7 RNA polymerase from the vectors pCT*ribo*, pCT*ribo1*, and pCT*ribo4* linearised at the EcoRI site in the experimental gene of pCTDel. The corresponding control ribozymes were likewise transcribed from the respective control vectors. The substrates for cleavage, luxtar, P1lux, and P1lux125, were transcribed with T3 RNA polymerase from their respective plasmid linearised with XbaI. All vectors were tested for linearity by agarose gel electrophoresis.

The *in vitro* transcription reactions were carried out in one of two ways: 1) a modification of standard transcription mixtures consisting typically of 1x commercially available buffer (Boehringer Mannheim: 40 mM Tris-HCl, pH 8, 6 mM $MgCl_2$, 2 mM spermidine, 10 mM DTT; Promega (Madison, Wisconsin): 40 mM Tris-HCl, pH 7.9, 6 mM $MgCl_2$, 2 mM spermidine, 10 mM NaCl), 0.5 mM each of ATP, CTP, GTP, and UTP, 10 mM DTT (if not supplied in the reaction buffer), 20 to 40 units of T3 or T7 RNA polymerase (Promega, or Boehringer Mannheim), 3 - 5 μCi [α-^{32}P]CTP (Amersham, Oakville, Ontario), and 1 μg of linearised template in a 20 μl volume, at 37°C for 1 to 2 hours, or 2) by using either a T3 or T7 Ambion (Austin, Texas) MEGAscript™ *in vitro* Transcription Kit , according to the manufacturer's instructions. In brief, 2 μg of linear plasmid was combined with 2 μl each of ATP, CTP, GTP, and UTP solutions (7.5 mM final concentration each), 2 μl of 10x reaction mix, 2 μl of enzyme mixture and 20-40 μCi of [α-^{32}P]CTP, in a final volume of 20 μl. Reactions proceeded at 37°C for a minimum of 3 hours. Following transcription, plasmid DNA was digested with 1 unit of RNase free DNase (Promega) for 15 minutes at 37°C. An equal volume of formamide loading

solution (80% formamide, 10 mM EDTA, 1 mg/ml xylene cyanol FF, 1 mg/ml bromophenol blue) was added, and 1 µl of each reaction was used for determining label incorporation by high acid precipitation of elongated transcripts in conjunction with liquid scintillation counting.

Transcripts were denatured at 95°C for 2 minutes, placed on ice, and loaded on an 8 M urea, 4% polyacrylamide gel (19:1) and electrophoresed for 1 hour at 400 volts. Full length transcripts were isolated by exposing the gels to Kodak (Rochester, New York) X-Omat XK-1 film for 10 minutes followed by developing in a Kodak M35A X-Omat processor, and excising the gel slices corresponding to the bands on the autoradiogram. RNA was eluted from the gels into PAGE elution buffer (without Mg^{2+}), either at room temperature or at 37°C for 2 hours to overnight. Eluted transcripts were precipitated with ethanol and resuspended in RNase free 50 mM Tris-HCl, pH 8. *In vitro* cleavage reactions carried out with gel purified transcripts gave superior results to those without gel purification.

2.2.7 *In vitro cleavage reactions*

Ribozyme-mediated cleavage of luxtar and P1lux125 RNA was analysed by mixing appropriate amounts of ribozyme and target RNA to obtain the desired ratios. These ratios were based on label incorporation (*i. e.*, cpm), rather than molarity. Solutions containing both RNAs were heated to 90°C, and cooled quickly on ice. Reactions were initiated by the addition of $MgCl_2$ to a final concentration of 20 mM, and incubated at various temperatures for various lengths of time (refer to results). Reactions were terminated by the addition of formamide loading solution containing 50 mM EDTA. Mixtures were denatured at 90°C, placed on ice, and resolved in 6% denaturing polyacrylamide gels.

Reactions with P1lux were done with more precision, in that ribozyme and substrate molar concentrations were determined. With the exception of the deviations listed below, gel purified transcripts were resuspended in 50 mM Tris-HCl, pH 8, heated to 90°C, cooled rapidly on ice, and prewarmed to the desired reaction temperature. A 1/10 volume of 200 mM $MgCl_2$ (20 mM final) was added to separate solutions of

ribozyme and substrate, and reactions were initiated by mixing the solutions 1:1 (vol:vol). All reactions, except those resolved on non-denaturing gels, were quenched by the addition of an equal volume of formamide loading solution (80% formamide, 1 mg/ml xylene cyanol FF, 1 mg/ml bromophenol blue) containing 50 mM EDTA. Prior to gel electrophoresis, all samples were heated to 90°C, and placed on ice. Electrophoresis was performed with 0.75 mm wide 6% denaturing polyacrylamide gels at 400-450 volts for 1 hour, or until the bromophenol blue had just run off the gel. In most cases, the gels were dried, and autoradiography was performed without intensifying screens.

P1lux and CT ribozyme transcripts were resuspended in 18 µl of 50 mM Tris-HCl, pH 8, and denatured at 90°C for two minutes, for the experiment described in Figure 2.5. Samples were cooled to 37°C and 2 µl of 200 mM $MgCl_2$ was added. Transcript concentrations were determined by scintillation counting, and diluted with 50 mM Tris-HCl, pH 8, 20 mM $MgCl_2$, to a final concentration of 50 nM for P1lux and 20 nM for each CT ribozyme. Dilutions were confirmed by repeating the scintillation counting. Each ribozyme was mixed 1:1 (vol:vol) with substrate to give a final concentration of 25 nM target, and 10 nM ribozyme in a 10 µl reaction. 5µl of each independent transcript was diluted 1/2, and used as T=0 control. Samples were incubated at 37°C for 2 hours and quenched. Autoradiography was for 4 hours at -70°C with an intensifying screen.

2.2.8 Temperature optimum

For the results presented in Figure 2.6, the concentration of P1lux RNA was adjusted to 60 nM, and each ribozyme was adjusted to 20 nM in 50 mM Tris-HCl, pH 8. Equal volumes of each ribozyme and P1lux target RNA were mixed and incubated for 2 hours at 32°C, 37°C, 42°C, 47°C and 53°C. Ribozymes and target were also incubated separately for two hours at each temperature to distinguish between the loss of substrate resulting from ribozyme activity, and non-specific degradation (data not shown). Resulting bands were quantified by densitometry. The percent cleavage was calculated by using the total amount of detectable substrate (uncleaved substrate plus 5' product, with densities standardised against transcript size) as the denominator, and the density of 5' product (standardised against transcript size) as the numerator.

2.2.9 Time course of cleavage reaction

For the experiment described in Figure 2.7, P1lux and CTribo1 RNA were resuspended to give 66 nM, and 22 nM concentrations, respectively. After addition of Mg^{2+}, 2.5 µl of each was removed for T=0 samples, and 35 µl of each ribozyme was mixed with 35 µl of P1lux target to initiate the reaction. 5 µl aliquots were removed at times indicated in Figure 2.6, and quenched. Densitometry was performed on the resulting autoradiogram. Similar procedures were used with CTribo, ribo1BS, and ribo4BS.

2.2.10 Determination of kinetic parameters

For ribozyme kinetic experiments, substrates and ribozymes were made up to concentrations 2.2 times that of the desired final concentration, denatured, supplemented with a 1/10 volume of 200 mM $MgCl_2$, and prewarmed to 47°C. Reactions were initiated by mixing equal volumes of the ribozyme and substrate solutions. Alternatively, for reactions initiated by Mg^{2+} (CTribo1 and CTribo4, see Results), ribozymes and substrate were mixed and prewarmed to 47°C at 1.1 times the desired final concentration, followed by the addition of 1/10 volume of 200 mM $MgCl_2$. For ribozyme excess, single turnover kinetic analysis of ribo1BS and ribo4BS, final P1lux concentrations were either 5 nM or 10 nM, and ribozyme concentrations ranged from 5 nM to 100 nM. For ribozyme excess, single turnover kinetic analysis of CTribo1 and CTribo4, final P1lux concentration was 5 nM, and ribozyme concentrations ranged from 5 nM to 100 nM. Aliquots of ribo1BS and CTribo1 reactions were taken at T=0, 5, 10, 15, 20, and 30 minutes, and at T = 0, 10, 20, 30, 45, and 60, minutes for ribo4BS and CTribo4. Reaction velocity (v) was determined by measuring product formation relative to substrate concentration by densitometry. For substrate excess, multiple turnover kinetics of ribo1, reactions were carried out as above using 5 nM ribo1BS and P1lux ranging from 5 nM to 200 nM. Aliquots of each were removed at T = 0, 10, 20, 30, and 60 minutes. Reaction velocity (v) was determined by measuring 3' product formation relative to ribozyme concentration by densitometry.

Kinetic parameters, V_{max} and K_M, were calculated with HYPERBOLIC REGRESSION ANALYSIS, version 1.02 (Copyright J. S. Easterby, 1993), by entering [r] (ribozyme excess), or [s] (substrate excess) and v values obtained from kinetic

experiments, according to the instructions supplied with the program. The k_{cat}/K_M values were either calculated from V_{max} and K_M values, or were obtained directly from the experimental results with the equation

$$-\ln(\text{FracS})/t = k_{cat}/K_M[R]$$

where ln(FracS) is the natural log of the fraction of substrate remaining, t is time in minutes, and [R] is the ribozyme concentration in nM.

2.2.11 Non-denaturing gel electrophoresis

Non-denaturing gels were run with a 50 mM Tris-acetate (pH 8.0), 20 mM magnesium acetate electrophoresis buffer to mimic conditions used for *in vitro* cleavage reactions. 6% acrylamide solutions (19:1) were prepared with the same buffer. Independent ribozyme and substrate solutions were pre-incubated at 47°C, a 1/10 volume of 200 mM $MgCl_2$ was added, and incubate at 47°C for an additional 5 minutes before mixing ribozymes and substrate. Ribozyme and substrates were also run independently. The final P1lux concentrations was 10 nM, and ribozyme concentrations ranged from 5 nM to 100 nM. Solutions were incubated at 47°C for 30 minutes before adding EDTA and dye loading solution (0.25% bromophenol blue, 0.25% xylene cyanol FF, 30% glycerol in water), and placing on ice. Samples were run into the gel at room temperature at 100 volts (the gel did not heat), and then transferred to 4°C and run for 6-8 hours at 80-100 volts.

2.2.12 Cleavage of a full length lux transcript in vitro

For the *in vitro* synthesis of a full length *lux* transcript, plasmid pLx709-*fab*2 was obtained from Dr. Alan Escher (Escher, *et al.*, 1989). pLx709-*fab*2 contains a *lux*A and *lux*B fusion gene downstream of a ϕ10 T7 promoter in pT7/T3-19. *In vitro* transcription was performed with an Ambion T7 MEGAscript™ *in vitro* Transcription Kit, as previously described, using 1 µg of pLx709-*fab*2 linearised with BamHI as template. Due to the size of the transcript (2.3 kb), polyacrylamide gel purification was not carried out. Cleavage reactions were performed for 2 hours at 47°C, in 50 mM Tris-HCl, pH 8.0, 20 mM $MgCl_2$, as previously described (section 2.2.7). The concentration of full length *lux*

transcript was10 nM, and ribozymes CTribo1, and CTribo4 were tested at concentrations of 10 nM and 100 nM each.

2.2.13 Protein facilitation of ribozyme activity

In vitro cleavage reactions were repeated in the presence of HeLa cell nuclear extracts to test for protein facilitation of ribozyme activity. HeLa cell nuclear extracts were a kind gift from Dr. Douglas Black, UCLA. Heat denatured P1lux was made up to a concentration of 10 nM in 20 mM $MgCl_2$, 140 mM KCl, 50 mM Tris-HCl, pH 8, and one of the following: 1) no protein, 2) BSA, 250 ng/µl, 3) BSA, 1000 ng/µl, 4) HeLa cell nuclear extract, 250 ng/µl, and 5) HeLa cell nuclear extract, 1000 ng/µl. Heat denatured ribozymes (riboBS, ribo1BS, and ribo1C), at final concentrations of 100 nM and 10 nM, were made up in an identical fashion. Solutions were pre-warmed to 37°C, and mixed 1:1 to initiate the reactions. Aliquots were removed at T = 0, 10, and 30 minutes (Figure 2.12), or T = 0 and 20 minutes (Figure 2.13), and quenched as previously described. Electrophoresis and autoradiography were as previously described.

2.2.14 Densitometry

Densitometry was only performed on autoradiograms produced without intensifying screens, and band densities were assumed linear for optical densities below 1.5, based on published reports (Laskey, Amersham Review #23), and an optical density standard curve obtained with Kodak X-Omat film developed in a Kodak M35A X-Omat processor (results not shown). Autoradiograms were scanned with 200 µm resolution on a Bio-Rad Model GS-670 Imaging Densitometer. Images were manipulated with Bio-Rad MOLECULAR ANALYST version 1.1 software. Bands of interest were quantitated with the Volume Analysis module of the above software, with local background subtraction. All procedures were performed as per the manufactures instructions.

2.2.15 Computer prediction of RNA secondary structures

Computer predictions of luxtar secondary structure were performed with the Dyad module of DNA STRIDER; sequences within luxtar capable of hybridising with other

luxtar molecules were predicted with the Hybrid module of DNA STRIDER. All other secondary structure predictions were performed with PCFOLD version 4 (Zuker, 1989). Energy files utilised by PCFOLD to simulate temperatures other than 37°C were created by NEWTEMP. Structures generated by PCFOLD were visualised with MOLECULE, EGA version. All programs were used according to the instructions supplied with each.

2.3 Results

2.3.1 Cleavage of three distinct targets by the BS series

Initial *in vitro* cleavage experiments were performed with the BS series of ribozymes with luxtar as the target transcript. These experiments demonstrated that ribo1BS and ribo4BS were active, and that the control ribozyme constructs were inactive under the conditions used. RiboBS, was however inactive (Figure 2.4, lanes 1-6).

Sequence analysis of luxtar in the region surrounding the riboBS cleavage site suggested stable secondary structures could form as a result of the vector construction. Specifically, the ClaI site used for insertion of the *lux* fragment placed the SalI site of the pBluescript KS+ multiple cloning site in close proximity to the SalI site at the junction of the P1 promoter and the luciferase gene (GTCGACGGTATCGATCCGTCGAC), such that either an intramolecular structure with an eight nucleotide stem and a seven nucleotide loop, or an intermolecular 23 nucleotide duplex with two single base bulges could form. Either structure was considered sufficient to prevent riboBS from accessing the cleavage site.

pP1luxBS was constructed to separate the SalI sites by approximately 135 nucleotides, and to create a vector suitable for *in vitro* transcription of a ribonuclease protection assay probe with T7 RNA polymerase. As well, transcription of pP1luxBS with T3 RNA polymerase (P1lux) more accurately mimics the mRNA produced in plants from the P1 promoter. However, riboBS was also inactive against P1lux. It was postulated that the SalI-ClaI sequence of pBluescript incorporated into riboBS could still form inactive conformations at the ClaI-SalI sequence at the cleavage site of the target transcript. The pBluescript SalI-ClaI sequences were therefore removed in the vector pP1Lux125, but RiboBS was still inactive (Figure 2.4, lanes 7-12).

The BS series of ribozymes and controls (riboBS, riboCBS, ribo1BS, ribo1CBS, ribo4BS, ribo4CBS) were tested against luxtar, P1lux, and P1lux125, at temperatures ranging from ambient, to 70°C, and for times ranging from 2 to 4 hours. As well, the ratio of ribozyme to substrate was varied to estimate the catalytic activity (Figure 2.4). Most of these experiments were subsequently repeated with greater precision, and are therefore

discussed in more detail below. However, these early experiments did establish that 1) ribo1BS and ribo4BS were active against several targets with different 5' sequences, 2) ribo1BS is active in less than stoichiometric amounts, over a 2 hour period at 50°C, and ribo4BS is less active than ribo1BS, 3) riboBS is inactive against several different targets, over a broad range of temperatures and incubation times, and 4) that the control constructs are inactive against several different targets, over a broad range of temperatures and incubation times.

2.3.2 Cleavage of P1lux by the CT series

The activity of the CT series (section 2.2.4) of ribozymes and controls (see Chapter 3 for details) was tested using a three fold molar excess of P1lux as a target, at 37°C (Figure 2.5). As expected, transcripts from pCTDel (cloning vector without a ribozyme insert), pCT*riboC*, pCT*ribo1C*, and pCT*ribo4C* do not demonstrate any cleavage activity (Figure 2.5, lanes 10, 12, 14, and 15). The transcript from pCT*ribo* is inactive (lane 11), as is the transcr from p*ribo*BS (Figure 2.4) - presumably for the same reason (see section 2.4.2). CTri is active at a less than 1:1 ratio, and CTRibo4 is less active than CTRibo1. The exten of activity for this experiment was not quantified since x-ray film does not respond in a linear fashion in the presence of scintillants (*i. e.*, intensifying screens) (Amersham, Guide to Autoradiography). Experiments were also performed at room temperature, and at 50°C, for 2 and 4 hour incubations. The results of these experiments (not shown) confirm that CTRibo1 and CTRibo4 are active under conditions described in subsequent experiments. The control ribozymes for both the BS series, and the CT series were inactive under conditions used in subsequent experiments, and were hence excluded from the experiments discussed below.

2.3.3 Temperature analysis of ribozymes.

The six ribozymes which are theoretically active (riboBS, ribo1BS, ribo4BS, CTribo, CTribo1, and CTribo4) were analysed at different temperatures to determine the optimal temperature for kinetic studies with P1lux as the target (Figure 2.6). Increasing incubation temperature resulted in increased cleavage activity, however, at temperatures

greater than 50°C, significant non-specific degradation of the target was evident. The values for percent cleavage (Figure 2.6b) are therefore over estimated at the higher temperatures as evident from CTribo (lane 32) which is represented as cleaving 46% of the substrate, even though no 5' cleavage product is visible (the "smudge" above the ribozyme (248 nt) was interpreted as a possible 3' cleavage product (252 nt), and used in the calculations), and it is unlikely that any of the ribozymes would cleave greater than stoichiometric amounts of substrate (33%). Enhancement of ribozyme activity with increasing temperature was previously observed (Taylor and Rossi, 1991; Chen, *et al.*, 1992; Bennet and Cullimore, 1992). However, a *cis*-acting ribozyme was demonstrated to perform better at 37°C than at 50°C (Ventura, *et al.*, 1993). Based on these temperature analysis results, 47°C was chosen as a temperature for subsequent experiments. Factors taken into consideration were the maximal rate of cleavage with minimal non-specific degradation. It was also desirable to use a temperature which was not excessively higher (*i. e.*, less than 2 fold) than that which ribozyme catalysed reactions would encounter *in vivo*.

2.3.4 Time course of cleavage reactions

Time course experiments were carried out to determine the linear range of the ribozyme-mediated cleavage reaction. Under the conditions used, CTribo showed no activity up to three hours of incubation time (data not shown). The reaction rate of CTribo1 was plotted as a function of 5' product formation relative to ribozyme quantity (Figure 2.7). Linear regression analysis of slopes reveals what appears to be two distinct phases in the reaction: 1) an intial rate of reaction up to T = 30 minutes, followed by 2) a slower steady state, indicating that product dissociation is rate-limiting (Taylor and Rossi, 1991; Fedor and Uhlenbeck, 1992; Bertrand, *et al.*, 1994).

Since the amount of product produced during the burst phase of the reaction is predicted to be stoichiometric with the amount of free ribozyme in a multiple turnover reaction, it is postulated that 50% of CTribo1 at the concentration utilised (10 nM), is involved in inactive higher order structures, since the slower multiple turnover rate extrapolates back to 0.5 product/ribozyme at T=0 (Fedor and Uhlenbeck 1990; Denman,

1993b). However non-denaturing gel electrophoresis suggest that CTribo1 concentrations below 50 nM do not form structures which migrate as distinct bands with lower mobility than the monomer, but an inactive conformation could migrate at the same rate, or there could be multiple inactive forms, each at concentrations below the level of detection.

Similar experiments were carried out for ribo1BS, and ribo4BS. From these results, it is concluded that under the conditions used, ribo1BS and CTribo1 catalysed reactions are linear, single turnover reactions up to at least 30 minutes, and ribo4BS catalysed reactions are linear up to 1 hour. CTribo4 reactions are assumed to be linear up to 1 hour, based on the ribo4BS results.

2.3.5 Ribozyme kinetic parameters

Kinetic parameters for the four functional ribozymes (ribo1BS, ribo4BS, CTribo1 and CTribo4) were established. Transcripts were synthesised by *in vitro* transcription with T3 or T7 MEGAscript™ *in vitro* Transcription Kits, as appropriate. The use of these kits was a great improvement over standard *in vitro* transcription reactions, yielding up to 100 µg of full length RNA per 20 µl reaction.

Burst phase kinetics (*i. e* , single turn over) with excess target were determined for ribo1BS to establish the initial rate of ribozyme activity. The ribozyme concentration was set at 5 nM, and substrate (P1lux) concentrations ranged from 5 nM to 200 nM (5, 10, 20, 30, 50, 75, 100, 150, and 200 nM). Based on time course experiments, aliquots were removed from the reaction mixture and quenched at T=0, 10, 20, 30, and 60 minutes, and kinetic parameters were established (Figure 2.8). Analysis of product formation over time indicated the reaction was still linear after 60 minutes. The observed K_M *and* V_{max} values were determined by averaging the velocity for each time point; error is stated as sample standard error (Table 2.1). The percentage of "active," monomeric substrate was not determined by non-denaturing gel electrophoresis over the entire concentration range used, however, concentration from 5 to 50 nM displayed approximately 50% of P1lux migrating as a slow band on non-denaturing gels. It was established that the ribozyme

transcripts form aggregates with increasing concentration (see below), and it is probable that P1lux does as well, thereby preventing a percentage from participating in the reaction.

Burst phase kinetics were also determined using excess ribozyme over target to eliminate the rate-limiting product dissociation effects (Fedor and Uhlenbeck, 1992). The kinetic parameters obtained therefore characterise the reaction up to, and including the formation of the EP1P2 complex (Figure 2.1). Reactions for ribo1BS and ribo4BS were both carried out with 5 nM and 10 nM substrate to test for concentration dependent changes in kinetic parameters, the ribozyme concentrations were 5, 10, 25, 50, and 100 nM. Reactions for CTribo1 and CTribo4 were carried out using 5 nM substrate (P1lux), and 5, 10, 25, 50, 75, and 100 nM of each ribozyme. Reactions the CT ribozymes were initiated in one of two ways: 1) substrate and ribozymes were preincubated with 20 mM Mg^{2+}, and the reactions were initiated by combining the two (as above), and 2) substrates and ribozymes were mixed at appropriate concentrations, incubated at 47°C for 15 minutes to allow annealing and the reactions were initiated by the addition of Mg^{2+} to 20 mM. This experiment was carried out to examine the effect of the association rate constant on the overall reaction. Reaction mixture aliquots were removed and quenched at T=0, 5, 10, 15, 20, and 30 minutes for those with ribo1BS and CTribo1, and T=0, 10, 20, 30, 45, and 60 minutes for those with ribo4BS and CTribo4. Figure 2.9 is a representation of the results obtained with ribo1BS.

With increasing concentrations of ribozyme, increasing amounts of higher order structure (and presumably inactive structure) was observed on non-denaturing gels. Figure 2.10 is a non-denaturing gel for the BS series, and similar patterns are observed on CT series non-denaturing gels (data not shown). The fastest migrating band was assumed to be monomeric (albeit, not necessarily linear) ribozyme, and the slower moving bands were assumed to be inactive aggregates. The ratios of active to inactive ribozyme were determined by densitometry (Table 2.2). The concentrations of ribozyme used to determine V_{max} and K_M values from ribozyme excess experiments (Figure 2.9) were adjusted based on these ratios.

The kinetic parameters for the four ribozymes, under the different conditions, were determined by averaging the three longest incubation times (15, 20, and 30 minutes for

ribo1BS and CTribo1; 30, 45, and 60 minutes for ribo4BS and CTribo4) (Table 2.3). The shorter time points gave poor results because the product bands were not significantly denser than the background, as determined by densitometry, making it difficult to obtain consistent density readings. The k_{cat}/K_M values reported in Table 2.3 are expressed from three different methods of determination. 1) k_{cat}/K_M (calculated) was determined from the values obtained for V_{max} and K_M, using the program HYPERBOLIC REGRESSION, which fits the velocity data (v), and the variable reactant concentration (usually [substrate], but in these experiments, [ribozyme]) to the best hyperbolic curve, to obtain a plot of (v) vs. [R]. The ribozyme concentrations used for [R] are the adjusted values of monomeric ribozyme, determined from non-denaturing gel electrophoresis (Table 2.2). 2) k_{cat}/K_M (adjusted) are the values obtained directly from the experimental results, with the adjusted concentrations of ribozyme, using the Michaelis Menton equation:

$$v = -d[S]/dt = \frac{kcat[R_o][S]}{[S]+Km} \quad . \tag{2.1}$$

where v is velocity, $-d[S]/dt$ is the loss of substrate over time, and $[R_o]$ is the total quantity of ribozyme. If $[S] << K_M$, then

$$-d[S]/dt = k_{cat}/K_M[R][S] \tag{2.2}$$

but this result also holds at any substrate concentration, where [R] is the concentration of free ribozyme (Fersht, 1977). Multiplying both sides of equation (2.2) by dt, and integrating gives

$$[S_t] = [S_o]e^{-kcat\cdot KM[R]t} \tag{2.3}$$

where $[S_o]$ is the initial amount of substrate, and $[S_t]$ is the amount of substrate remaining after time, t. Dividing through by $[S_o]$, and taking the natural logarithm of each side gives

$$\ln(\text{FracS}) = -k_{cat}/K_M[R]t \tag{2.4}$$

where (FracS) is $[S_t]/[S_o]$, and a final rearrangement gives

$$-\ln(\text{FracS})/t = k_{cat}/K_M[R] \tag{2.5}$$

such that the slope of the line obtained by plotting the natural logarithm of the fraction of substrate remaining, after time t, with various concentration of ribozyme [R], represents the k_{cat}/K_M value (Figure 2.11) (Heidenreich and Eckstein, 1992). Using this formula, the k_{cat} and K_M values can not be separated, but this important parameter is determined directly from the experimental results. *3)* k_{cat}/K_M (observed) is obtained by the same equation

(2.5), without adjustment of the ribozyme concentrations based on the non-denaturing gel electrophoresis. k_{cat}/K_M (observed) is the most appropriate method of calculation when measuring the activity of a ribozyme against a substrate, since it measures the apparent activity under the conditions used. Adjusting the concentrations based on non-denaturing gel electrophoresis has the effect of artificially reducing the K_M values from those observed, thereby increasing k_{cat}/K_M. For example, k_{cat}/K_M (calculated, or adjusted) for reactions catalysed by ribo1BS and ribo4BS suggest that the activities are more or less equal under nonsaturating conditions, however, examination of Figure 2.6 (lanes 24 and 25), for example, clearly demonstrate that ribo1BS is more active. That the values obtained for k_{cat}/K_M (calculated) and k_{cat}/K_M (adjusted) are generally within 2 to 3 fold of each other strongly supports the validity of the results obtained.

Comparing non-denaturing gels with ribozymes and substrate mixed, and ribozyme and substrate run independently does not reveal a significant difference in migration patterns. This would imply that a very small amount of substrate and ribozyme are involved in an ES or EP1P2 complex at any given time. Removing aliquots at various times after mixing at 47°C did not affect the migration of the bands, indicating that intra-molecular secondary structures which form, form rapidly and are not time-dependent, whereas inter-molecular structures necessary for cleavage form slowly, supporting the premise that the association rate, k_1, is rate-limiting (results not shown).

2.3.6 A full length luciferase target is not cleaved

To compare the activity of the ribozymes against a truncated target with the activity against a full length (2.3 kb) luciferase gene fusion transcript, as would be produced *in vivo*, pLx709-*fab*2 was obtained from Dr. Alan Escher (Escher, *et al.*, 1989). pLx709-*fab*2 is a pT7/T3-19 derivative with the *lux* fusion gene downstream of the ϕ10 T7 promoter. It does not contain a Shine Delgarno sequence, nor does it contain the complete binding sequence of Ribo. The latter sequence was deemed unnecessary since ribo failed to demonstrate activity against the proper sequence, and the former sequence is of no importance for *in vitro* transcription.

Under standard cleavage conditions, a 123 nt 5' end cleavage product was expected to migrate into the 6% denaturing poyacrylamide gel. However, after several attempts, the expected band was not visible, demonstrating that ribozymes active against a 449 nt *lux* truncation were inactive against a 2333 nt full length *lux* transcript. Failure of the ribozymes to cleave the longer target could be the result of a further decrease in k_{cat}, due to the increased complexity on the substrate (Bertrand, *et al.*, 1994), or the ribozyme binding sites could be blocked by secondary structure. Although these results are of significance to experiments discussed in later chapters since the luciferase transcripts produced *in vivo* are approximately 2.3 kb in length, the results obtained *in vitro* can not be interpreted as direct indication of those which may be obtained in the cellular environment.

2.3.7 Hammerhead ribozyme activity in the presence of nuclear proteins

Rates of ribozyme catalysis in the presence of proteins was studied to establish if proteins in HeLa cell nuclear extracts could enhance the catalytic activity of the ribozymes. An experiment with riboBS, and ribo1BS was set up to compare cleavage activity in the absence of, and in the presence of 250 ng/µl and 1000ng/µl of HeLa cell nuclear extracts. The same concentrations of bovine serum albumin (BSA) were used to control against volume displacements effects, and since these conditions deviate significantly from previously tested conditions, ribo1CBS was tested in parallel. Substrate concentration (P1lux) was fixed at 5 nM, and each ribozyme was tested at 5 nM and 50 nM final concentrations. The results for 50 nM Ribo1BS are represented in Figure 2.12. Samples containing no protein, and the two concentrations of BSA demonstrate cleavage rates similar to those discussed above. 250 ng/ml of HeLa cell nuclear extract also demonstrated similar cleavage characteristics, although RNA degradation is more pronounced due to RNase in the extract. However in the presence of 1000 ng/µl, all of P1lux, and approximately 50% of ribo1BS is either degraded, or retained in the well. It is also significant that substantial label is retained in the wells for the other protein containing samples. From these results, it is evident that HeLa cell nuclear factors are in association with the RNA, however, it cannot be concluded that the factors are promoting RNA-RNA

interactions. In parallel experiments with ribo1C, cleavage of the target was not evident, but the migration patterns of the target and ribozyme were similar to those observed in experiments with ribo1BS (Results not shown).

In a second experiment, SDS was added to a final concentration of 1.0% with tRNA as carrier, and a phenol/chloroform extraction was performed to eliminate RNA-protein interactions after the cleavage reaction in order to prevent retention of the RNA in the wells of the gel. Ribozyme riboBS was tested along side ribo1BS to establish if factors in the nuclear extracts could bestow catalytic activity upon riboBS, since it is demonstrated that nuclear factors can melt inactive structures in favour of active ones (RNA chaperone functions; Portman and Dreyfuss, 1994). However, no evidence of P1lux cleavage by riboBS was observed (results not shown). Furthermore, HeLa cell nuclear extracts did not improve the activity of ribo1BS, under the conditions used (Figure 2.13), although the SDS/phenol/chloroform treatment was effective at disrupting the RNA-protein interactions.

2.4 Discussion

Ribozymes in general, and hammerhead ribozymes in particular, are a relatively new class of molecule with enzymatic activity, and as such, little is known about the kinetic mechanisms involved in RNA-mediated RNA cleavage reactions. *In vitro* analysis of the ribozymes utilised in this study was primarily carried out to characterise the activity of each in a cell free system, and to establish the legitamacy of the controls used. The purpose of the controls was to differentiate between gene repression resulting from a cleavage event, and gene repression resulting from the intrinsic antisense properties of ribozymes *in vivo*, which alone can result in significant repression (Saxena and Ackerman, 1989; Cotten, *et al.*, 1989; Steinecke, *et al.*, 1992; Perriman, *et al.*, 1995). The negative controls used in this study were inactive *in vitro* over a wide range of conditions, and it is assumed that they are also inactive *in vivo*.

2.4.1 Mutant ribozymes as antisense controls

The single base mutation in the controls, A14T, alters one of ten conserved nucleotides in the hammerhead domain which is not base paired by standard Watson-Crick interactions. Computer analysis of the minimal ribozyme sequences does not predict an alteration in secondary structure resulting from the mutation, supporting the premise that the controls are not disabled through formation of an inactive conformation with the target. However, an identical mutation in a different hammerhead affected UV cross linking patterns substantially, without affecting substrate binding (Woissard, *et al.*, 1994), suggesting that tertiary folding in the ribozyme/substrate complex is affected. Specifically, a substrate with 2' deoxy-4-thiouridine substitution at position 16.1 failed to crosslink to the mutant, while crosslinking was strong in the wild type. X-ray crystallography predicts a non-Watson-Crick duplex at the base of stem II which includes A14, (Pley, *et al.*, 1994), and FRET analysis predicts a base stacking interaction between A6, A15.1 and A14 (Tuschl, *et al.*, 1994). Therefore, an A14 to T14 mutation may disrupt tertiary interactions, which may in turn affect the overall stability of the control-substrate complex. Fedor and Uhlenbeck (1992), report that the substrate dissociation rate (k_{-1}) for an active ribozyme is higher than would be expected based on the length of duplex formed, whereas

a mutant ribozyme was substantially more stable. Therefore, mutations which alter tertiary interactions may increase the antisense properties of hammerhead constructs.

2.4.2 Ribozymes containing the ribo sequences are inactive

That ribozymes targeted to cleave *mas* P1 sequences immediately upstream of the *lux*F ATG codon (riboBS and CTribo), are inactive under the conditions tested is unfortunate, since the 5' untranslated region of a transcript is believed to be a good target for either antisense RNA, or ribozyme-mediated gene repression. 5' untranslated regions of highly expressed genes are predicted to be more susceptible to these technologies since these regions contain less secondary structure, particularly close to the 5' cap structure, presumably to facilitate 40S ribosome subunit binding and scanning (Hershey, 1991).

Modifications of the sequence surrounding the cleavage site strongly suggests that the cause of this inactivity is not in the substrate strand (*i. e.*, compare sequences of luxtar, P1lux, and P1lux125). Flanking sequences beyond the ribozyme guide arms are not involved either, since riboBS and CTribo do not contain any sequence homology beyond the synthetic gene insert. The cause of inactivity must therefore be internal to the hammerhead domain.

Computer analysis of the minimal ribo ribozyme structure with PCFOLD (*i. e.*, BamHI site to BamHI site, Figure 2.14) suggests stable intramolecular secondary structure, which sequesters 17 of 19 nucleotides in the two guide arms, as well as preventing formation of stem loop II. It is unlikely that formation of stem loops I and III could compete with the intramolecular structures. PCFOLD also predicts secondary structure in the minimal ribozymes, ribo1 and ribo4, however it is not as extensive, and sequences involved in duplex formation with the target molecule are found in single stranded regions, which presumably facilitates strand exchange. Indeed, there is a correlation between the stabilities of the potential secondary structure within each ribozyme studied and the activity *in vitro*. Using free energy per nucleotide as a representation of the internal stability of secondary structure within each minimal ribozyme, the order Ribo1 (ΔG = 0.138 kcal/mole) < Ribo4 (ΔG = 0.142 kcal/mole) < Ribo (ΔG = 0.196 kcal/mole) is inversely related to the observed activity (k_{cat}/K_M),

Ribo1>Ribo4>Ribo. Although this correlation is supported in the literature (Denman, 1993), it's validity is not directly tested in this work. However, since the nucleotides in stem loop II are not conservered, the sequence of ribo could be mutated to prevent the predicted secondary structure, and reanalysed.

2.4.3 Two (hammer)heads are not better than one

The dual hammerhead, ribo4, was designed with the idea that "two heads are better than one". It was also assumed that since ribo4 incorporates ribo1 3' to a unique hammerhead catalytic domain targeted to a GUU sequence, the activity of ribo4 against a target transcript would be at least equivalent to that of ribo1. However, as evident from kinetic data, the activity of ribo4BS is only 33% that of ribo1BS (Table 2.3: V_{max}, and k_{cat}/K_M (observed)), presumably as a result of the increased length and complexity of ribo4BS. Generally, as evident from the kinetic experiment performed with minimal ribozymes and substrates (*i. e.*, Fedor and Uhlenbeck, 1992), simpler sequences demonstrate greater activity, and transcripts containing multiple ribozymes are not as active as their single ribozyme counterparts (Ohkawa, *et al.*, 1993; Bertrand, *et al.*, 1994).

Furthermore, the two hammerheads of ribo4 are not active to the same extent (for example, Figure 2.4, lane 11). The 3' hammerhead cleaves the 5' target site everytime a cleavage event occurs, as evident from the single 5' product band with a migration pattern identical to the migration pattern of the 5' cleavage product of ribo1BS (Figure 2.4, lane 9). The two 3' product bands resulting from target cleavage by ribo4, each of approximately equal intensity, suggest that the 3' target site is cleaved by the 5' hammerhead with 50% efficiency of the 3' hammerhead domain. Mutagenesis of the hammerhead domain (Symons, 1992) indicate that the sequence GUU is cleaved with only 5% the efficiency of GUC, explaining the lower activity. Alternatively, the secondary structure of the 5' ribozyme may be incompatible with cleavage in a proportion of the ribo4/substrate complexes. In the former case, the extent of cleavage at the 3' site is dependent on the stability of the intermolecular structure, in that the rate of dissociation relative to the rate of cleavage determines the extent of cleavage. Time course experiments at different temperatures (which would affect the stability of the duplexes)

could be designed to test this hypothesis. The increased number of nucleotides in the guide arms of ribo4 (total = 22) could also decrease the specificy of catalysis (Herschlag, 1991).

2.4.4 Kinetics

Kinetic parameters were determined for both the CT series and the BS series to analyse the affects of non-complementary sequences beyond the guide arms. These experiments are significant since ribozymes expressed *in vivo* will contain additional sequences from the promoter and terminator elements of the ribozyme gene (with some clever exceptions - *i. e.*, self-cleaving ribozymes, discussed in Chapter 6). The pBluescript sequences, and pCTDel sequences are completely different beyond the synthetic gene inserts. During a two hour incubation period, the extent of cleavage is roughly equivalent for both types (Figure 2.6), and during the initial steady state phase of the cleavage reaction, there is little difference between the two families of constructs (Table 3). The BS series contain 80 nt apart from the ribozyme gene inserts, whereas the CT series contain 202 nt apart from the inserts, such that a difference in kinetic values might be expected based on the increased complexity of the CT series. PCFOLD, however, predicts significant secondary structure in the BS series resulting from the pBluescript KS+ MCS, which is absent in the CT series. Therefore, the CT series may be more active "per nucleotide" than the BS series.

The overall kinetic parameters established are characteristic of similar ribozyme-substrate complexes, and the rate-limiting step is attributed to substrate association. However, preincubation of the ribozymes and substrates, followed by the addition of Mg^{2+} to initiate the reaction did not alter the reaction kinetics significantly, even though this experiment was expected to measure the k_2 rate. There are two possible explanation for this: 1) the reactions were not preincubated long enough to allow sufficient formation of the ribozyme substrate complexes, or 2) Mg^{2+} is required to form the intermolecular interaction. According to several reports (section 1.4), Mg^{2+} is predicted to stabilise the structure, and the reaction intermediates, rather than participate in the formation of ribozyme/substrate complexes. However, salt concentrations,

particularly Mg^{2+}, play an important role in nucleic acid interactions, and initiating reactions with Mg^{2+} can result in anomalous initial rates, possibly due to slow adoption of Mg^{2+} dependent structures. (Fedor and Uhlenbeck, 1990; 1992). Replacing Mg^{2+} with a non-catalytic monovalent cation may overcome potential problems with duplex formation. It is unlikely that incorporation of Mg^{2+} into the active structure is rate-limiting.

Analysis of secondary structure by non-denaturing gel electrophoresis reveals extensive secondary structure at the concentrations used in these experiments. Ribozymes and substrate resolved independently, or together, do not show differences in the migration patterns. Removing aliquots of each reaction during a time course after mixing also does not result in changes in migration pattern, suggesting that intermolecular structures between the ribozyme and substrate are slow to form (results not shown). This is not surprising considering the low V_{max} values obtained, and the assumption that substrate association is rate-limiting for the reaction up to, and including, the formation of the EP1P2 complex. Since, the concentrations of ribozyme used exceeds the K_M values, the slow substrate association rate is not a reflection of a concentration dependent interaction. Although Larson, *et al.*, (1993) report using non-denaturing gels to establish the association rate constant (k_1) for ribozyme-mediated cleavage reactions, this method would appear to be inadequate for this system. However, in the reference provided, the authors incubate the ribozyme and substrate for three hours prior to analysis, whereas the non-denaturing gel analysis herein was performed after a maximum of 30 minutes.

2.4.5 Protein facilitation

HeLa cell nuclear extracts were added to *in vitro* cleavage reactions to look for protein mediated enhancement of the reaction rate. Nuclear extracts contain 20 abundant heterogeneous nuclear ribonucleoproteins (hnRNPs), which are involved in mRNA processing (Portman and Dreyfuss, 1994). RNA-RNA base pairing plays a critical role in the interactions between pre-mRNA and transacting factors during the processing of pre-mRNAs into mRNA, and these interactions must be dynamic and efficient to ensure rapid splicing (Dreyfuss, *et al.*, 1993). Therefore, proteins found in nuclear extracts could

potentially affect ribozyme kinetic rates by enhancing substrate association and product dissociation.

Several HeLa factors are reported to have RNA annealing activity: hnRNP A1, hnRNP C1/C2, mRNA binding proteins SF2/ASF, and U2AF-65, and tumour suppressor p53 (Dreyfuss, *et al.*, 1993; Portman and Dreyfuss, 1994). A1 is characterised in detail (Munroe and Dong, 1992): the RNA annealing activity is assigned to the carboxy terminal domain, and the helix destabilising properties are localised to the amino terminus, which contains 2 copies of an RNA binding motif, the ribonucleoprotein (RNP) consensus domain. In the presence of A1, annealing of two RNA sequences was 80% complete in 30 seconds, and less than 2% complete after 5 minutes in the absence of A1. Isolated A1 is shown to enhance ribozyme activity *in vitro* (section 2.1.6)

The addition of Hela cell nuclear extracts to *in vitro* cleavage reactions did not have a significant affect on the reaction rates (Figures 2.12 and 2.13), contrary to published reports with purified proteins (Tsuchihashi, *et al.*, 1993; Bertrand and Rossi, 1994) and experiments with nuclear extracts (J. Rossi, personal communication). The extracts were demonstrated to be efficient in RNA splicing, and resistant to long term storage at -70°C (D. Black, personal communication), however, degradation of certain factors cannot be ruled out. The optimal protein to nucleotide ratios are determined for several of the factors, and are generally in the range sufficient to coat the RNA. Bertrand and Rossi (1994) found purified protein (NCp7, and hnRNP A1) concentrations of 50 ng/µl sufficient to have at least one protein interacting with each transcript molecule at a concentration of 22 nM. The maximal RNA concentrations used in this study was 55 nM, however, the total amount of RNA in these reactions was approximately 7.5 times that used by Bertrand and Rossi, since the transcripts utilised herein were significantly longer. Of the proteins concentrations used herein, 250 ng/µl of total extract is certainly subsaturating with respect to hnRNPs, but 1000 ng/µl was predicted to approach adequate levels. That substrate transcripts were retained in the well at 1000 ng/µl, demonstrates protein association with the RNA. However, since approximately 50% of the ribozyme migrated at the size expected for unbound ribozyme, and that the same pattern was

observed for reactions containing 5 nM ribozyme (not shown), which contain significantly less total RNA, the extent of RNA saturation with protein may be the cause of the failure to increase the ribozyme activity. Cooperative binding is predicted for both RNA chaperones and matchmakers (Portman and Dreyfuss, 1994), so it is plausible that proteins bound the larger target molecule in a co-operative fashion until exhausted, explaining why a portion of ribozyme transcript did not have a retarded migration pattern.

Figure 2.1

A. Minimal kinetic mechanism for intermolecular hammerhead catalysis.

B. Secondary structure of hammerhead 16 (HH16) (Hertel, *et al.*, 1994). R, ribozyme strand; S, substrate (or target) strand; arrow, cleavage site.

C. Summary of determined rate constants difined in **A**, for hammerhead 16 (Hertel, *et al.*, 1994).

A

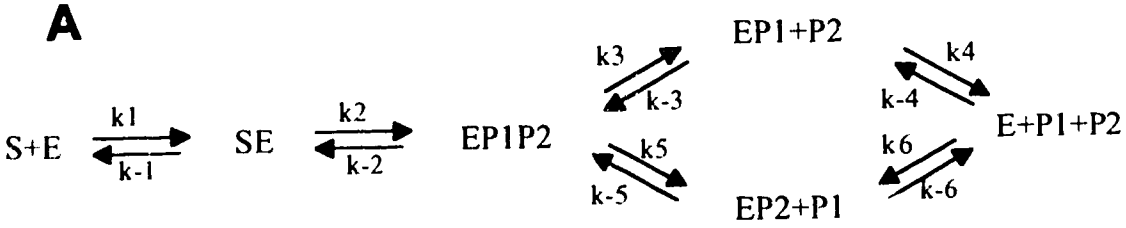
S+E
k1
k-1
SE
k2
k-2
EP1P2
k3
k-3
EP1+P2
k4
k-4
E+P1+P2
k5
k-5
EP2+P1
k6
k-6

B

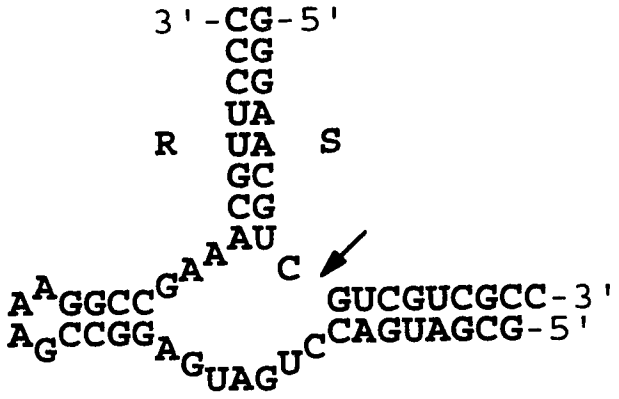
3'-CG-5'
CG
CG
UA
R UA S
GC
CG
AU
GUCGUCGCC-3'
CAGUAGCG-5'

C

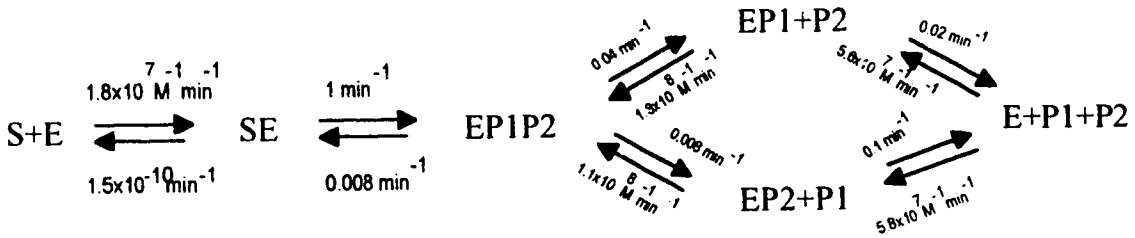
S+E
1.8x10 7 M -1 min -1
1.5x10 -10 min -1
SE
1 min -1
0.008 min -1
EP1P2
0.04 min -1
1.8x10 8 M -1 min -1
EP1+P2
0.02 min -1
5.8x10 7 M -1 min -1
E+P1+P2
0.008 min -1
1.1x10 8 M -1 min -1
EP2+P1
0.1 min -1
5.8x10 7 M -1 min -1

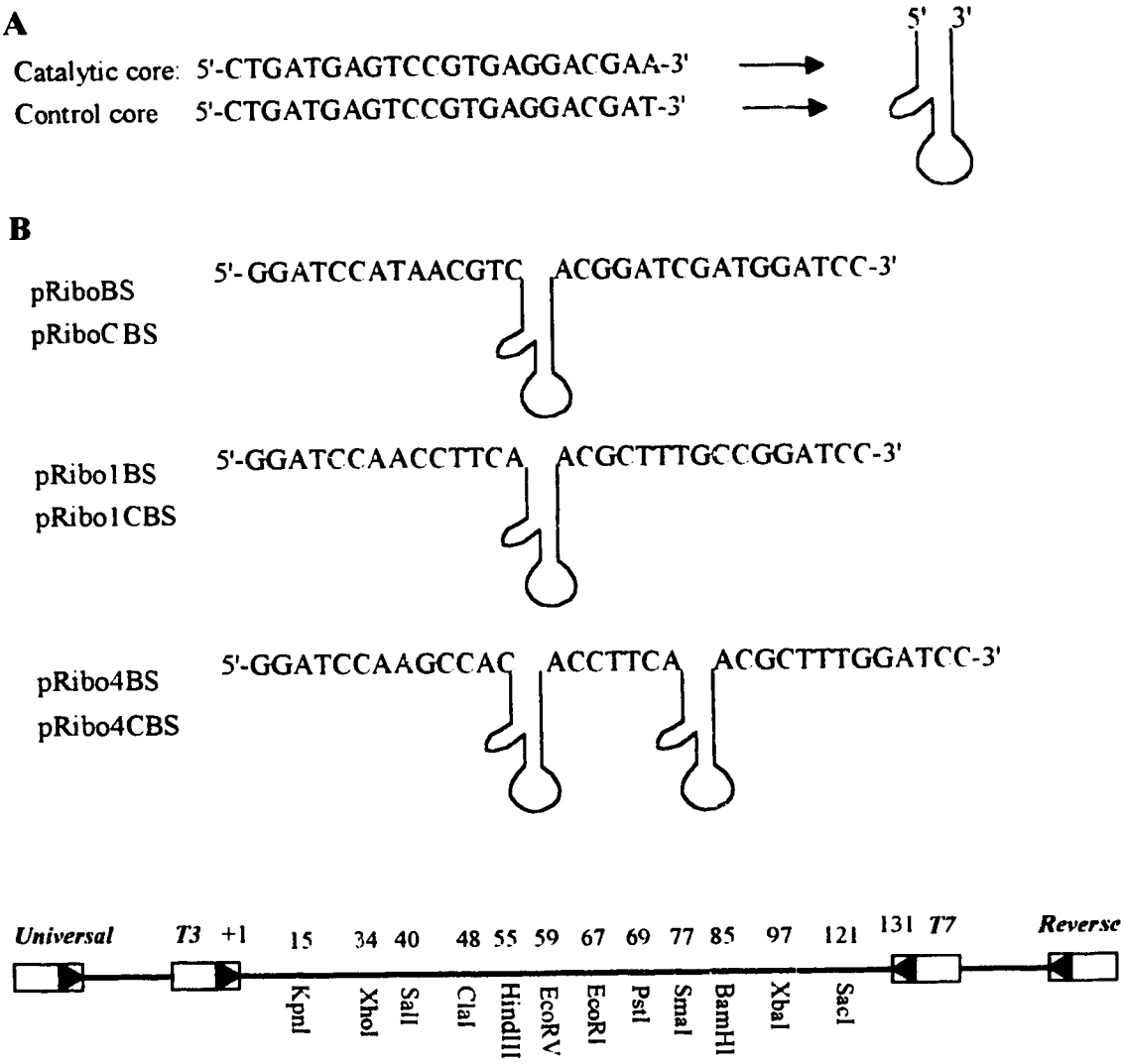

Figure 2.2

Construction of the BS series of ribozymes. **A.** Ribozyme catalytic domain, derived from the satelite RNA of tobacco ringspot virus, and the A to T mutation in the control domain. **B.** Sequences of the synthetic ribozyme genes (and controls) inserted into the BamHI site of pBluescript KS +. Restriction sites are as marked; Universal, universal priming site; T3, T3 promoter sequence; T7, T7 promoter sequence, Reverse, reverse priming site. Nucleotide numbering is relative to the T3 RNA polymerase transcription start site.

Figure 2.3

Construction of plasmids for *in vitro* transcription of target molecules.

Top: region of pPCV701-*lux*-FP1 between the left and right T-DNA borders. Please see Figure 1.2 for explanation of labels.

Middle: enlarged view of pPCV701-*lux*-FP1, with ribozyme cleavage sites indicated by arrows, and sequences involved in ribozyme binding underlined.

Bottom: Linear map of pBluescript KS + between the Universal and Reverse priming sites. T3, T3 promoter; T7, T7 promoter; restriction sites as labelled; nucleotide numbering is relative to T3 RNA polymerase start site. pluxtarBS: sequences -17 to +221 of pPCV701-*lux*-FP1 inserted into the ClaI-PstI sites of pBluescript KS +. pP1luxBS: sequences -145 to +221 of pPCV701-*lux*-FP1 inserted into the EcoRV-PstI sites of pBluescript KS +. pP1lux125BS: deletion of KpnI-HindIII sites of the pBluescript KS + multiple cloning site (MCS).

pPCV701-*lux*-FP1

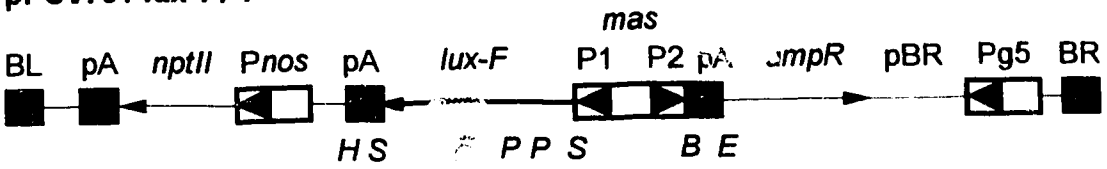

pBluescript KS+ MCS

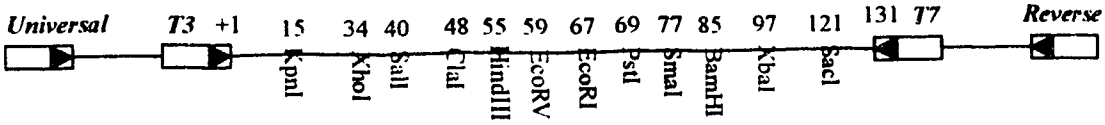

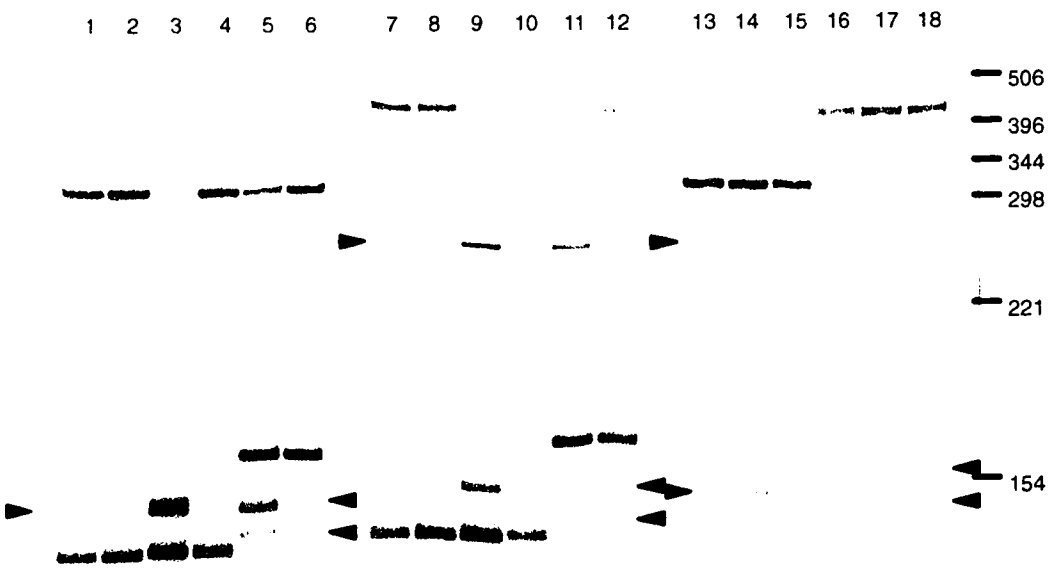

Figure 2.4

Cleavage of luxtar (307 nt, Lanes 1-6, and 13-15), and P1lux125 (419 nt, Lanes 7-12, and 16-18) by the BS series of ribozymes and controls, after 2 hours incubation at 50 degrees Celsius. Size marker is to the right. Lanes 1-12, 1:1 ribozyme to target RNA ratio; lanes 13-18, 1:10 ribozyme to target RNA ratio. Lane 1, riboBS (142 nt); Lane 2, riboCBS; Lane 3, ribo1BS (142 nt); Lane 4, ribo1CBS; Lane 5, ribo4BS (167 nt); Lane 6, ribo4CBS. Lanes 7-12, identical to Lanes 1-6, using P1lux125 rather than luxtar. Lane 13, riboBS; Lane 14, ribo1BS; Lane 15, ribo4BS; Lanes 16-18, identical to Lanes 13-15, using P1lux125 rather than luxtar. Substrate bands are the slowest migrating band in each lane, 5' cleavage products are labelled with right pointing arrows, 3' cleavage products are labelled with left point arrows. luxtar 5' and 3' cleavage products overlap.

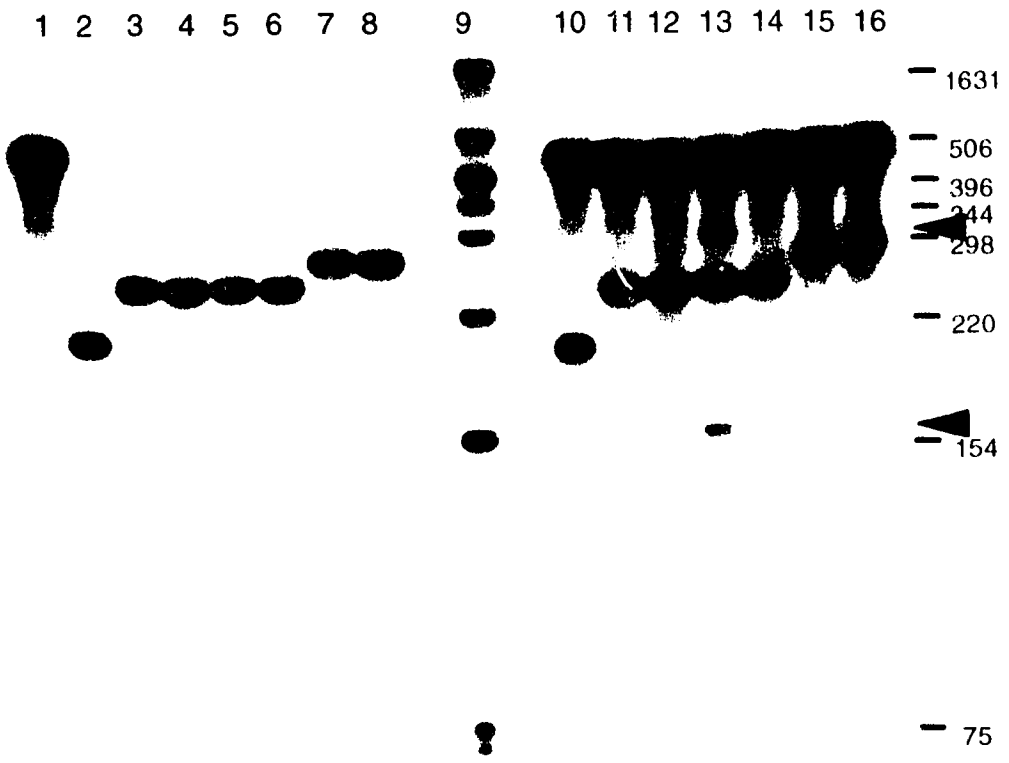

Figure 2.5

Activity of the CT ribozyme series (10 nM each) against P1lux (25 nM). Lane 1, P1lux target RNA, Lane 2, transcript from pCTdel, Lanes 3-8, ribozymes CTribo, CTriboC, CTribo1, CTribo1C, CTribo4, CTribo4C, respectively. Lane 9, size marker (pBR322 digested with HinfI); sizes are labelled to the right. Lane 10-16, ribozymes (same order as lanes 2-8) mixed with P1lux target under cleavage conditions at 37 degrees C, for 2 hours. Cleavage products are marked with arrows; 5' product resulting from cleavage of P1lux by CTribo1 is 297 nt, the 3' cleavage product is 152 nt..

Figure 2.6

Determination of temperature optima for ribozyme activity against P1lux.

A. Lane 1 and 16, size marker. All reactions represented in the remaining lanes consisted of 30 nM P1lux RNA as substrate and the 10 nM of the indicated ribozyme as catalyst. Reactions proceeded for two hours, at the temperatures indicated. Lanes 2-8, 32°C reaction temperature; Lane 2, riboBS; Lane 3, no ribozyme; Lane 4, ribo1BS; Lane 5, ribo4BS; Lane 6, CTribo; Lane 7, CTribo1; Lane 8, CTribo4. Lanes 9-15, 37°C reaction temperature; Lane 9, no ribozyme; Lane 10, riboBS; Lane 11, ribo1BS; Lane 12, ribo4BS; Lane 13, CTribo; Lane 14, CTribo1; Lane 15, CTribo4. Lanes 17-22, 42°C reaction temperature; Lane 17, riboBS; Lane 18, ribo1BS; Lane 19, ribo4BS; Lane 20, CTribo; Lane 21, CTribo1; Lane 22, CTribo4. Lanes 23-28, 47°C reaction temperature; same order as for Lanes 17-22. Lanes 29-34, 53°C reaction temperature; same order as for Lanes 17-22. Ribozymes are boxed (Lanes 2-8), and cleavage products are indicated by arrows. The band corresponding to CTribo1 is not visible in this image due to an error in quantification in this particular experiment.

B. Graphic representation of percent cleavage as determined by densitometry.

C. Schematic representation of the various bands resulting from incubating ribozymes and substrates together for 2 hours at 47°C, corresponding to lanes 23 - 28 in **A**: Lane 23, riboBS; Lane 24, ribo1BS; Lane 25, ribo4BS; Lane 26, CTribo; Lane 27, CTribo1; Lane 28, CTribo4. Colour scheme: black, residual substrate; blue, ribozyme; orange, 5' product; and magenta, 3' product.

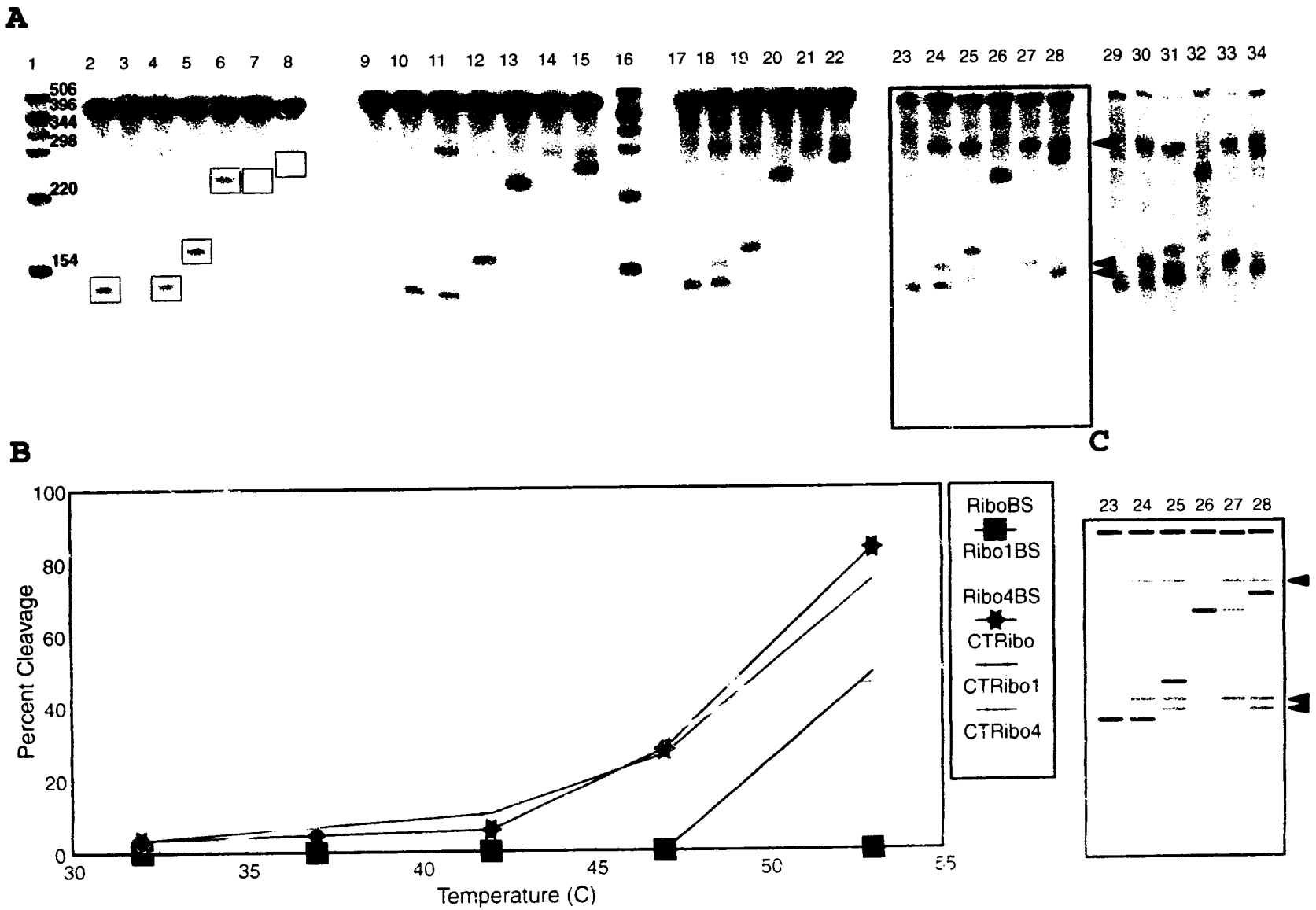
A
1 2 3 4 5 6 7 8 9 10 11 12 13 14 15 16 17 18 19 20 21 22 23 24 25 26 27 28 29 30 31 32 33 34
506
396
344
298
220
154
B
Percent Cleavage
100
80
60
40
20
0
30
35
40
45
50
55
Temperature (C)
RiboBS
Ribo1BS
Ribo4BS
CTRibo
CTRibo1
CTRibo4
C
23 24 25 26 27 28

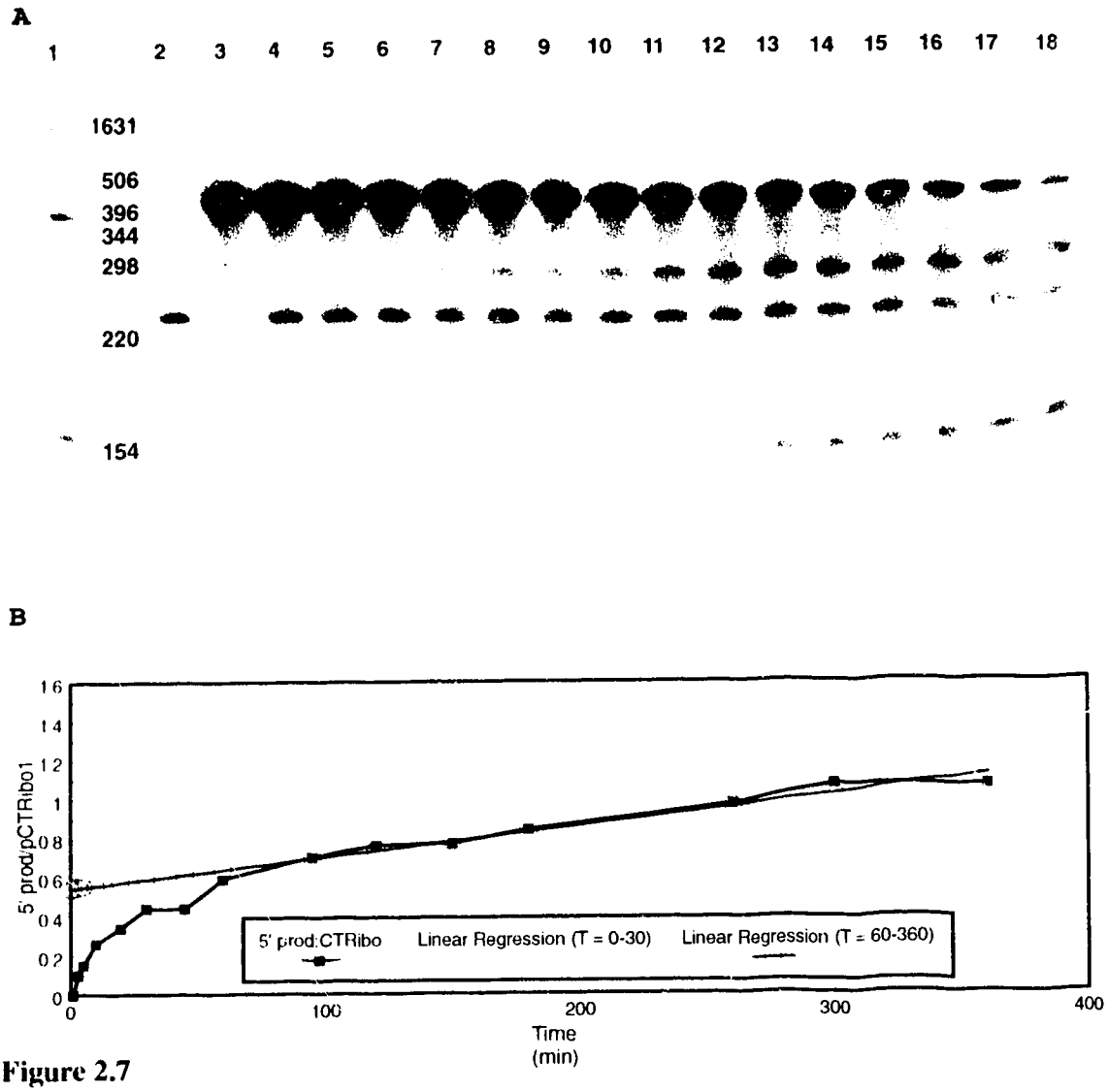

Figure 2.7

A. Cleavage activity of CTribo1 (10 nM) against P1lux (30 nM), relative to time, at 47 degrees C. Lane 1, size marker; Lane 2, CTribo1 prior to mixing with target (T=0); Lane 3, P1lux prior to mixing with CTribo1; Lane 4, T=1 min; Lane 5, T=3 min; Lane 6, T=5 min; Lane 7, T=10 min; Lane 8, T=20 min; Lane 9, T=30 min; Lane 10, T=45 min; Lane 11, T=60 min; Lane 12, T=95 min; Lane 13, T=120 min; Lane 14, T=150 min; Lane 15, T=180 min; Lane 16, T=260 min; Lane 17, T=300 min; Lane 18, T=360 min.

B. Graphical representation of the band densities in A. Blue, measured values; yellow, linear regression of values from T=0 min to T=30 min; green, linear regression of values from T=60 min to T=360 min.

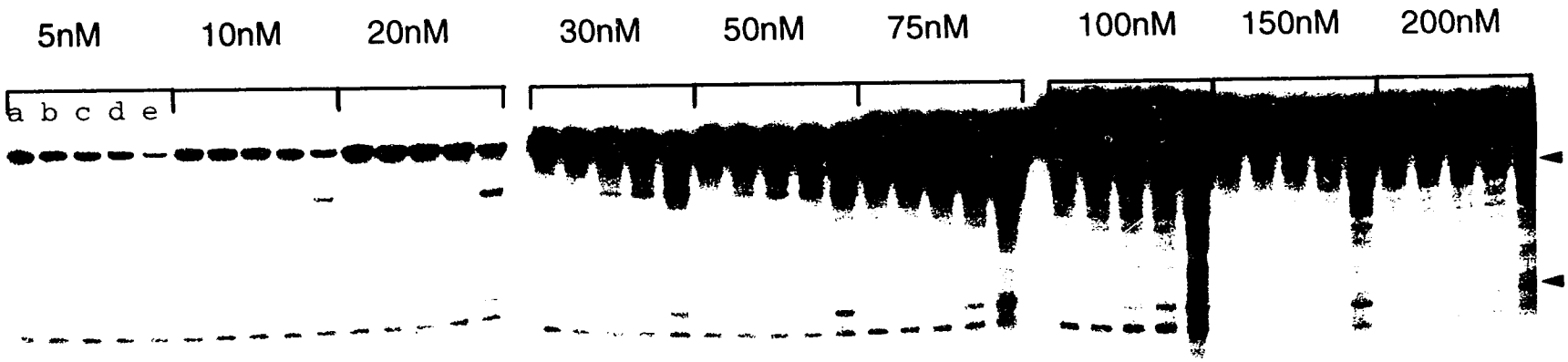

Figure 2.8

Burst phase kinetics of Ribo1BS against P1LuxBS: substrate excess over ribozyme. Substrate concentrations are as labelled, ribozyme concentration is 5 nM; a, T=0 (minutes); b, T=10; c, T=20; d, T=30; e, T=60. For substrate = 150 nM and 200 nM, 1/5 of the reaction volume was loaded relative to the lower concentrations.

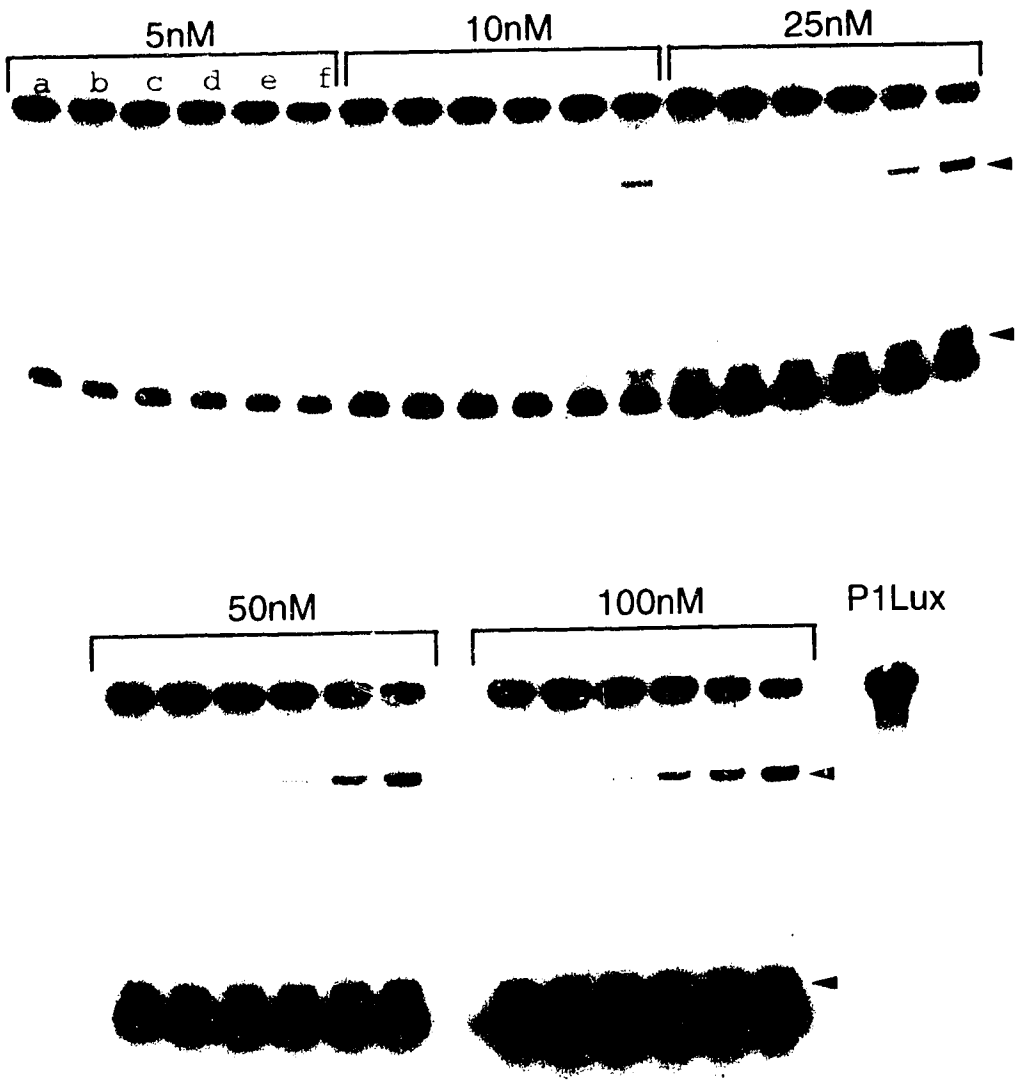

Figure 2.9

Burst phase kinetics of ribo1BS against P1luxBS RNA: ribozyme excess. Ribozyme concentrations are as labelled, substrate concentration is 5 nM; a, T=0 (minutes); b, T=5; c, T=10; d, T=15; e, T=20; f, T=30. P1lux cleavage products are indicated by arrows; 5' product is 297 nt, and the 3' product is 152 nt.

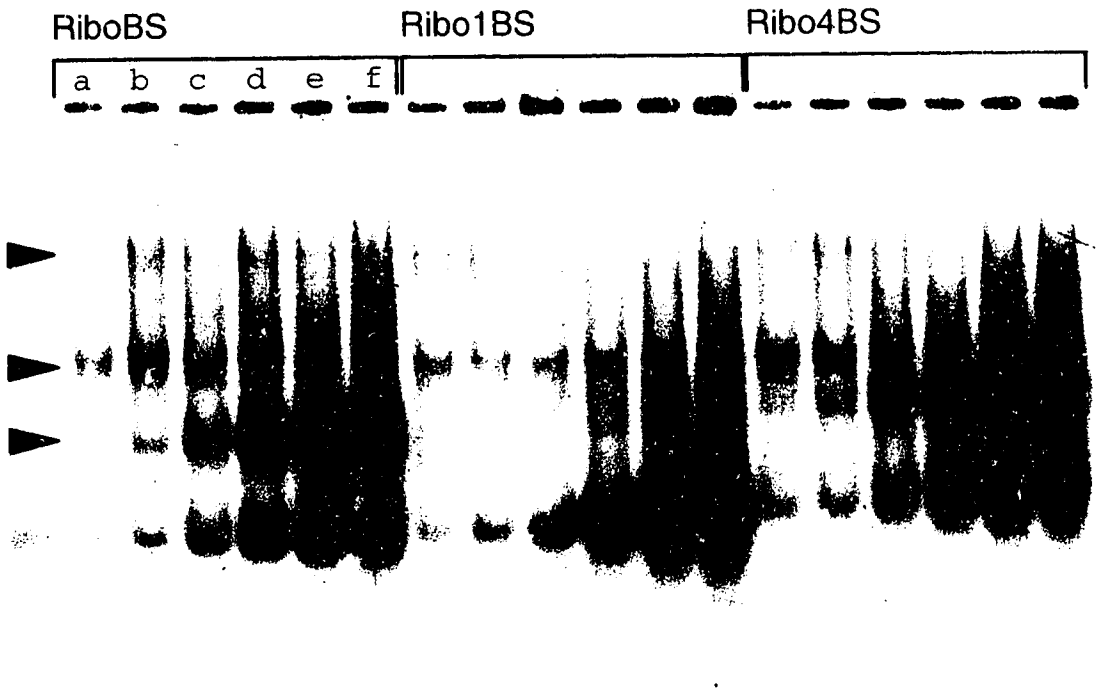

Figure 2.10

Non-denaturing gel electrophoresis of BS ribozymes at various concentrations with substrate P1luxBS at 5 nM, mixed, and preincubated for 30 minutes. Ribozymes are as labeled, ribozyme concentrations are: a, 5 nM; b, 10 nM; c, 25 nM; d, 50 nM; e, 75 nM; f, 100 nM. Red, P1luxBS aggregates; blue, P1luxBS monomers; green, ribozyme aggregates; orange, ribozyme monomers.

Table 2.1. Kinetic parameters determined for ribo1BS using excess substrate over ribozyme (Figure 2.8). V_{max} and K_M values were determined by plotting (v) against [S] with HYPERBOLIC REGRESSION software.

V_{max} (nM/min)	K_M (nM)	k_{cat} (min^{-1})	k_{cat}/K_M (min^{-1} nM^{-1})
0.1762 +/- .0387	118.6 +/-36.6	0.0350	0.0003
Error is expressed as standard error			

Table 2.2 Percentage of each ribozyme in the fastest migrating band on non-denaturing polyacrylamide gels: assumed to be monomeric (Figure 2.10).

nM	RiboBS	Ribo1BS	Ribo4BS	CTRibo	CTRibo1	CTRibo4
5	69	100	70	100	100	100
10	62	100	66	100	100	94
25	49	100	50	100	100	93
50	37	89	45	85	92	89
75	31	89	25	84	86	76
100	27	85	27	78	87	65

Table 2.3. Kinetic parameters determined for each of the four active ribozymes (ribo1BS, ribo4BS, CTribo1, and CTribo4), under conditions described in the text, and as in Figure 2.11.

Ribozyme	Conditions	V_{max} (nM/min)	K_M (nM)	k_{cat} (min^{-1})	k_{cat}/K_M (min^{-1} mM^{-1}) calculated	k_{cat}/K_M (min^{-1} mM^{-1}) adjusted	k_{cat}/K_M (min^{-1} mM^{-1}) observed
ribo1BS	5nM P1Lux	0.091 +/- 0.012	34 +/- 10	0.018	540	160 +/-20	133 +/- 18
ribo1BS	10nM P1Lux	0.33 +/- 0.07	80 +/- 28	0.033	410	240 +/-30	195 +/- 24
ribo4BS	5nM P1Lux	0.028 +/- 0.010	18 +/- 12	0.006	330	110 +/-20	31 +/- 2
ribo4BS	10nM P1Lux	0.14 +/- 0.06	38 +/- 26	0.014	380	230 +/-20	59 +/- 7
CTribo1	Mg^{2+} Preincubation	0.10 +/- 0.05	80 +/- 70	0.019	240	130 +/-10	111 +/- 8
CTribo1	Mg^{2+} Initiation	0.029 +/- 0.004	11 +/- 5	0.006	510	40 +/-20	35 +/- 11
CTribo4	Mg^{2+} Preincubation	0.053 +/- 0.016	58 +/- 32	0.011	180	90 +/-10	62 +/- 6
CTribo4	Mg^{2+} Initiation	0.092 +/- 0.018	54 +/- 20	0.018	340	190 +/-10	125 +/- 6

Figure 2.11

Graphs used to established k_{cat}/K_M (adjusted) (Table 2.3). -ln(FracS)/t was established by averaging the time points (in minutes) T=15, 20, and 30 for ribo1BS and CTribo1, and T=30, 45, and 60 for ribo4BS and CTribo4. Error in the average values are expressed for each ribozyme concentration, on each graph, as sample standard error, by way of error bars. All ribozyme concentrations are adjusted based on results from non-denaturing gel electrophoresis.

A. Various concentration of ribo1BS, with 5 nM P1lux as substrate.

B. Various concentration of ribo1BS, with 10 nM P1lux as substrate.

C. Various concentration of ribo4BS, with 5 nM P1lux as substrate.

D. Various concentration of ribo4BS, with 10 nM P1lux as substrate.

E. Various concentration of CTribo1, with 5 nM P1lux as substrate, incubated with 20 mM Mg^{2+} prior reaction initiation by mixing.

F. Various concentration of CTribo1, with 5 nM P1lux as substrate, mixed prior to the addition of Mg^{2+}. Reactions were initiated by the addition of Mg^{2+} to 20 mM.

G. Various concentration of CTribo4, with 5 nM P1lux as substrate, each incubated with 20 mM Mg^{2+} prior reaction initiation by mixing.

H. Various concentration of CTribo4, with 5 nM P1lux as substrate, mixed prior to the addition of Mg^{2+}. Reactions were initiated by the addition of Mg^{2+} to 20 mM.

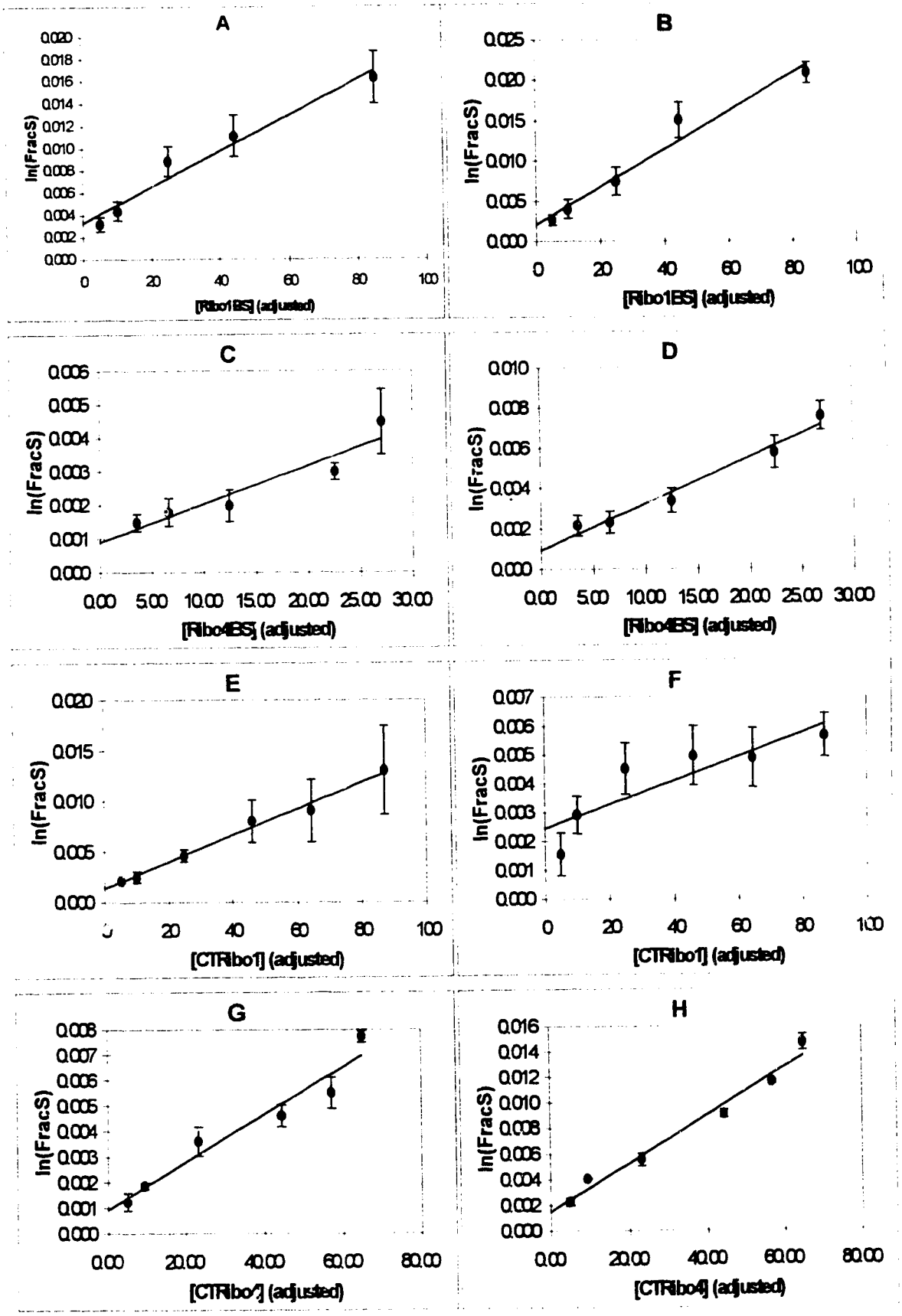
A
ln(FracS)
[Ribo1BS] (adjusted)
B
ln(FracS)
[Ribo1BS] (adjusted)
C
ln(FracS)
[Ribo4BS] (adjusted)
D
ln(FracS)
[Ribo4BS] (adjusted)
E
ln(FracS)
[CTRibo1] (adjusted)
F
ln(FracS)
[CTRibo1] (adjusted)
G
ln(FracS)
[CTRibo4] (adjusted)
H
ln(FracS)
[CTRibo4] (adjusted)

Figure 2.12

Protein facilitation of ribo1BS (50 nM) cleavage activity against P1luxBS (5 nM). 1, no protein; 2, BSA (250 ng/µl); 3, BSA (1000 ng/µl); 4, HeLa cell nuclear extract (250 ng/µl); 5, HeLa cell nuclear extract (1000 ng/µl). a, T=0 (minutes); b, T=10; c, T=30. 5' cleavage product is marked, 3' cleavage product is obscured by the ribozyme bands. Wells are at the top of the figure.

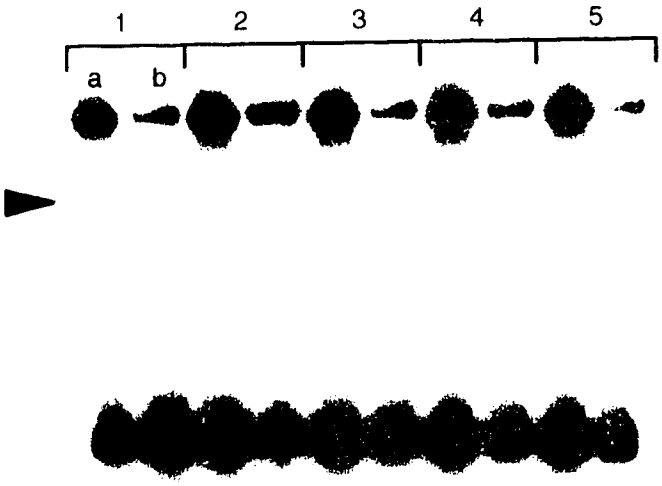

Figure 2.13

Protein facilitation of ribo1BS (50nM) cleavage activity against P1luxBS (5nM), with addition of SDS and a phenol/chloroform extraction after the incubation period. Protein concentrations are as labeled in Figure 2.11. a, T=0; b, T=20 minutes. 5' cleavage product is marked, 3' cleavage product is obscured by the ribozyme bands. Wells are not shown.

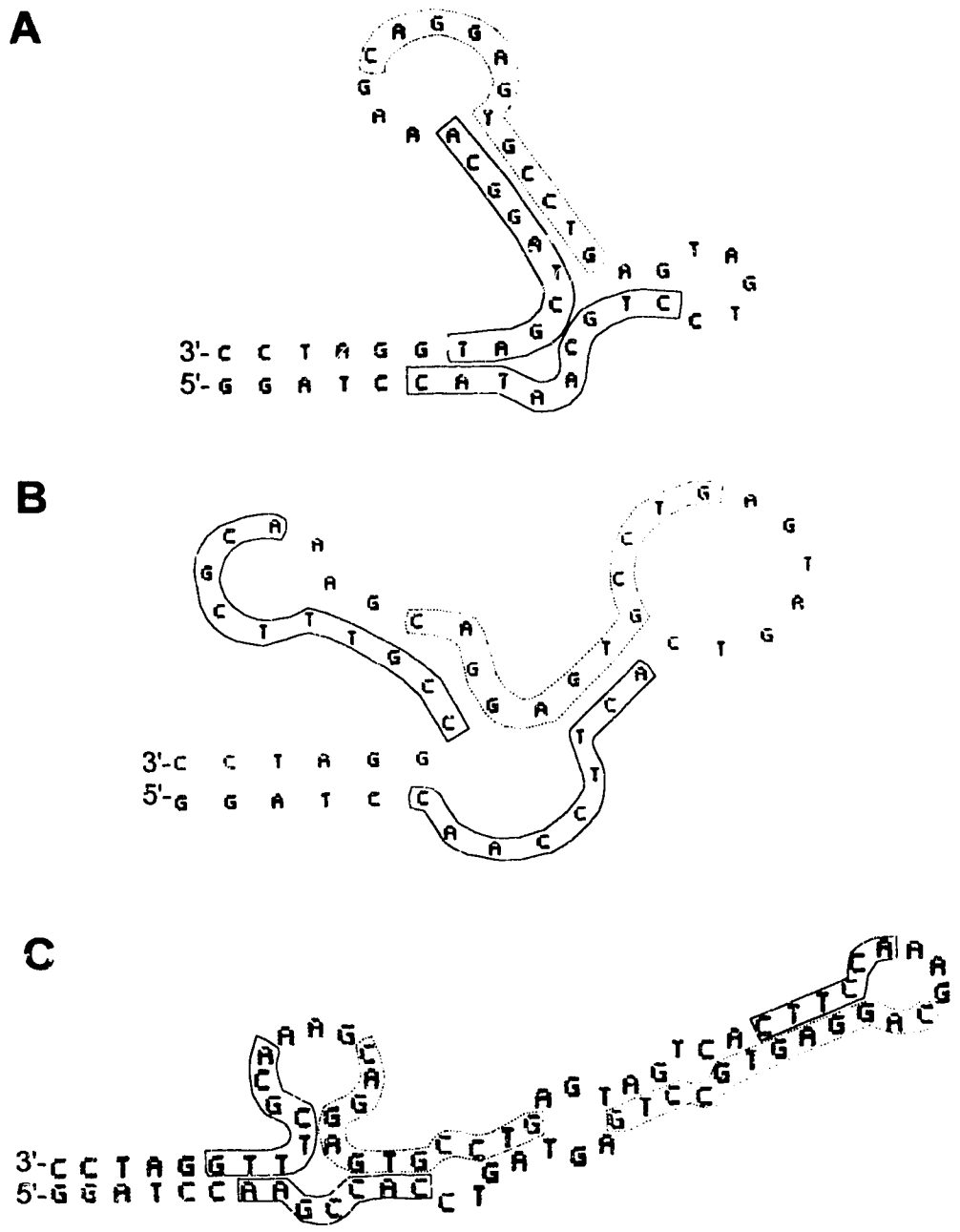

Figure 2.14

Secondary structure of the minimal ribozymes (BamHI site, to BamHI site), as determined by PCFOLD, at 47degrees C. Ribozyme guide sequences are indicated by the solid lines, sequences involved in forming stem-loop structre II are indicated by the dashed lines. 5' and 3' orientations are indicated. A. ribo; B. ribo1; C. ribo4. Note that the DNA sequences are provided.

2.5 Bibliography

Amersham: *Guide to Autoradiography*. Distributed by Amersham, Oakville, Ontario.

Ausubel, F. M., Brent, R., Kingston, R. E., Moore. D. D., Seidman, J. G., Smith, J. A., Struhl, K., (eds.) (1994) *Currect Protocols in Molecular Biology*. John Wiley and Sons, Inc., New York.

Bennett, M. J., and Cullimore, J. V. (1992). Selective cleavage of closely related mRNAs by synthetic ribozymes. *Nucleic Acids Res.* **20**, 831-837.

Bertrand, E. B., Rossi, J. J. (1994) Facilitation of hammerhead ribozyme catalysis by the nucleocapsid protein of HIV-1 and the hetergeneous nuclear ribonucleoprotein A1. *EMBO J.* **13**, 2904-2912.

Bertrand, E., Pictect, R., Grange, T. (1994). Can hammerhead ribozymes be efficient tools to inactivate gene function? *Nucleic Acids Res.* **22**, 293-300.

Chen, C., Banerjea, A. C., Harmison, G. G., Haglund, K., and Schubert, M. (1992). Multitarget-ribozyme directed to cleave up to nine highly conserved HIV-1 *env* RNA regions inhibits HIV-1 replication - potential effectiveness against most presently sequenced HIV-1 isolates. *Nucleic Acids Res.* **20**, 4581-4589.

Chung, C. T., Niemela, S. L., Miller, R. H. (1989) One-step preparation of competent *Escherichia coli*: transformation and storage of bacterial cells in the same solution. *Proc. Natl. Acad. Sci. USA* **86**, 2172-2175.

Coetzee, T., Herschlag, D., Belfort, M. (1994) *Escherichia coli* proteins, including ribosomal protein S12, facilitate in vitro splicing of phage T4 introns by acting as RNA chaperones. *Genes and Development* **8**, 1575-1588.

Cotten, M., Schaffner, G., Birnstiel, M. L. (1989). Ribozyme, antisense RNA, and antisense DNA inhibition of U7 small nuclear ribonucleoprotein-mediated histone pre-mRNA processing *in vitro*. *Mol. and Cell. Bio.* **9**, 4479-4487.

Denman, R. B. (1993a). Using RNAFOLD to predict the activity of small catalytic RNAs. *Biotechniques* **15**, 1090-1094.

Denman, R. B. (1993b). Cleavage of full-length βAPP m RNA by hammerhead ribozymes. *Nucleic Acids Res.* **21**, 4119-4125.

Dreyfuss, G., Matunis, M. J., Pinol-Roma, S., Burd, C. G. (1993). hnRNP proteins and the biogensis of mRNA. *Annu. Rev. Biochem.* **62**, 289-321.

Escher, A., O'Kane, D. J., Lee, J., Szalay, A. A. (1989). Bacterial luciferase αβ fusion proteins is fully active as a monomer and highly sensitive in vivo to elevated temperature. *Proc. Natl. Acad. Sci. USA* **86**, 6528-6532.

Fedor, M. J., Uhlenbeck, O. C. (1992). Kinetics of intermolecular cleavage by hammerhead ribozymes. *Biochemistry* **31**, 12042-12054.

Fedor, M. J., Uhlenbeck, O. C. (1990). Substrate sequence effects on "hammerhead" RNA catalytic efficiency. *Proc Natl. Acad. Sci. USA* **87**, 1668-1672.

Fersht, A. (1977). In: *Enzyme Structure and Mechanism.* W. H. Freeman and Company, San Francisco.

Heidenreich, O., Eckstein, F. (1992). Hammerhead ribozyme-mediated cleavage of the long terminal repeat of human immunodefiency virus type I. *J. Biol. Chem.* **267**, 1904-1909.

Herschlag, D. (1991). Implications of ribozyme kinetics for targeting the cleavage of specific RNA molecules *in vivo*: More isn't always better. *Proc. Natl. Acad. Sci. USA* **88**, 6921-6925.

Herschlag, D., Khosla, M., Tsuchihashi, Z., Karpel, R. L. (1994) An RNA chaperone activity of non-specific RNA binding proteins in hammerhead ribozyme catalysis. *EMBO J.* **13**, 2913-2924.

Hershey, J. W. B. (1991). Translational control in mammalian cells. *Annu. Rev. Biochem.* **60**, 717-755.

Hertel, K. J., Herschlag, D., Uhlenbeck, O. C. (1994). A kinetic and thermodynamic framework for the hammerhead ribozyme reaction. *Biochemistry* **33**, 3374-3385.

Larson, G. P., Bertrand, E., Rossi, J. J. (1993). Designing and testing of ribozymes as therapeutic agents. *Methods: A Companion to Methods in Enzymology* **5**, 19-27.

Laskey, R. A. *Review 23. Efficient detection of biomolecules by autoradiography, flourography, or chemiluminescence.* Distributed by Amersham, Oakville, Ontario.

Muller, G., Strack, B., Dannull, J., Sproat, B. S., Surovoy, A., Jung, G., Moelling, K. (1994) Amino acid requirements of the nucleocapsid protein of HIV-1 for increasing catalytic activity of a *Ki-ras* ribozyme *in vitro*. *J. Mol. Biol.* **242**, 422-429.

Munroe, S. H., Dong, X. (1992) Hetergeneous nuclear ribonucleoprotein A1 catalyzes RNA-RNA annealing. *Proc. Natl. Acad. Sci. USA* **89**, 895-899.

Ohkawa, J., Yuyama, N., Yutaka, T., Hishikawa, S., Taira, K. (199_ Importance of independence in ribozyme reactions: kinetic behavior of trimmed and of simply connected multiple ribozymes with potential activity against human immunodeficiency virus. *Proc. Natl. Acad. Sci. USA* **90**, 11302-11306.

Perriman, R., Bruening, G., Dennis, E. S., Peacock, W. J. (1995). Effective ribozyme delivery in plant cells. *Proc. Natl. Acad. Sci. USA*. **92**, 6175-6179.

Pley, H. W., Flaherty, K. M., and McKay, D. B. (1994). Three dimensional structure of a hammerhead ribozyme. *Nature* **372**, 68-74.

Portman, D. S., Dreyfuss, G. (1994) RNA annealing activities in HeLa nuclei. *EMBO J.* **13**, 213-221.

Ruffner, D. E., Dahm, S. C., Uhlenbeck, O. C. (1989). Studies on the hammerhead self-cleaving domain. *Gene* **82**, 31-41.

Sambrook, J., Fritsch, E. F., Maniatis, T. (1989). *Molecular Cloning: A Laboratory Manual, Second Edition.* Cold Spring Harbour Laboratory Press, Cold Spring Harbour, NY.

Saxena, S. K., Ackerman, E. J. (1989). Ribozymes correctly cleave a model substrate and endogenous RNA *in vivo*. *J. Biol. Chem.* **265**, 17106-17109.

Steinecke, P., Herget, T., Schreier, P. H. (1992). Expression of a chimeric ribozyme gene results is endonucleolytic cleavageof target mRNA and a concomitant reduction of gene expression *in vivo*. *EMBO J.* **11**, 1525-1530.

Taylor, N. R., Rossi, J. J. (1991). Ribozyme-mediated cleavage of an HIV-1 gag RNA: The effects of non-targetted sequences and secondary structure on ribozyme cleavage activity. *Antisense Research and Development* **1**, 173-186.

Tsuchihashi, Z., Khosla, M., Herschlag, D. (1993). Protein enhancement of hammerhead ribozyme catalysis. *Science* **262**, 99-102.

Tuschl, T., Gohlke, C., Jovin, T. M., Westhof, E., and Eckstein, F. (1994). A three-dimensional model for the hammerhead ribozyme based on fluorescence measurements. *Science* **266**, 785-789.

Ventura, M., Wang, P., Ragot, T., Perricaudet, M., Saragost, S. (1992). Activation of HIV-specific ribozyme activity by self-cleavage. *Nucleic Acids Res.* **21**, 3249-3255.

Woisard, A., Fourrey, J-L., Favre, A. (1994). Multiple folded conformations of a hammerhead ribozyme domain under cleavage conditions. *J. Mol. Biol.* **239**, 366-370.

Zuker, M. (1989). Computer prediction of RNA structure. *Methods in Enz.* **180**, 262-288.

3. RIBOZYME ACTIVITY IN *E. coli* CELLS

3.1 Introduction

An *E. coli* model system was established for analyzing ribozyme activity *in vivo*. Sioud and Drlica (1991), demonstrated that hammerhead ribozymes can cleave RNA from the integrase gene of the human immunodeficiency virus (HIV), in bacteria, and Inokuchi *et al.* (1994), report the specific reduction of transcripts from the A2 gene of RNA coliphage SP *in vivo*. Expression of ribozymes in *E. coli* has several potential advantages over analysis in plant tissues. First, the speed and ease of manipulation allows faster analysis of new constructs. Second, the large number of well characterised promoters facilitate experimental design. Third, the simplicity of the genome facilitates detection of transcripts of interest, as does the relative abundance of transcripts of interest.

An experiment was designed to take advantage of the extremely high levels of expression attainable with a T7 RNA polymerase expression system. Each ribozyme gene, and control ribozyme gene utilised in this study was inserted into a unique T7 RNA polymerase expression cassette. The cassette consists of a dicistronic element upstream of a promoter recognised by T7 RNA polymerase (ϕ10), and downstream of a T7 RNA polymerase termination signal (Tϕ). At the 5' end of each gene in the dicistronic element is a T7 strong translational start signal (s10), and each gene is separated from the other, and from other flanking elements by RNase III cleavage sites (R0.3) (Figure 3.1). The promoter proximal cistron contains sequences from gene 9 of bacteriophage T7, and a short multiple cloning site, into which the synthetic ribozyme genes were inserted. The second cistron consists the complete coding sequence of gene 9 of bacteriophage T7, which could be used to indirectly quantitate the level of ribozymes produced. The cassette is carried on an ampicillin resistance plasmid, pCTDel, derived from vectors pCT1 and pCT3, obtained from Dr. John Dunn (Rosenberg, *et al.*, 1993). This construct therefore allows high levels of ribozyme gene transcription after induction of a T7 RNA polymerase gene located on the chromosome of an appropriate *E. coli* host strain. The ribozyme transcripts produced are of a defined size (197 nt, plus the length of the inserted ribozyme

gene (section 2.2.3, and 2.2.4), since ribozymes transcribed from the T7 promoter are trimmed both 5' and 3' by RNase III endogenous to the host.

Two constructs were used to study luciferase regulation in *E. coli* cultures harbouring pCTDel derived vectors. pLx403-*fab*9 was obtained from Dr. Alan Escher, which consists of a luciferase fusion gene with a correctly positioned Shine Delgarno sequence inserted into the BamHI site of pACYC184, thereby inactivating the gene encoding tetracycline resistance (*Tet*^{R}). (Escher, *et al.*, 1989; Escher and Szalay, 1993). Plasmid pACYC184 carries the origin of replication from plasmid p15A, and the gene encoding resistance to chloramphenicol, which enables it to co-exist with vectors carrying the *Col*E1 origin of replication, and the gene for ampicillin resistance.

Plasmid pLx403-*fab*9 was designed for the expression of the *lux* fusion gene in *E. coli*, and does not contain the *mas* P1 promoter sequences upstream of the *lux*F ATG codon required, and ergo, does not contain the ribo and riboC target sequence. Therefore, a second vector was created, p403-15, by inserting a DNA fragment consisting of a luciferase fusion gene downstream of sequences derived from the *mas* P1 promoter into the BamHI site of pACYC184. This vector does not contain a Shine Delgarno sequence upstream of the *lux*F ATG, and translation efficiency in *E. coli* is low. The low levels of light emission which are obtained are possibly the result of read through translation, or spurious initiation at the *lux* ATG.

The host strain for pCTDel and the pCT series of ribozyme vectors was the *E. coli* K12 strain HMS174. For expression of the ribozymes, the strain HMS174(DE3) was used. Bacteriophage DE3 is a λ phage derivative which carries the T7 RNA polymerase gene under the control of the *lac*UV5 promoter. DE3 is inserted into, and inactivates, the integrase gene (*int*) on the *E. coli* chromosome, and because the *int* gene is inactivated, DE3 needs a helper for integration and excision from the chromosome. The *lac*UV5 promoter driving the polymerase gene is inducible with isopropyl-β-D-thio-galactopyranoside (IPTG) (Studier, *et al.*, 1990).

The *in vivo* activity of each ribozyme against luciferase target transcripts was analysed indirectly by comparing Lux enzyme activities between cultures containing

ribozyme genes, and those containing control ribozyme genes, with a sensitive photon detection camera, following induction of the *lac*UV5 promoter. Ribozyme activity against luciferase RNA was measured directly by comparing quantities of luciferase target transcripts by ribonuclease protection assays. In the case of the latter technique, cultures induced to transcribe large quantities of each ribozyme were incubated at 47°C to mimic the cleavage conditions used for *in vitro* analysis of ribozyme activity. Since the ribozyme expression cassette contains a strong translation start signal, an experiment was performed in which IPTG-induced cultures were incubated w[illegible]tomycin to inhibit ribosome initiation, and prevent possible interference of ribozy[illegible]ity by migrating ribosomes.

3.2 Materials and Methods

3.2.1 Suppliers, media, and strains

Unless otherwise stated, suppliers are as described for Chapter 2. Media for bacterial growth was either LB, or 2xYT, as described in Chapter 2. Antibiotics for plasmid maintenance were ampicillin (Ap, 100 mg/L), and chloramphenicol (Ch, 50 mg/L).

3.2.2 Plasmid construction

Plamid pCTDel was derived from plasmids pCT1 and pCT3, obtained from Dr. John Dunn (Rosenberg, *et al.*, 1993). Approx[illegible] 30 µg of both pCT1 and pCT3 were digested with NheI and BamHI from Promeg[illegible] resolved on a LMP agarose gel. A 4330 nt band was isolated from the pCT1 lane, corresponding to the entire pCT1 vector minus the 1928 bp BamHI-NheI fragment. A 1043 bp BamHI-Nhe fragment was isolated from the pCT3 lane. The 1043 BamHI-NheI fragment of pCT3 was ligated into the 4.33kb pCT1 fragment, creating a "CT-type" vector, pCTDel, with 885 nucleotides deleted from the "test gene" (Figure 3.1). Plasmid integrity was checked by restriction digest with BglII.

[illegible]tic ribozyme gene was cut out of 20 µg of the respective BS vectors (sectio[illegible] 2.4) with BamHI and isolated from 15% non-denaturing polyacrylamide gels by passi[illegible] elutio[illegible] and precip[illegible]ated with 95% ethanol. Plasmid pCTDel (7.5 µg) was diges[illegible] with BamHI, and [illegible]reated with CIP. Each synthetic ribozyme gene was ligated into pCTDel, and transformed into HMS174 (F-, *rec*A, r^-_{k12}, m^+_{k12}, Rif^R).

Recombinant vectors were screened by restriction digest analysis with EcoRI and XbaI to identify clones with a single ribozyme gene insert. Appropriate vectors were sequenced by the ABI Taq cycle sequencing method, using either a T7 primer obtained from Dr. John Elliot and dye terminators from ABI, or T7 dye primers from ABI. Collectively, ribozyme genes inserted into pCTDel are referred to as the pCT series, and individually are pCT*ribo*, pCT*riboC*, pCT*ribo1*, pCT*ribo1C*, pCT*ribo4*, and pCT*ribo4C*.

Plasmid pLx403-*fab*9 was obtained from Dr. Alan Escher (Escher and Szalay, 1993). For the construction of p403-15, a DNA fragment consisting of the *mas* P1

promoter fused to the *lux*-F cassette was amplified from pPCV701-*lux*-FP1 by PCR, using the P1start oligo (section 2.2.5) for the 5' sense strand primer, and oligonucleotide LuxBend as the 3' antisense strand primer (CCT GCA ATG ACC ATT GCT GAG GAG). The 5' end of P1start is 145 nt upstream of the luciferase ATG, and the 5' end of LuxBend is 186 nt downstream of the *lux*-F TAA stop codon on pPCV701-*lux*-FP1. 60 pmoles of each primer were used with 10 ng of plasmid in a standard 100 µl PCR reaction. The cycling program consisted of 30 cycles of 1 minute at 94°C, 1 minute at 55°C, and 2.5 minutes at 72°C. The PCR reaction mixture was extracted with phenol/chloroform, precipitated with ethanol, and resuspended in ddH_2O. Klenow enzyme was used to remove the 3' T overhangs created by Taq polymerase, and the 5' ends were phosphorylated with T4 polynucleotide kinase and ATP.

Plasmid pACYC184 was linearised with BamHI and the products were resolved by agarose gel electrophoresis for detection of complete digestion. 5' overhangs were repaired with Klenow in the presence of dNTPs, and treated with CIP. Both the CIP treated vector, and the kinase treated PCR products were extracted with phenol/chloroform, precipitated, and resuspended to 125 ng/µl in H_2O. The two fragments were ligated together and transformed into DH5α.

Colonies containing recombinant vectors were selected based on photon emission by an Argus 100 low light imaging system (Hamamtsu Photonics), and further screened by digestion with EcoRI and PstI, and independently with BamHI (BamHI sites were expected to be recreated during the construction). A single colony with a P1-*lux* insert the correct orientation was obtained, and labelled p403-15.

Plasmid pCATBS was constructed for synthesis of an RNA probe suitable for quantifying chloramphenicol acetyltransferase (CAT) mRNA levels in *E. coli* cultures harbouring pACYC184 derived vectors, via ribonuclease protection assays. Plasmid p403-15 was digested with EcoRI and ScaI, and a 414 nt fragment from the CAT structural gene was isolated from by LMP agarose. This fragment was then ligated into pBluescript KS+, which had been digested with EcoRV and EcoRI, and treated with CIP. Recombinant vectors were screened by α-complementation, and digestion with ClaI and

EcoRI. Plasmid DNA was isolated from an appropriate clone by CsCl centrifugation. The orientation of the insert was such that transcription with T3 RNA polymerase would produce an RNA probe complementary to the CAT mRNA.

3.2.3 Measurement of luciferase activity in E. coli cultures

E.coli strain HMS174(DE3) carrying pLx403-*fab*9 was transformed with the pCT series of vectors, including pCTDel, and colonies were selected on LB agar + Ap + Ch. p403-15 was transformed into HMS174(DE3) simultaneously with the pCT vector series.

Overnight cultures of HMS174(DE3)(pLx403-*fab*9) with each of the the pCT series of vctors were diluted 1:200 with fresh media (100 µl->20 ml), and grown for 3 hours at 37°C ($O.D._{600}$ = 0.6). At T = 0 minutes, 100 µl of each culture was mixed with 2 µl of a 1:1000 decanal solution, and analysed in a prewarmed microtitre plate under a Siemens Videolum low light camera for 1 minute at maximum intensity. Simultaneously, 1 ml of each culture was placed on ice for RNA isolation and analysis, and 500 µl was used to determine the $O.D._{600}$ of each culture, and to verify the presence of both plasmids. The remainder of each 20 ml culture was divided into two prewarmed erlenmeyer flasks and allowed to cool to room temperature. To one flask of each culture, IPTG was added to a final concentration of 0.4 mM for induction of the *lac*UV5 promoter/T7 RNA polymerase fusion gene, while the second was left as an uninduced control. At T = 30, 60, 90, and 120 minutes, 100 µl of each culture was analysed by low ligh imaging, 1 ml was put aside for RNA isolation and analysis, and 500 µl was used to determine the optical density.

3.2.4 Verification of the presence of both plasmids in the same E. coli cell

Plasmid retention was determined for each of the 7 cultures at T = 0 by inocculating 100 µl of the desired dilution into 3 ml of soft top agar (with the appropriate selection) kept at 47°C, followed by pouring onto the appropriate selection plates. The proportion of cells in each culture which retained a vector of the pCT series was determined from the number of colony forming units in 100 µl of a 10^{-6} dilution on LB,

and LB + Ap plates. The proportion of cells in each culture which retained pLx403-*fab*9 was similarly determined from the number of colonies resulting from 100 µl of a 10^{-6} dilution on LB, and LB + Ch plates. The proportion of cells in each culture which lost the respective pCT vector was established by plating 100 µl of 10^{-5} dilutions on LB plates containing 0.4 mM IPTG, and the proportion of cells with a dysfunctional T7 expression system was determined by plating 100 µl of 10^{-5} dilutions on LB + IPTG + Ap (Studier, *et al.*,1990).

3.2.5 Analysis of ribozymes isolated from E. coli cells

A truncated luciferase RNA was transcribed *in vitro* with T3 RNA polymerase from plasmid pP1luxBS, gel purified, and heat denatured, (section 2.2.6) and made up to a final Mg^{2+} concentration of 20 mM. Total RNA isolated from cultures of HMS174(DE3) harbouring pLx403-*fab*9 and one of the pCT vectors, which were induced with IPTG for 2 hours, was diluted to 400 ng/µl in 50 mM Tris-HCl pH 8. In one set of experiments, the *E. coli* RNA was heat denatured prior to adding Mg^{2+} to a final concentration of 20 mM, and in another, the heat denaturation step was eliminated. Total *E. coli* RNA solutions, and luciferase target transcript solution were preincubated at 47°C, and a cleavage reaction catalysed by the ribozymes in the cellular RNA was initiated by mixing 5 µl of each (final target concentration was 27 nM). The reaction mixtures were incubated at 47°C for 2 hours, and quenched with 10 µl of formamide dye solution containing 50 mM EDTA, and electrophoresis and autoradiography was as described (section 2.2.7). Autoradiograhy was performed with an intensifying screen.

3.2.6 Analysis of RNA from E. coli cultures

Overnight cultures of HMS174(DE3) harbouring either pLx403-*fab*9, or p403-15, and each of the pCT vectors, including pCTDel, were cultured overnight in LB broth + Ap + Ch. Cultures were diluted 1:200 with fresh media, grown to an $O.D._{600}$ of 0.6, and ribozyme gene transcription was induced for 2 hours at 37°C with addition of IPTG to 0.4 mM. 1 ml of each culture was incubated at 37°C for another 30 minutes, and 1 ml was incubated at 47°C for 30 minutes, both without agitation. For translation inhibition

studies, streptomycin was added to a final concentration of 50 mg/L, prior to the final 30 minute incubation. Cells were pelleted by centrifugation, and RNA was isolated by one of two methods:

1) Bacterial pellets were resuspended in solution I (50 mM sucrose, 10 mM Tris-HCl pH 7.5, 1 mM EDTA) with a trace of lysozyme to weaken the cell wall. Total RNA was isolated by a scaled down acid guanidinium isothiocyanate phenol chloroform (AGPC) extraction (Chomczynski and Sacchi, 1987).

2) Bacterial pellets were resuspended in 300 µl of lysis buffer (0.5% SDS, 10 mM Tris-HCl pH 7.5, 1 mM EDTA), and 300 µl of phenol was added with vortexing for 30 seconds. Samples were incubated for 10 minutes at 65°C, with vortexing every 2 minutes. Organic and aqueous phases were separated by centrifugation at 13000g for 5 minutes, and the aqueous phase was transferred to a fresh tube and mixed with 30 µl of 3 M sodium acetate, pH 4.8. RNA was precipitated with ethanol. Both procedures resulted in high quality RNA preparations, however, the latter was much easier to perform. In some cases, RNA was treated with 1 unit of RQ1 DNase (Promega) for 30 minutes at 37°C to remove potential DNA contamination.

RNA structure and quantity were determined by ribonuclease protection assay, using an RPA II Ribonuclease Protection Assay Kit from Ambion, according to the manufacturer's instructions. Luciferase RNA probes were synthesised by *in vitro* transcription with T7 RNA polymerase from pP1luxBS linearised with HindIII as a template. Chloramphenicol acetyl transferase (CAT) RNA probes were synthesised with T3 RNA polymerase, with pCATBS linearised with BamHI. Plasmid p*ribo*BS was the template for CTRibo and CTRiboC RNA probes, p*ribo1*BS was the template for CTRibo1 and CTRibo1C RNA probes, and p*ribc4*BS was the template for CTRibo4 and CTRibo4C RNA probes; each template vector was linearised with EcoRI and transcribed with T7 RNA polymerase. A standard transcription reaction for probe synthesis contained 1 µg of template, 500 µM each ATP, GTP, and UTP, 1x commercial buffer (section 2.2.6), 10 mM DTT (if not supplied in the buffer), 20-40 units of either T3 or T7 RNA polymerase, 20 units of RNAsin (Promega), and [α-^{32}P]CTP exceeding 15 µM (about 200

μCi) in a 20 μl reaction. The quantity of label used for ribozyme probes was reduced and replaced with . reduce the specific activity. Reaction mixtures were incubated at room temperatur °C for 1 - 2 hours, and terminated by the addition of 1 unit RQ1 DNase (Promega). Transcripts were quantified, and gel purified as described in section 2.2.6. RPA analysis was performed with a large excess of probe, to ensure quantitative hybridisation with the mRNA of interest. Unless stated, autoradiography was performed without intensifying screens.

3.3 Results

3.3.1 Plasmid retention.

To ensure overnight cultures of HMS174(DE3) were retaining both the *lux* vector, and a pCT vector, cultures were diluted, and plated as described in section 3.2.4. Each of the cultures had approximately the same number of colonies growing on plates without selection, as on plates with either Ap or Ch, indicating that a significant loss of either vector (pCT or pLx403-*fab*9, respectively) did not occur. The LB IPTG plates did not have any colonies forming, suggesting the majority of cells retained the respective pCT vectors (induction of the T7 RNA polymerase gene by IPTG interferes with colony formation due to the taxation of cellular transcription and translation machinery). The results obtained from plating the cultures on LB IPTG media support those obtained from LB + Ap plates, in that the pCT vectors were retained in the majority of cells. The LB + Ap IPTG plates did not develop any colonies, indicating that there were no cells in which the pCT vector was retained, but the T7 expression system had become dysfunctional (Studier, *et al.*, 1990).

3.3.2 Analysis of luciferase activity in vivo

Ribozyme activity against luciferase mRNA was indirectly analysed *in vivo* by comparing luciferase enzyme activity levels between cultures harbouring ribozyme gene constructs, and those harbouring control ribozyme constructs and pCTDel. Photon emissions from cultures induced to express ribozyme genes by the addition of IPTG, and photon emissions from uninduced cultures were also compared to test for increased *lux* repression upon overexpression of the ribozyme genes. After induction of ribozyme gene transcription, bacterial cultures were cooled to ambient temperatures, since the Lux fusion protein utilised is more active at room temperature than at 37°C (Escher, *et al.*, 1989), and aliquots of each culture were analysed for luciferase activity at increasing times post induction. Figure 3.2a is a collage of the data collected from each time point by a Siemens Videolum low light camera, constructed by overlaying the images obtained for each time point. Increasing photon emission from each culture with increasing time is the result of

increased cell density. Figure 3.2b is the numerical value of photon emission measured as $1x10^4$ photons/second, standardised against culture density (OD_{600}). (T 120 OD values for the induced cultures, and T = 90, and 120 for uninduced cultures were not measured, and the values reported were calculated by linear regression extrapolation of the previous growth rates). The results presented in Figure 3.2 indicate that luciferase activity is not significantly repressed by over production of the CT series of ribozymes, since there is not a reduction in photon emission from cultures harbouring a ribo[illegible]onstruct, versus a control ribozyme gene construct. The IPTG-induced [illegible] has photon emission levels lower than those cultures harbou[illegible] with synthet gene inserts, indicating that the ribozymes and control ribo[illegible] sequences in the luciferase RNA do not have significant antisense RN[illegible]ity, either

3.3.3 Ribozymes synthesised <u>in vivo</u> are active against their target sequence

To demonstrate that functional ribozymes are produced in *E. coli*, 2 µg of total RNA isolated from cultures induced with IPTG for 120 minutes was mixed with luciferase target RNA transcribed *in vitro,* in an *in vitro* cleavage assay. This experiment was set up in duplicate: for the first set, 2 µg of bacterial RNA was heated to 90°C to denature any secondary structure, and placed on ice. For the second set, 2 µg bacterial RNA was used without the denaturation step. The purpose of these two treatments was to test for possible effects of secondary structure on ribozyme activity. Luciferase target RNA transcribed *in vitro* from pP1luxBS with T3 RNA polymerase, and labelled with ^{32}P was mixed 1:1 (vol/vol) with the bacterial RNA, and incubated at 47°C for 2 hours. 47°C was used since ribozyme activity under these conditions are well characterised (Table 2.3).

The resulting autoradiogram is represented in Figure 3.3. As expected, pCTDel and the control ribozymes in the *E. coli* RNA do not demonstrate any cleavage. Ribozyme CTribo is also inactive, as expected from *in vitro* analysis. However, RNA isolated from cultures harbouring pCT*ribo1* and pCT*ribo4*, and induced for 120 minutes with IPTG do demonstrate site-specific cleavage, as evident from the bands migrating as expected for cleavage of the P1lux target (for comparison, see Figure 2.5).

These results indicate that the cultures analysed in Figure 3.2 did produce functional ribozymes, and suggest that the failure to reduce luciferase expression *in vivo* may be the result of the ribozyme's inability to gain access to the target, or that the reaction rate is too slow (section 2.3.6). Denaturing the ribozymes present in the total RNA prior to to the cleavage reaction did not enhance activity.

3.3.4 Full-length luciferase fusion gene transcripts are not cleaved by ribozymes

To determine the structure and quantity of luciferase mRNA in cells carrying either pLx403-*fab*9 or p403-15, ribonuclease protection assays were performed. The full length probe produced from pP1luxBS digested with EcoRI by T7 RNA polymerase is 432 nt. The length of the probe fragment protected by hybridisation to full length luciferase mRNA from plasmid pLx403-*fab*9 is 227 nt, whereas the length of the probe fragment protected by hybridisation to luciferase mRNA from p403-15 is 369 nt. The expected size of the probe fragments resulting from hybridisation to ribozyme-mediated luciferase transcript cleavage products are given below.

luciferase vector	Ribozyme CTribo		Ribozyme CTribo1		Ribozyme CTribo4	
	5'*	3'	5'	3'	5'	3'
pLx403-*fab*9	N/A	N/A	95	132	95	124
p403-15	139	230	237	132	237	124

* 5' and 3' refer to the 5' and 3' luciferase RNA cleavage products, N/A, not applicable

Overnight cultures of HMS174(DE3) harbouring either pLx403-*fab*9, or p403-15, and each of the pCT vectors were prepared as described in section 3.2.6, and total RNA was isolated. Figure 3.4 is a representation of an RPA performed on RNA isolated from cultures harbouring p403-15, and one of the pCT vectors, incubated at 37°C, and 47°C for 30 minutes after 2 hours of IPTG induction. RNA was probed individually with the *lux* probe, (left half) and simultaneously with the CAT probe and the ribozyme probes. The CAT probe is included as an internal standard, since levels of CAT mRNA present in the cells should be independent of the gene carried by the pCT vector. Therefore, expressing

the intensity of the band resulting from the luciferase-protected probe fragment relative to the corresponding band resulting from the CAT-protected probe fragment allows *lux* transcript levels to be compared between cultures containing different pCT vectors. Analysis of the bands in Figure 3.4 by densitometery does not indicate a reduction in the ratio of *lux* band intensity to CAT band intensity greater than 10% in any of the samples containing potentially active ribozymes (CTribo, CTribo1, and CTribo4). Surprisingly, for the samples incubated for a further 30 minutes at 37°C after the 2 hour induction with IPTG, *lux* band to CAT band ratios for the inactive constructs (pCTDel, pCT*riboC*, pCT*ribo1C*, and pCT*ribo4C*) are reduced approximately 30% relative to the average ratio obtained from the other samples, indicating the level of error that may be obtained in experiments of this nature. No bands are evident in the locations expected for cleavage products of the luciferase mRNA.

The probes used to detect the ribozymes in Figure 3.4 had specific activities 0.64 times that of the *lux* probes, and the ribozyme-protected probe fragments are on average 0.16 the size of the *lux*-protected probe fragment. The density of the bands corresponding to the ribozyme-protected fragments are at least 10 times the intensity of the *luc*-protected fragments (more exact measurements are not possible since the X-ray film is saturated). The ribozymes are therefore estimated to be present in the cell in at least a 100 fold molar excess.

The extent of degradation in Figure 3.4 is characteristic of all experiments performed with p403-15. This degradation is occuring intra-cellularly, since RNA degradation is not as extensive with RNA isolated from cultures transformed with pLx403-*fab*9 in the same manner (compare figures 3.4 and 3.5), and probe degradation is minimal (not shown). The reason for the differential degradation patterns is not known.

3.3.5 Inhibition of ribosome initiation does not enhance ribozyme-mediated cleavage

The pCT series of vectors contain an s10 translation start signal, such that the cell may attempt to translate the ribozyme RNAs (CTribo, CTriboC, CTribo4, and CTribo4C contain in-frame stop codons, and HMS174 does not contain any suppressor mutations). The sequence of the potential peptides was not determined. It was considered that

ribosome migration would be efficient in blocking ribozyme activity (Chuat and Galibert, 1989; Inokuchi, *et al.*, 1994), therefore, cultures were supplemented with streptomycin to prevent ribosome initiation during the 30 minute incubation following the 2 hour induction with IPTG. Total *E. coli* RNA was hybridised with the luciferase RNA probe alone, and in triple hybridisation with the *lux*, CAT, and ribozyme probes in ribonuclease protection assays (Figure 3.5). Cleavage products are not evident in the resulting autoradiograms, and the ratios of *lux* RNA to CAT RNA fluctuate less than 10% from the sample mean.

Ribosome migration along a transcript is believed to protect bacterial RNA from degradation, so the addition of streptomycin may reduce the already short half-life of *E. coli* RNAs. In these experiments, the ribozymes are estimated to be present in a 20 fold molar excess (Figure 3.5), rather than the 100 fold molar excess observed without the streptomycin treatment (Figure 3.4, and results not shown). This observation supports the possibility that RNA is being degraded faster, since the longer luciferase transcripts would be protected as a function of size, and in turn supports the premise that the addition of streptomycin was efficient at preventing ribosome initiation. The actual rate of degradation cannot be determined from these experiments, since controls without streptomycin were not analysed. A faster rate of RNA degradation would be deleterious to ribozyme activity.

3.3.6 lux mRNA synthesised in vivo is not cleaved by ribozymes synthesised in vivo

In one experiment, a portion of RNA isolated from each culture containing pLx403-*fab*9 and a pCT vector, and induced with IPTG, was treated with RQ1 DNase to remove residual DNA, in an attempt to reduce background in the RPAs. Ethidium bromide stained agarose gels demonstrated the disappearance of a large molecular weight band (presumably sheared chromosomal DNA) from the treated samples. However, background levels in RPA results were not reduced (Figure 3.6, for comparison: left, untreated RNA, and right, RQ1 DNase treated RNA). The DNase digestion step was therefore eliminated from the RNA isolation procedure.

RQ1 DNase requires Mg^{2+} for activity (Promega technical support). The RQ1 DNase digestions were carried out in 40 mM Tris-HCl, pH 8, 10 mM NaCl, and 6 mM

$MgCl_2$, and the presence of 6 mM Mg^{2+} is sufficient to activate hammerhead ribozyme cleavage reactions (Uhlenbeck, 1987). Significantly, the addition of Mg^{2+} to isolated total RNA for 30 minutes at 37°C did not result in the appearance of cleavage products, even though the ribozymes present in the samples are active (see Figure 3.3). Heat denaturation of the ribozymes in cellular RNA prior to initiating the cleavage reactions is not required (Figure 3.3, right side), although it may be required for the luciferase transcipts. A follow-up experiment in which total *E. coli* RNA was heat denatured and incubated with 20 mM Mg^{2+} for 2 hours at 47°C, followed by quenching with formamide and EDTA, also did not result in site-specific cleavage, as determined by RPA analysis (results not shown).

It was reported in section 2.3.6 that ribozymes produced *in vitro* were inactive against a full length luciferase fusion transcript produced *in vitro*. It is probable that the ribozymes, whether synthesised *in vivo*, or *in vitro*, are similarly inactive against a full length transcript produced *in vivo*. It should be noted that the *lux* transcripts originate from the tet^R promoter in pLx403-*fab*9, and p403-15, and the transcription termination site was not determined for this study. Therefore, the *lux* transcripts produced in *E. coli* are significantly longer than the full length transcripts synthesised *in vitro* with T7 RNA polymerase from plasmid pLx709-*fab*2 (section 2.3.6), and the transcripts generated in transfected, or transformed plants (Chapter 4, and 5, respectively).

3.4 Discussion

Increasing the quantity of ribozyme molecules within a cell would increase the chance of interaction with the substrate, and in turn, increase the level of repression of the target transcript. In this study, ribozyme transcription was driven by the strong T7 bacteriophage ϕ10 promoter in a cell line with an inducible promoter/T7 RNA polymerase gene fusion. Transcription of the target gene was driven by the constitutive tet^R promoter. In experiments without streptomycin to inhibit protein synthesis by prevention of ribosome initiation, the level of ribozyme transcript was estimated to be 100 fold that of the *lux* transcripts, whereas *in vitro*, a 20 fold excess catalysed significant cleavage of a truncated luciferase RNA (section 2.3.5). However, *in vivo*, with ribozyme transcripts similar to those used *in vitro*, and demonstrated to cleave an *in vitro* transcribed truncated target, no reduction in luciferase enzyme activity, or reduction in full length luciferase transcript levels were observed. This finding argues that the ribozymes did not access the full length substrate. Inability to access the target could be the result of separate compartmentalisation of either the ribozyme or the target RNA due to protein sequestering of the RNA, formation of incompatible secondary structure in the full length target, or mRNA turnover rates exceeding the k_{cat} of the reaction.

Sioud and Drlica (1991), demonstrated that hammerhead ribozymes can function in bacteria. The authors report that a plasmid-borne ribozyme designed to cleave RNA from the integrase gene of the human immunodeficiency virus (HIV), led to destruction of integrase RNA and complete blockage of integrase protein synthesis. The ribozyme gene was driven by a T7 promoter carried on a plasmid derived from pACYC184. The ribozyme transcript was terminated by a T7 transcription termination signal, resulting in expression of a ribozyme of defined size (86 nt) *in vivo*. The integrase target gene was driven by either a T7 promoter, or by the 5' region of the *E. coli trp*E gene, which is inducible by the addition of indoleacrylic acid (IAA). Experiments were performed in *E. coli* strain BL21(DE3), which contains the T7 RNA polymerase gene driven by the *lac*UV5 promoter, which is inducible with IPTG (Studier, *et al.*, 1990). Ribozyme activity was tested *in vitro* against total RNA isolated from *E. coli* induced to express integrase

RNA. The extent of cleavage was greater at 50°C than at 37°C, as determined by northern blot hybridisation. *In vivo*, co-induction of the ribozyme gene and the integrase gene with IPTG resulted in the failure to detect full length integrase RNA, or cleavage products, whereas full length transcripts were abundant in control experiments. However, if the target was induced independently with IAA from the *trpE* promoter, followed by the induction of the ribozyme, the 3' cleavage product was visible in northern blots. Simultaneous induction of the ribozyme with IPTG, and induction of the target with IAA resulted in a partial loss of target RNA, and preinduction of the ribozyme resulted in a complete loss of target. These findings indicated that the ribozyme efficiently cleaved the intended target transcript, and the cleavage products were degraded rapidly by cellular RNases.

Inokuchi *et al.* (1994), also reported specific transcript reduction *in vivo* with a ribozyme targeted to the A2 gene of RNA coliphage SP. The authors of this report were unable to detect cleavage products, but do make a strong case for repression by cleavage rather than by an antisense effect. The ribozyme and controls used were driven by the *lac* promoter, such that expression was presumably significantly less than that with the T7 promoter used in this study.

The above reports are in contrast with the results of Chuat and Galibert (1989), who designed a ribozyme against β-galactosidase mRNA. In this system, a *trans*-acting ribozyme was ineffective, while a *cis*-acting ribozyme was found to be active *in vivo*. The two ribozymes were not, however, targeted to the same sequence. The authors of this report concluded that the coupled transcription-translation system in bacteria prevented activity of the *trans*-acting construct. Inokuchi, *et al.*, (1994) provide indirect evidence that ribosomes can block ribozyme activity.

Ribosome inhibition of ribozyme-catalysed reactions was addressed in this study by using the antibiotic, streptomycin, to inhibit ribosome initiation. The extent of inhibition was not determined, but the apparent increase in ribozyme degradation rates argue that the ribozymes were not protected from degradation by ribosomes migrating along the RNA. Despite ribosome inhibition, no cleavage products, nor reduction in luciferase transcript levels are evident.

Another potential inhibiting factor is the short doubling time of *E. coli*, and the rapid turn over of mRNA, which averages approximately 2 minutes (Watson, *et al.*, 1987). As determined by *in vitro* kinetic analysis herein, and in other published reports, the k_{cat} of non-minimal ribozymes targeted to mRNA length transcripts is significantly less than the ideal 1 min^{-1} (Bertrand, *et al.*, 1994). The *in vitro* transcribed ribozymes utilised in this study which mimic those produced in *E. coli* cells (CTribo1, and CTribo4), demonstrate k_{cat} values of less than 0.02 min^{-1} (Table 2.3). Assuming that the k_{cat} values obtained *in vitro* approximate those obtainable *in vivo*, the target transcript would require a half-life of approximately 50 minutes, which exceeds the doubling time of the cell. A similar phenomenon may occur in *Sacchromyces cerevisae*, which has a doubling time significantly longer than that of *E. coli* (J. Rossi, personal communication). Despite, the results obtained *in vitro*, the *in vivo* experiments were worth pursuing since ribozymes may behave quite differently in a cell than in an Eppendorf tube, and because ribozymes are demonstrate to function in *E. coli*.

Ribozyme activity in relation to mRNA half-life is not addressed in the reports mentioned above, nor is it addressed in these experiments. However, this study, and others, do utilise secondary structures to enhance transcript stability. In this case, ribozyme sequences are protected at the 3' end by a stem loop structure left behind after RNase III cleavage (Studier, *et al.*, 1990). mRNA turnover in *E. coli* is believed to proceed from the 3' end (Carpousis *et al.*, 1994), which may explain why Sioud and Drlica (1991) were able to identify a 3' cleavage product, and not a 5' cleavage product (the 5' product is not protected at the 3' end).

The ribozymes produced *in vivo*, herein, are active, as evident from the expected bands resulting from cleavage of an *in vitro* transcribed substrate. Incubating total RNA under conditions known to result in cleavage, and probing with *lux* specific RPA probes, however, fails to identify cleavage products, suggesting that the substrate produced *in vivo* is not participating in active ribozyme/substrate complex formation. The reason for this is unknown, and PCFOLD does not predict obvious secondary structures in the regions of the target sites (PCFOLD is, however, limited to 425 nt, whereas the *lux* transcript originating from the tet^R promoter is in excess of 3 kb). These results

correspond with those presented in section 2.3.6 with a full length *lux* transcript in an *in vitro* cleavage reaction. For this reason, the effects of RNA turnover rates, and ribosome migration along the mRNA, may be irrelevant. The use of a truncated luciferase gene, similar to the ones used *in vitro*, would help to resolve this issue. These experiments emphasise the importance of substrate target site selection for future experimental designs of ribozyme-mediated gene inactivation .

Figure 3.1

Construction of the pCT series of vectors.

A. Linear diagrams of the T7 expression cassettes from pCT3, pCT1, and pCTDel: ϕ10, promoter recognised by T7 RNA polymerase; R, ribonuclease III recognition site; s10, strong translational start site from gene 10 of T7 phage; Tϕ, T7 RNA polymerase transcription terminator sequence. Restriction sites: Bg, BglII; B-E, MCS containing BamHI, HindIII, and EcoRI sites; N, NheI. **B**. Ribozyme genes isolated from the BS series of vectors were inserted into the BamHI site of pCTDel; catalytic core is from the satellite RNA of the tobacco ringspot virus.

A

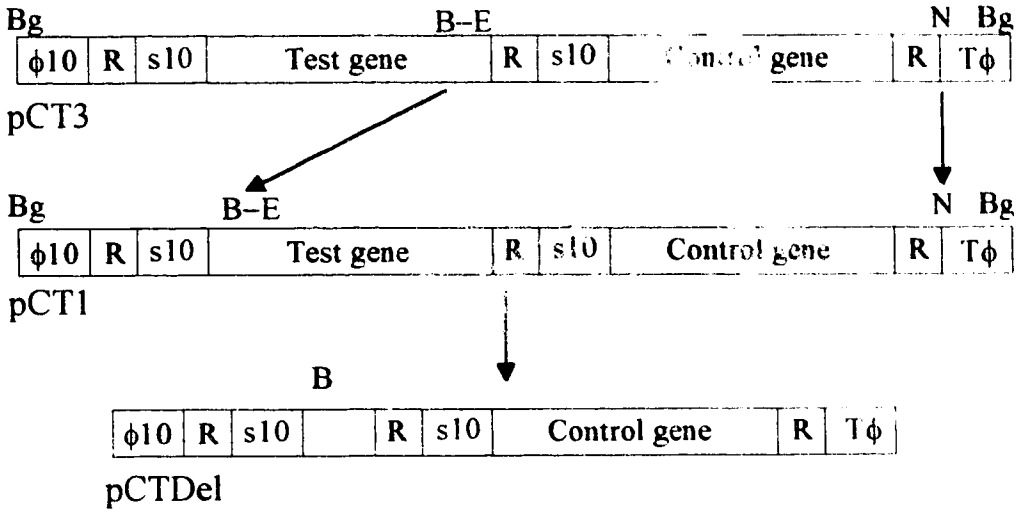
Bg
B–E
N Bg
ϕ10 R s10 Test gene R s10 Control gene R Tϕ
pCT3
Bg
B–E
N Bg
ϕ10 R s10 Test gene R s10 Control gene R Tϕ
pCT1
B
ϕ10 R s10 R s10 Control gene R Tϕ
pCTDel

B

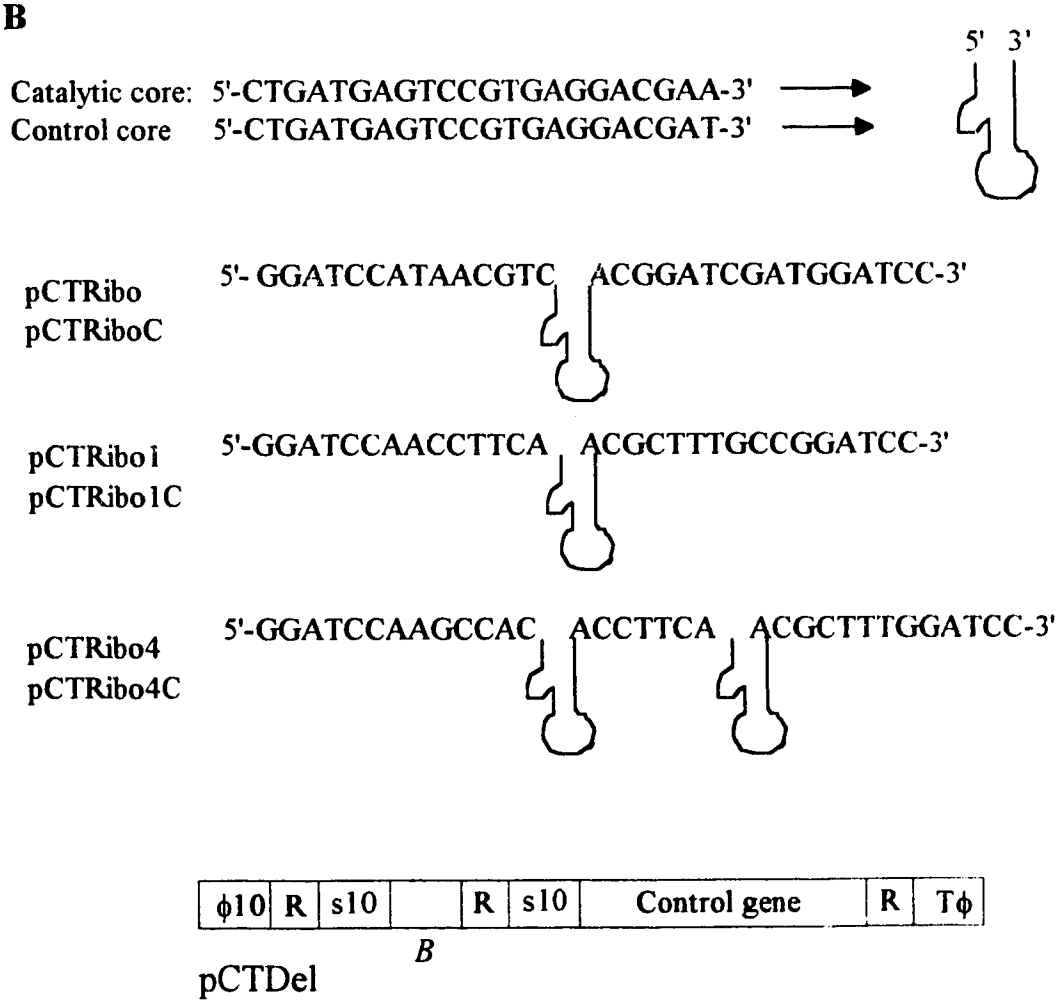
Catalytic core: 5'-CTGATGAGTCCGTGAGGACGAA-3'
Control core 5'-CTGATGAGTCCGTGAGGACGAT-3'
5' 3'
pCTRibo
pCTRiboC
5'- GGATCCATAACGTC ACGGATCGATGGATCC-3'
pCTRibo1
pCTRibo1C
5'-GGATCCAACCTTCA ACGCTTTGCCGGATCC-3'
pCTRibo4
pCTRibo4C
5'-GGATCCAAGCCAC ACCTTCA ACGCTTTGGATCC-3'
ϕ10 R s10 R s10 Control gene R Tϕ
B
pCTDel

Figure 3.2

Analysis of ribozyme activity *in vivo*, in *Escherichia coli* cultures.

A. Collage of bacterial cultures expressing luciferase from plasmid pLx403-*fab*9, and ribozymes from a plasmid in the pCT series in a microtitre plate, generated by a Siemens Videolum low light imaging system. Time points relative to induction of ribozyme expression with IPTG are labelled across the top. The first column for each time point is an uninduced control, the second column is induced with 0.4 mM IPTG. Ribozyme vectors are indicated to the right. The colour bar on the extreme right indicates the intensity of light emission: colours at the top represent higher activity than those at the bottom. T=0 is at 37°C, the remainder are at room temperature.

B. Photon emmission from T=0, and uninduced microtitre plate wells, standardised against culture density.

C. Photon emmission from T=0, and induced microtitre plate wells, standardised against culture density.

A

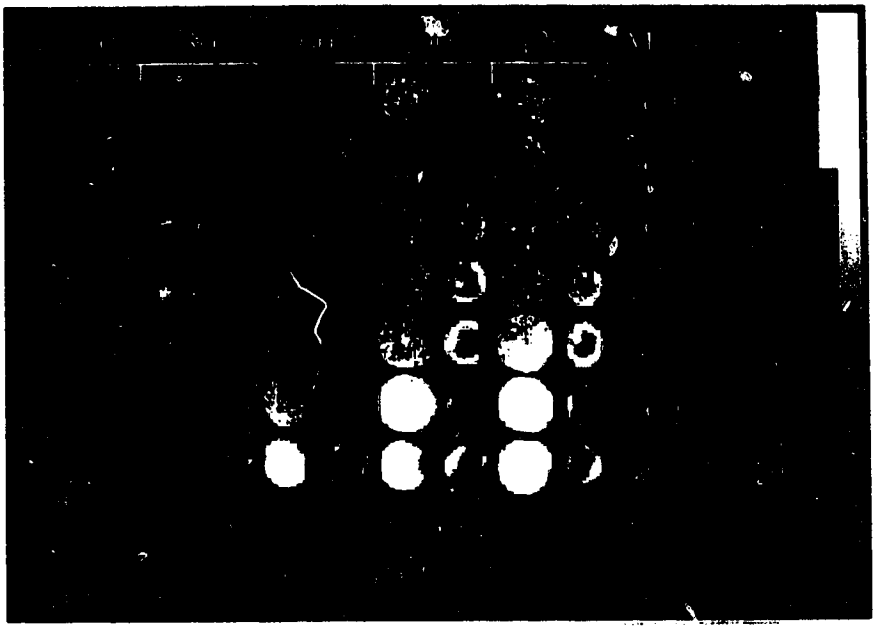

B

Uninduced	T=0	T=30	T=60	T=90	T=120
pCTDel	4.04	4.51	9.03	9.11	8.48
pCTRibo	3.83	6.47	8.88	7.36	6.64
pCTRiboC	4.47	7.97	9.54	7.94	7.35
pCTRibo1	4.10	6.37	9.11	7.61	7.07
pCTRibo1C	4.18	5.56	9.71	7.87	7.38
pCTRibo4	4.42	4.66	11.21	9.44	8.78
pCTRibo4C	3.56	5.81	12.32	10.10	9.97

C

Induced	T=0	T=30	T=60	T=90	T=120
pCTDel	4.04	4.73	5.51	4.85	4.08
pCTRibo	3.83	5.27	5.34	5.62	4.43
pCTRiboC	4.47	5.57	8.92	8.19	8.14
pCTRibo1	4.10	4.90	7.69	7.66	8.15
pCTRibo1C	4.18	5.92	6.49	6.61	7.98
pCTRibo4	4.42	3.70	5.01	4.33	5.50
pCTRibo4C	3.56	4.76	6.23	5.79	5.97

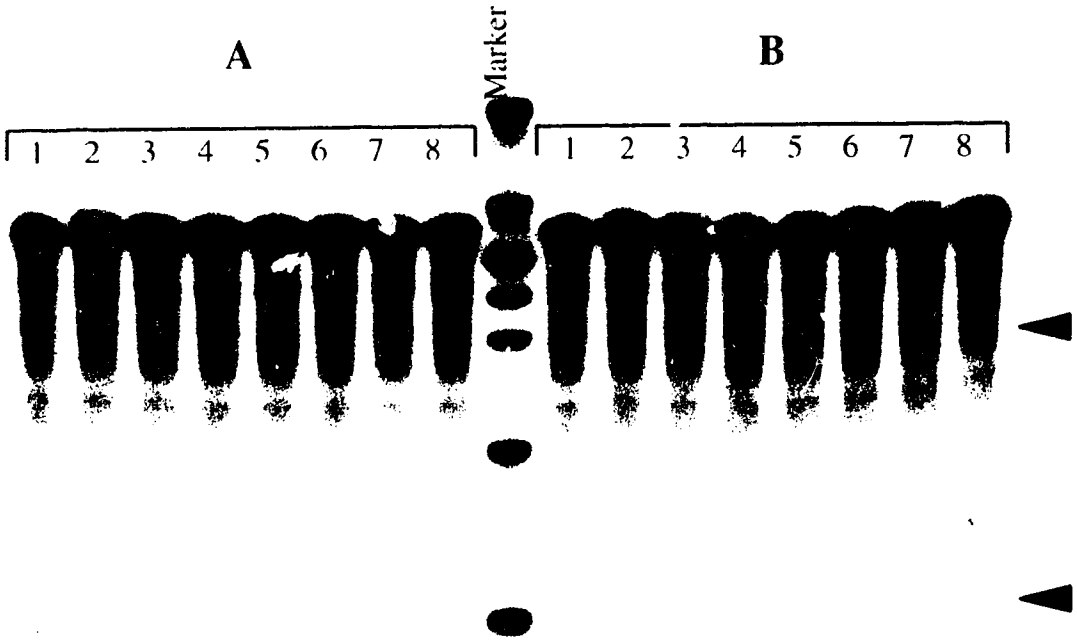

Figure 3.3

Ribozymes synthesised in *E. coli* cells are active against a luciferase target transcribed *in vitro* from pP1luxBS. Cleavage products are indicated by the arrows on the right. Size marker is pBR322 digested with HinfI.

A. 2 µg of total RNA isolated from *E. coli* cultures expressing luciferase from plasmid pLx403-*fab*9, and ribozymes from the following pCT vectors: 1, no pCT vector; 2, pCTDel; 3, pCT*ribo*; 4, pCT*riboC*; 5, pCT*ribo1*; 6, pCT*ribo1C*; 7, pCT*ribo4*; 8, pCT*ribo4C*. Total RNA was heat denatured prior to initiating the reaction.

B. As for A, without prior heat denaturation of the toat bacterial RNA.

Figure 3.4

Ribonuclease protection assay analysis of *lux*, CAT, and ribozyme mRNA from HMS174(DE3) cultures harbouring p403-15, and the indicated ribozyme vector.

A. 5 μg total RNA probed with transcripts from pP1luxBS digested with EcoRI, and transcribed with T7 RNA polymerase. Cultures were induced with IPTG for two hours at 37°C, followed by a further incubation for 30 minutes at 37°C (Lanes 1-7), or 47°C (Lanes 8-14). Lane 1, pCTDel; Lane 2, pCT*ribo*; Lane 3, pCT*riboC*; Lane 4, pCT*ribo1*; Lane 5, pCT*ribo1C*; Lane 6, pCT*ribo4*; Lane 7, pCT*ribo4C*. Lanes 8-14 are the same as Lanes 1-7, except incubated at 47°C. Luciferase probe fragments protected by full length luciferase mRNA is indicated by the arrow to the left. The size marker is pBR322 digested with HinfI.

B. As for **A**, probing for CAT mRNA and ribozyme RNAs. The CAT probe was generated by T3 RNA polymerase transcription from pCATBS digested with BamHI. Ribozyme probes were generated by T7 RNA polymerase transcription from the following plasmids digested with EcoRI: p*Ribo*BS for CTDel, CTribo, and CTriboC (Lanes 1-3, 8-10); p*ribo1*BS for CTribo1, and CTribo1C (Lanes 4-5, 11-12); p*ribo4*BS for CTribo4, and CTribo4C (Lanes 6-7, 13-14). Probe fragments protected by full length CAT mRNA, and ribozyme mRNA, are indicated to the right by the blue arrow, and the red arrow, respectively. The size marker is pBR322 digested with HinfI.

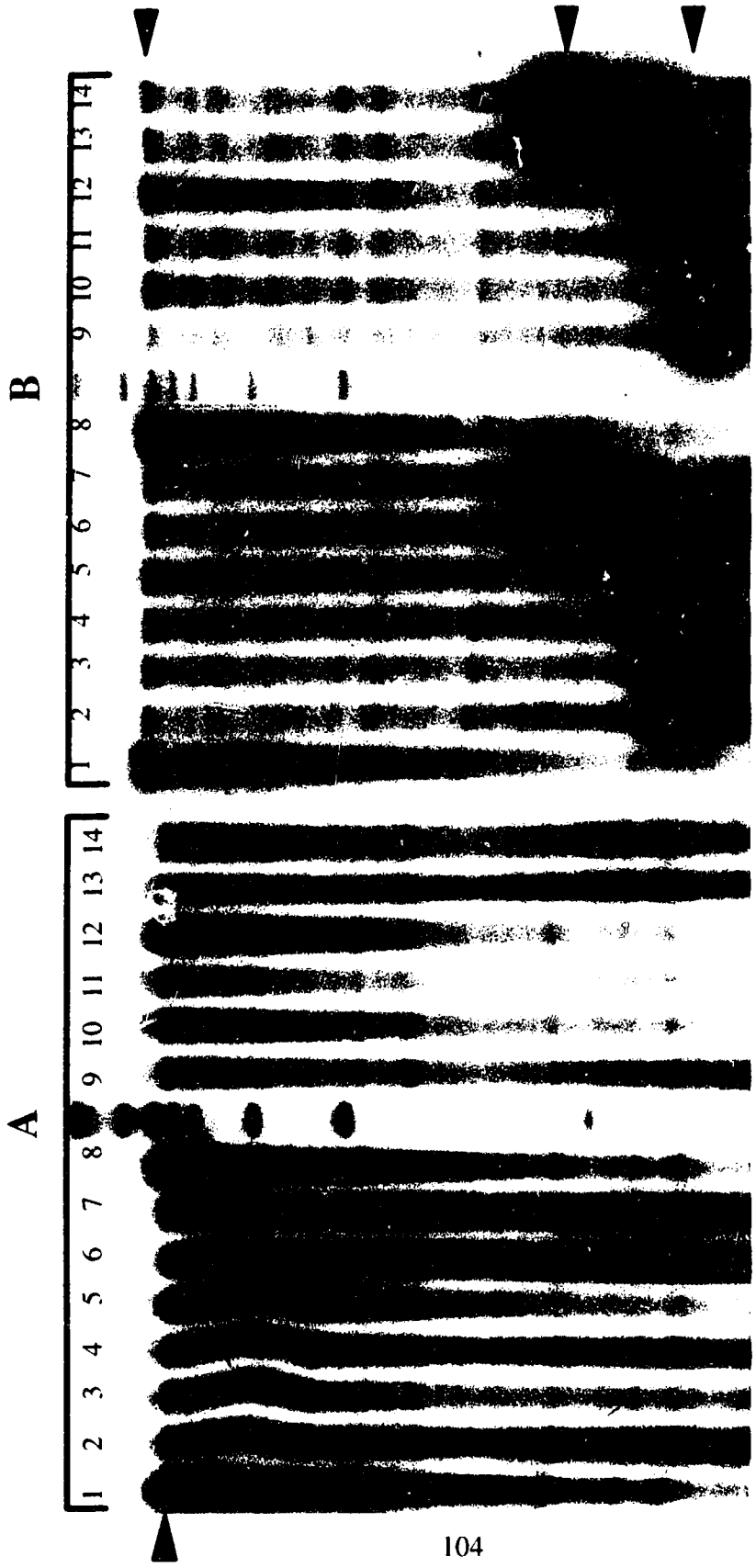
A
B
1 2 3 4 5 6 7 8 9 10 11 12 13 14
1 2 3 4 5 6 7 8 9 10 11 12 13 14

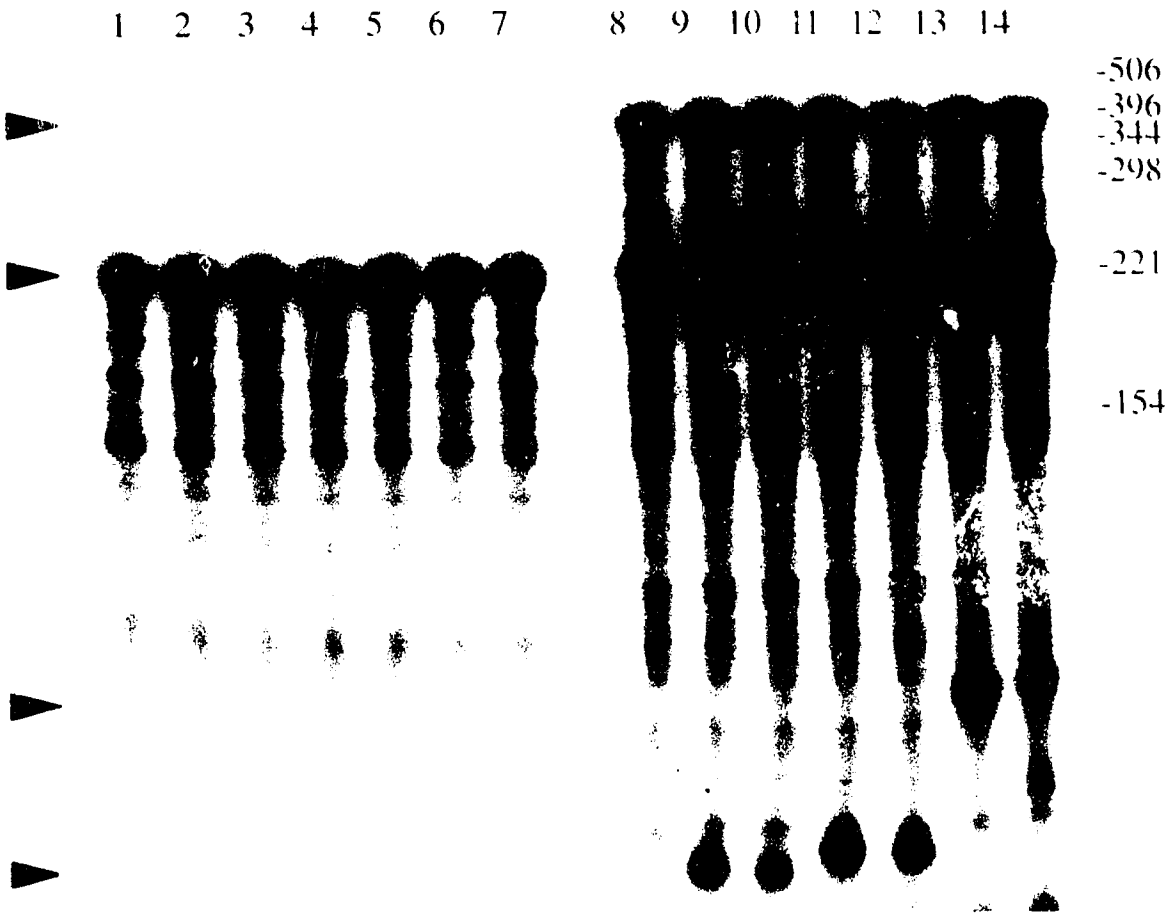

Figure 3.5

Ribonuclease protection assay analysis of lux, CAT, and ribozyme mRNA from HMS174(DE3) cultures harbouring pLx403-*fab*9, and the indicated pCT vector. Lanes 1 - 7; 5 µg total RNA probed with transcripts from pP1luxBS digested with EcoRI, and transcribed with T7 RNA polymerase. Cultures were induced with IPTG for two hours at 37oC, followed by supplementing the media with 50mg/L streptomycin and a further incubation for 30 minutes at 37oC. Lane 1, pCTDel; Lane 2, pCTribo; Lane 3, pCTriboC; Lane 4, pCTribo1; Lane 5, pCTribo1C; Lane 6, pCTribo4; Lane 7, pCTribo4C. Lanes 8-14 are the same as Lanes 1-7, using probes suitable for detection of lux mRNA, CAT mRNA, and the ribozymes present in total RNA. Probe fragments protected by full length lux mRNA, CAT mRNA, and ribozyme mRNA, are indicated to the left by the blue, black, and red arrows, respectively. The size marker is pBR322 digested with HinfI.

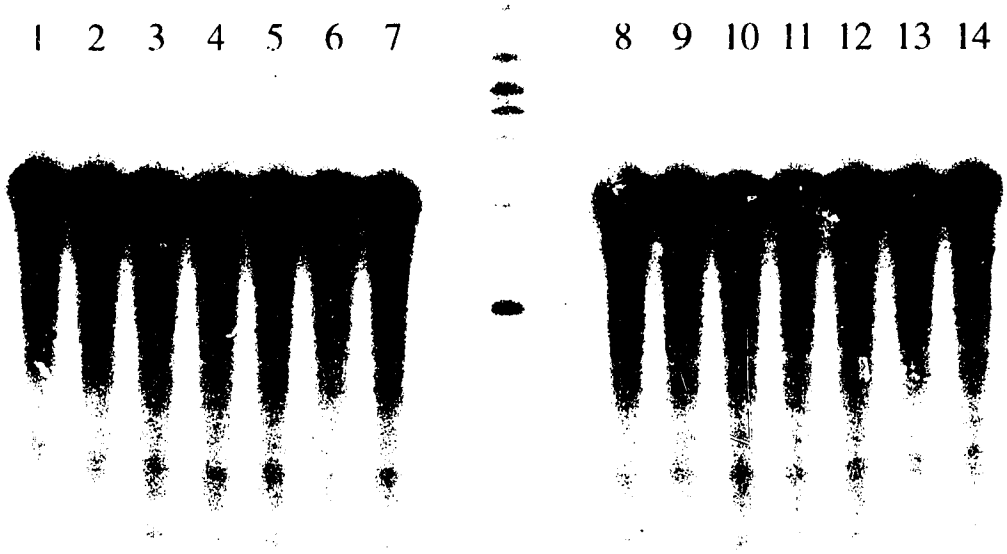

Figure 3.6

Ribonuclease protection assay analysis of isolated RNA treated with (lanes 1-7), and without (lanes 8-14), RQ1 DNase from cultures harbouring pLx403-*fab*9, and one of the pCT series of vectors. The luciferase probe was synthesised by T3 RNA polimerase *in vitro* transcription with of pP1luxBS digested with XbaI as template. Lane 1, pCTDel; Lane 2, pCT*ribo*; Lane 3, pCT*ribo*C; Lane 4, pCT*ribo1*; Lane 5, pCT*ribo1*C; Lane 6, pCT*ribo4*; Lane 7, pCT*ribo4*C; lanes 8-14, identical order as for lanes 1-7.

3.5 Bibliography

Carpousis, A. J., Houwe, G. V., Ehretsmann, C., Krisch, H. M. (1994). Copurification of *E. coli* RNAase E and PNPase: Evidence for a specific association between two enzymes important in RNA processing and degradation. *Cell* **76**, 889-900.

Chomczynski, P., Sacchi, N. (1987). Single-step method of RNA isolation by acid guanidinium thiocyanate phenol chloroform extraction. *Analytical Biochemistry* **162**, 156-159.

Chuat, J. C., Galibert, F. (1989). Can ribozymes be used to regulate procaryote gene expression. *Biochem. Biophys. Res. Commun.* **162**, 1025-1029.

Denman, R. B. (1993). Cleavage of full-length βAPP mRNA by hammerhead ribozymes. *Nucleic Acids Res.* **21**, 4119-4125.

Escher, A., Szalay, A. A. (1993). GroE-mediated folding of bacterial luciferases *in vivo*. *Mol. Gen. Genet.* **238**, 65-73.

Escher, A., O'Kane, D. J., Lee, J., Szalay, A. A. (1989). Bacterial luciferase αβ fusion protein is fully active as a monomer and highly sensitive *in vivo* to elevated temperature. *Proc. Natl. Acad. Sci. USA* **86**, 6528-6532.

Inokuchi, Y., Yuyama, N., Hirashima, A., Nishikawa, S., Ohkawa, J., Taira, K. (1994). A hammerhead ribozyme inhibits the proliferation of an RNA Coliphage SP in *Escherichia coli*. *J. Biol. Chem.* **269**, 11361, 11366.

Levitz, R., Wang, J., Sioud, M., Drlica, K. (1993). Expression of functional ribozymes in bacteria. *Methods: a Companion to Methods in Enzymology* **5**, 29-35.

Rosenberg, A. H., Goldman, E., Dunn, J. J., Studier, F. W., Zubay, G. (1993). Effects of consecutive AGG codons on translation in *Escherichia coli* demonstrated with a versatile codon test system. *J. Bact.* **175**, 716-722.

Sioud, M., Drlica, K. (1991). Prevention of human immunodeficiency virus type 1 integrase expression in *Escherichia coli* by a ribozyme. *Proc. Natl. Acad. Sci. USA*. **88**, 7303-7307.

Studier, F. W., Rosenberg, A. H., Dunn, J. J., Dubendorff, J. W. (1990) Use of T7 RNA polymerase to direct expression of cloned genes. *Methods in Enzymology* **189**, 60-89.

Uhlenbeck, O. C. (1987). A small catalytic oligoribonucleotide. *Nature* **328**, 596-600.

Watson, J. D., Hopkins, N. H., Roberts, J. W., Stietz, J. A., Weiner, A. M. (1987) In: *Molecular Biology of the Gene, Fourth Edition.* The Benjamin/Cummings Publishing Company, Inc., Menlo Park, California.

4. RIBOZYME ACTIVITY IN PLANT CELLS

4.1 Introduction

The use of hammerhead ribozymes to control the expression of deleterious genes in general, or to immunise against viral infection in plant cells has attracted attention from many laboratories. To date, the *in vivo* activity of hammerhead ribozymes in plants is not well characterised. Two reports claim to have identified ribozyme-mediated reduction of reporter gene transcript levels (Steinecke, *et al.*, 1992; Perriman, *et al.*, 1995), while a third (Massolini, *et al.*, 1992), reports on the failure of a ribozyme to inhibit target gene activity. All three were done in transiently transfected protoplasts, and the first two report the requirement for high levels of ribozyme transcript relative to target transcript.

Protoplast transfection for testing ribozyme constructs has advantages in comparison to stable transformation of plant tissues because it eliminates many of the variables involved with stable integration of genes into plant chromosomes. Particularly, position effects, in which the inserted gene takes on the expression characteristics of the surrounding chromatin, are eliminated because the transfecting DNA does not insert into the chromosome, and variation between transformants is avoided since a statistically significant population is generated, *i. e.*, $3x10^6$,or more, cells are transfected at a time. Expression levels obtained can be modulated by altering the amount of vector used per transfection, and promoters can be induced by incubation in media containing appropriate inducers post-transfection: a process which is hampered in whole plants by the complex morphology. In additon, the time requirements are reduced from months (regenerated transformed plants), or weeks (transformed callus tissue), to less than 48 hours after transfection.

In this chapter, experiments are discussed in which ribozymes designed to cleave various sites on the luciferase reporter gene transcript are tested by transient expression in plant protoplasts. The versatile plant cloning vector, pPCV701 (Koncz, *et al.*, 1987), is utilised as a gene delivery vector. The luciferase fusion gene is driven by the P1 promoter of the mannopine synthase dual promoter from the *Agrobacterium* Ti plasmid, while

expression of the ribozyme genes are driven in the opposite direction by the P2 promoter (Velten, *et al.*, 1984; Figure 4.1). Both components of the mannopine synthase dual promoter are induced by the addition of auxin, or by wounding, such that the substrate and catalyst are induced simultaneously (Langridge, *et al.*, 1989). This system is particularly advantageous since digestion of the cell wall in creating protoplasts presumably triggers a wound response, and protoplast culture media contains a high auxin to cytokinin ratio. The proximity of the two promoters (transcription start sites of the P1 and P2 promoter are approximately 350 nt apart (Velten, *et al.*, 1984)), may enhance ribozyme activity by co-localising the substrate and catalyst at the site of transcription. Co-localisation of ribozymes and target in virus particles is shown to significantly increase ribozyme effectiveness (Sullenger and Cech, 1993)

Transfection experiments were carried out with several plant cell suspension culture lines, with varying success. The popular tobacco Bright Yellow 2 (BY-2) (An, 1985), and the maize Black Mexican Sweet (BMS) (Fromm, *et al.*, 1987) lines worked very poorly in the hands of this investigator. An alfalfa (*Medicago sativa*) line, A2, was very robust and responded well to both Ca-PEG mediated transfection and electroporation. Repression of luciferase expression levels were analysed via enzyme activity, and mRNA quantification

4.2 Material and Methods

4.2.1 Media and Strains

Tobacco Bright Yellow (BY-2) suspension culture was obtained from Dr. Monica Bega. Maize Black Mexican Sweet (BMS) cultures were grown in the laboratory of Dr. A. Good, University of Alberta. Alfalfa A2 suspension cultures were obtained from Dr. Laszlo Bogre. Murashige Skoog (MS) minimal organic media (Murashige and Skoog, 1962) was obtained from JRH Biosciences, Lenexa, KS, and plant hormones were obtained from Sigma. Cell wall digestion enzymes, cellulase Y-C and pectolyase Y23 were obtained from Seishin Pharmaceutical Co., Ltd. (Tokyo, Japan). *E. coli* strain DH5α was used for all plasmid manipulations and isolations. All other suppliers are as previously described.

Tobacco BY-2 suspension cultures were grown as previously described (Maas and Werr, 1989). Alfalfa cultivar A2 suspension cultures were grown in A2 suspension media, consisting of MS minimal organic media supplemented with 2% sucrose, 0.25 g/L casamino acids, 180 mg/L KH_2PO_4, 1 mg/L thiamine, and 100 mg/L myo-inositol, 1.0 mg/L 2,4-D, 0.2 mg/L kinetin, pH 5.6. Cultures were grown in 50 ml volumes in 250 ml erlenmeyer flask with rotation at 100 rpm, at room temperature. Every three days, 20 ml of culture was subcultured into 30 ml of fresh A2 media.

4.2.2 Construction of ribozyme-containing plant cloning vectors

The *ribo*, and the *ribo4C* gene fragments were isolated by polyacrylamide gel purification following BamHI digestion of plasmids p*ribo*BS, and p*ribo4C*BS respectively. The *ribo1*, *ribo1C*, and *ribo4* ribozyme genes were prepared as described in Section 2.2.3. The *riboC* gene fragment was isolated by polyacrylamide gel purification following BamHI digestion of plasmid pPCV701FP$_1$R$_1$C, obtained from Dr. Alan Escher. pPCV701FP$_1$R$_1$C consists of the *riboC* synthetic gene downstream of the *mas* P2 promoter, and the luciferase fusion gene downstream of the *mas* P1 promoter in pPCV701. Dr. Escher identified the serendipitous mutation, A14T, in the sequence

GAAAC -> GATAC after sub-cloning the *ribo* gene fragment into pPCV701 (Alan Escher, personal communication).

Plasmid pmp19 was obtained from Dr. Monica Baga. pmp19 is a derivative of pPCV701-*lux*-A+B (Koncz, *et al.*, 1987), in which the luciferase genes A and B were removed (pmp19 is therefore identical to pPCV701). pmp19 was digested with BamHI and treated with CIP to prevent self ligation of the vector ends. The ribozyme genes with BamHI cohesive ends were ligated into the vector, downstream of the *mas* P2 promoter, and transformed into DH5α. Potential recombinant plasmids were isolated by alkaline lysis miniprep and screened by restriction endonuclease digestion with SalI and EcoRI in conjunction with agarose gel electrophoresis. To determine the orientation, and to ensure the correct sequence, vectors with a single insert were sequenced with Sequenase and the P2 sequencing primer (CCA ATA CAT TAC ACT AGC ATC TG), which produces a sequence initiating 31 nucleotides 5' of the BamHI restriction site. Suitable plasmids were amplified, and purified by CsCl gradient ultracentrifugation. Collectively, these ribozyme containing vectors are referred to as the 701 series, and individually are pPCV701R, pPCV701RC, pPCV701R1, pPCV701R1C, pPCV701R4, and pPCV701R4C.

Plasmid pPCV701-*lux*-FM1 was obtained from Dr. Jiang Chao, in which the BamHI and SalI sites at the 3' end of the *lux*F cassette of pPCV701-*lux*-FP1 were disrupted (Jiang, *et al.*, 1993). A 2.3 kb SalI-HindIII fragment consisting of the *lux* fusion gene upstream of the octopine synthase polyA tail signal (*Ocs*pA) was isolated from low melting point agarose. Each plasmid of the 701 series was digested with SalI and HindIII, treated with CIP to prevent the *Ocs*pA fragment from reinserting, and ligated with the *lux*F-*Ocs*pA fusion. Recombinant colonies were screened by colony hybridisation using a random-primed probe synthesised from an EcoRI/ClaI fragment from the *lux*B gene (Koncz, *et al.*, 1987). Colonies were also analysed by low light video imaging to check for insert orientation (ironically, strong light emission indicates a reverse orientation, since *lux* is not expressed from the P1 promoter in *E. coli)*. Colonies containing a *lux* insert were further analysed by EcoRI/PstI double digests. Constructs containing the luciferase fusion gene and the synthetic ribozyme genes are referred to collectively as the 701-*fab* series, and individually are referred to as pPCV701R-*fab*, pPCV701RC-*fab*,

pPCV701R1-*fab*, pPCV701R1C-*fab*, pPCV701R4-*fab*, and pPCV701R4C-*fab* (Figure 4.1).

4.2.3 Construction of pnptIIBS

Vector p*npt*IIBS was constructed for *in vitro* transcription of a probe suitable for ribonuclease protection assay analysis of transcript levels from the neomycin phosphotransferase gene (*npt*II) in plant tissues either transfected, or transformed with pPCV701 based vectors. pPCV699 (pPCV701 minus the *mas* P1 and P2 promoters) was digested with SphI, and the 5' overhangs were repaired with Klenow. The vector was digested with PstI, and a 350 nt fragment from the *npt*II gene, with one blunt end, and one PstI cohesive end was isolated from LMP agarose. pBluescript II KS+ was digested with BamHI, and the 5' overhangs were repaired with Klenow to create blunt ends. The vector was digested with PstI, and treated with CIP, before the 350 nt *npt*II gene fragment was ligated into it. Recombinant vectors were selected by alpha complementation, and screened by digestion with PvuII. Several clones were sequenced by Taq cycle sequencing with universal and reverse dye primers from ABI, and a single construct was selected for large scale plasmid isolation by CsCl centrifugation.

4.2.4 Ca-PEG mediated transfection of plant protoplasts

Suspension cultures were harvested in 50 ml falcon tubes, typically 25-40 ml of culture at a time. Cells were sedimented by centrifugation at 600 rpm for 4 minutes in a Sorvall Technospin bench top centrifuge. Culture media was decanted, and replaced with an equal volume of cell wall digestion media (0.1% cellulase Y-C, 0.01% pectolyase Y23, 2 mM MES, 5 mM $CaCl_2$, 0.5 mM Na_2HPO_4, 0.4 M mannitol, pH 5.6), transferred to petri dishes in 10 to 15 ml aliquots and incubated at room temperature in the dark with rotation at 40 rpm for a minimum of 5 hours. Prior to harvesting, cells were examined by light microscopy to ensure complete protoplasting.

Protoplasts were collected in 50 ml Falcon tubes by centrifugation at 30g for 4 minutes, and washed with an equal volume of protoplast wash solution (0.4 M mannitol, 25 mM $CaCl_2$ pH 5.8). Following the second wash, protoplasts were resuspended in

20 ml of protoplast wash solution, and the concentration was determined with a haemocytometer and inverted light microscope. Protoplasts were again sedimented and resuspended in a volume of protoplast wash solution to give a concentration of $1x10^7$ protoplasts per ml.

Typically, 20 µg of CsCl purified plasmid DNA (1 mg/ml) was placed in a 15 ml falcon tube, and 300 µl of protoplast solution was added with gentle mixing. 500 µl of Ca-PEG solution (20% PEG 8000, 100 mM $Ca(NO_3)_2$, 20 mM MES, 0.4 M mannitol, pH 6.0) was added immediately by introducing the solution to the side of the tube, and complete mixing was obtained by gentle tapping. Cultures were incubated for 20 minutes at room temperature, followed by the addition of 5 ml of transformation washing solution (0.275 M $Ca(NO_3)_2$, 44 mM mannitol, 20 mM MES, pH 5.6). Cultures were incubated at room temperature for a further 5 minutes and the protoplasts were sedimented by centrifugation at 600 rpm for 4 minutes. After decanting the supernatant, protoplasts were resuspended in 5 ml of protoplast culture media (MS salts, 0.4 M mannitol, 0.5% sucrose, 1.3 mM KH_2PO_4, 0.55 mM myo-inositol, 3 mM thiamine, 0.2 mg/L 2,4-D, 0.5 mg/L zeatin, pH 5.8) and transferred to small petri dishes (60 x 15 mm). Protoplasts were incubated in the dark for 24-48 hours prior to analysis.

Typically, four transfections were performed for each plasmid being analysed. Two transfections were used for analysing Lux expression levels by luminometry, and total RNA was isolated from the remainder.

4.2.5 Electroporation

Electroporation of BY-2 and alfalfa cells was carried out essentially as described (Langridge, *et al.*, 1985; Ecker and Davis, 1986), in a Bio-Rad Gene Pulser with Capacitance Extender. Protoplasts were prepared as above, washed in electroporation buffer (10 mM HEPES, pH 7.1, 150 mM NaCl, 4 mM $CaCl_2$, 0.2 M mannitol), and resuspended to $1x10^7$ cells/ml. Aliquots of protoplast suspension (500 µl) were gently mixed with 30 µg of the appropriate CsCl purified vector in a 4 mm gap electroporation cuvette (Bio-Rad), and incubated on ice for 10 minutes. Protoplasts were resuspended immediately prior to delivery of a single 250 volt discharge from a 500 microfarads (µF)

capacitor. Cuvettes were immediately returned onto ice for ten minutes, before gently transferring the cells to 60 mm diameter petri plates. Cultures were left for another ten minutes before adding 5 ml of protoplast culture media, as above.

4.2.6 Luciferase enzyme assay

Luciferase enzyme activity was quantified by luminometry, essentially as previously described (Koncz, *et al.*, 1987). Protoplasts were disrupted by sonication with a Model W-225R Heat Systems Ultrasonics Inc. (Plain View, NY.) sonicator for 5 seconds, with a standard tapered microtip probe, at a power setting of four. Luciferase activity from each transfection was expressed as a ratio, standardised against the activity obtained from cultures transfected with pPCV701-*lux*-FM1.

4.2.7 RNA isolation

Different RNA isolation procedures were utilised to extract RNA from the plant tissues used in this study.

1) Total RNA isolation using LiCl precipitation

Protoplast cultures ($3x10^6$ protoplasts, approximately 50 µl) were lysed by the addition of 200 µl of lysis buffer (5 M guanidinium *iso*-thiocyanate, 10 mM EDTA, 50 mM Tris-HCl, pH 7.5, 8% β-mercaptoethanol) followed by vortexing. Cellular debris was pelleted by centrifugation for 15 minutes at maximum speed in a microcentrifuge. The supernatant was transferred to a fresh Eppendorf tube and 7 volumes of 4 M LiCl was added. Total RNA was precipitated overnight at 4°C. RNA was pelleted by centrifugation for 30 minutes, and washed with an equal volume of 3 M LiCl, and centrifugation was repeated. RNA was resuspended in 100 µl solubilisation buffer (10 mM Tris-HCl pH 7.5, 1 mM EDTA, 0.5% SDS), and extracted with an equal volume of phenol, followed by phenol/chloroform (1:1), and finally with chloroform. Sodium acetate (pH 5.2) was added to a final volume of 0.3 M prior to the chloroform extraction to force the polysaccharides to the interface. RNA was precipitated with 2.5 volumes of -20°C 85%ethanol/15% methanol, for 1 hour at -20°C. The RNA pellet was washed with 70% ethanol and allowed to air dry.

2) Isolation of total RNA by centrifugation through a CsCl density gradient

Tissue was homogenised in solution D, as outlined for the AGPC method (below), followed by centrifugation to remove the cellular debris. 1.5 ml of RNase free CsCl solution (5.7 M CsCl, 0.1 M EDTA, pH 7.0) was placed in 5 ml polyallomer tubes (for the Beckman SW51 rotor), and the homogenate was carefully layered on top of the CsCl cushion to within 2 mm of the top of the tube. Solution D was loaded on top of the homogenate when not enough homogenate was available to fill the tube. The samples were then subjected to ultracentrifugation at 35 000 rpm, for 23 hours at 20°C, and the supernatant was carefully removed so as not to disturb the glass-like RNA pellet.

3) RNA isolation by acid guanidinium thiocyanate phenol chloroform (AGPC) extraction

This procedure is based on the protocol of Chomczynski and Sacchi, (1987). Fresh plant tissue was lysed in a 5 - 10 fold volume of solution D (4 M guanidinium thiocyanate, 25 mM sodium acetate, 0.5% sarcosyl, 0.1 M β-mercaptoethanol, pH 7.0). 0.1 volume of 2 M sodium acetate, pH 4.0, 1 volume of water-saturated phenol, and 0.2 ml of chloroform/isoamyl alchohol mixture (49:1) were added in sequence, with thorough mixing after the addition of each reagent. The solution was vortexed for 10 seconds and cooled on ice for 15 minutes at 4°C. The aqueous phase was transferred to a fresh tube without disturbing the interface (which contains proteins and DNA, due to the acidity of the aqueous phase). One volume of isopropanol was added to precipitate the RNA, and the tubes were incubated at -20°C for at least one hour, followed by centrifugation at maximum speed in a microcentrifuge at 4°C for 15 minutes. The RNA pellet was resuspended in 0.3 ml of solution D and transferred to a 1.5 ml Eppendorf tube. The RNA was again precipitated with 1 volume of isopropanol at -20°C for one hour, and pelleted by centrifugation for 15 minutes. The resulting pellet was washed with 75% (v/v) ethanol and air dried.

For each method described, isolated RNA was solubilised in DEPC-treated H_2O to a concentration of 1-3 mg/ml, as determined by spectrophotometry. RNA quality was

determined by resolving 1 μg on an agarose gel and comparing the intensities of the 28S and 18S ribosomal bands. If necessary, an additional chloroform extraction step with 0.3 M sodium acetate was used to reduce the amount of insoluble material, followed by precipitation of the RNA.

4.2.8 RNA analysis

High resolution mapping, and quantifying of specific transcripts was performed by ribonuclease protection assays on 20 μg of total RNA, using an RPA II Ribonuclease Protection Assay Kit from Ambion, according to the manufactures instructions. RPA probes specific for luciferase and ribozyme mRNA were prepared as described in section 3.2.6. Plasmid p*npt*IIBS linearised with HindIII was the template for *in vitro* transcription with T7 RNA polymerase to produce probes specific for neomycin phosphotransferase mRNA. *In vitro* transcription was performed as described in section 3.2.6, with the exception that the specific activity of ribozyme probes was not reduced.

4.3 Results

4.3.1 Selection of suspension cultures

Ca-PEG transfection of plasmid DNA for transient expression studies were initiated with BY-2 tobacco suspension cultures. Although other members of the laboratory had had success with this line, in the hands of this investigator, luciferase expression, as determined by luminometry, was very low, frequently indiscernible from background. Similar poor results were obtained with maize BMS. An alfalfa cell line, A2, however, worked surprisingly well, with very little alteration of the methodologies used for BY-2 cultures. Microscopic analysis of BY-2 cultures following cell wall digestion revealed a significant proportion of lysed, and generally unhealthy protoplasts, indicating that protoplasting was too harsh. Microscopic analysis of digested alfalfa cells revealed primarily healthy protoplasts, spherical in shape with central vacuoles and nuclei.

Electroporation of protoplasts was carried out with 200, 300, and 450 volt discharges, with either 500 μF, or 960 μF capacitance. Increasing voltage and capacitance resulted in increased clumping, as determined by microscopy, following electroporation and dilution of the cultures in protoplast culture media. Clumping was interpreted as deleterious since it indicates excessive disruption of the outer memberane. Also, after the desired incubation time, increased voltage and capacitance resulted in bleached pellets after harvesting, indicating numerous dead cells. BY-2 cultures failed to produce measurable light emission, whereas alfalfa cultures gave good expression with even the harshest treatments tested. 200 and 300 volts, with capacitance of either 500 μF or 960 μF gave essentially the same results in terms of photon emission, and 250 volts with 500 μF resistance was chosen for future experiments.

4.3.2 Analysis of luciferase activity

Luciferase activity in transfected protoplasts was determined by luminomety, and the expression of each transfection was standardised against pPCV701-*lux*-FM1 transfection controls. pPCV701-*lux*-FP2 (Langridge, *et al.*, 1991) was included in all experiments as an indication of expression from the *mas* P2 promoter (Figure 4.1), and

therefore as an indirect measure of ribozyme transcript levels. In most experiments, ribozyme genes, and ribozyme control genes carried by the 701-*fab* series were transfected in parallel to control for antisense affects. In co-transfection studies (*i. e.*, luciferase fusion genes and ribozyme genes were delivered on separate plasmids), equal masses of pPCV701-*fab*-FM1 and the desired 701 series vector were used. Cultures incubated between 32 and 42 hours post-transfection gave the best luciferase expression, as determined by photon emission.

The results of 20 independent studies are documented in Table 4.1, according to the date of the transfection. The values for each date are the averages of between 2 and 6 measurements. The overall average, and sample standard error for each vector, or combination of vectors, is also given.

Luciferase activity of pPCV701-*lux*-FP2 transfected cultures relative to pPCV701-*lux*-FM1 transfected cultures indicate the *mas* P2 promoter is on average 5.8 times more active than the *mas* P1 promoter, and suggest that ribozymes are 5.8 fold more prevalent than *lux* transcripts. Levels of luciferase activity in transfections with the 701-*fab* series, except pPCV701R-*fab*, are within standard error limits of pPCV701-*lux*-FM1, indicating that ribozyme, or antisense-mediated luciferase repression is not occurring. Luciferase activity in pPCV701R-*fab* transfected cultures, however, is on average 43% lower than that of pPCV701-*lux*-FM1, demonstrating that luciferase activity is repressed in these cultures. That expression levels of pPCV701RC-*fab* are not reduced implies that the observed reductions may be occurring via target transcript cleavage, or could potentially be artifact, as discussed below.

Plasmids utilised in these experiments were isolated by CsCl density gradient centrifugation, and analysed by electrophoresis to ensure that there was no visible chromosomal DNA contamination, and that concentrations of covalently closed circular plasmid were consistent. However, slight differences in plasmids concentration, or structure resulting from breakage during freeze-thaw cycles, could result in the observed differences through cumulative effects. Plant expression vectors derived from pPCV701 contain a ColE1 origin of replication, and are therefore present in each *E. coli* cell in relatively low copy numbers. A mutation occurring in the luciferase fusion gene on one

plasmid during plasmid amplification would be replicated throughout the growth of the culture, and therefore could also contribute to the reduce levels of *lux* gene activity in pPCV701R-*fab* transfected protoplasts. It is noted that the most significant reductions in luciferase activity between pPCV701R-*fab* and pPCV701-*lux*-FM1, and particularly between pPCV701R-*fab* and pPCV701RC-*fab*, occur prior to the experiment performed on April 22, 1992, and fresh plasmid was isolated on April 1, 1992, supporting the second possibility. The ribozyme gene on pPCV701R-*fab* was sequenced from the freshly isolated plasmid and found to be correct, indicating that the increase in *lux* expression after April 1, 1992 was not a result of a mutation in an otherwise active ribozyme.

To test for the possibility of luciferase repression resulting from a random mutation in the *lux*F gene, pPCV701-*lux*-FM1 was co-transfected with pPCV701R and pPCV701RC. Ribozyme, or antisense mediated repression of *lux* expression would therefore require uptake of both plasmids into a single cell. The proportion of cells taking up both plasmids is the square of the fraction of cells taking up a single plasmid, so repression to the same extent as observed with pPCV701R-*fab* is not expected. Nevertheless, no significant repression was found, suggesting that the repression occurring in pPCV701R-*fab* is specific to that construct. Two possible pPCV701R-*fab* specific factors which could repress luciferase expression are 1) co-localisation effects of having the ribozyme and substrate genes on the same plasmid, or 2) differences in plasmid stock solutions, such as those discussed above.

4.3.3 Analysis of RNA isolated from transfected plant protoplasts

Different RNA isolation procedures were used to obtain high quality total RNA from protoplast cultures. All utilised the chaotropic agent, guanidinium isothiocyanate (GIT), to rapidly lyse the cells, and denature proteins (Berger and Chirwin, 1989). RNA was purified by 1) precipitation with LiCl, 2) sedimentation through a CsCl cushion, or 3) by acidic phenol removal of proteins and DNA. The first two protocols were eventually deemed inadequate, since LiCl and CsCl do not efficiently pellet small molecular weight RNA (Bird, 1986; and results not shown), which could jeopardise the recovery of the

ribozymes. The acid guanidinium thiocyanate phenol chloroform method was used for most isolations (Chomczynski and Sacchi, 1987).

Attempts to analyse RNA by Northern blotting, S1 nuclease analysis, and primer extension were unsuccessful, presumably due to low levels of mRNA of interest in total RNA populations. Ribonuclease protection assays (RPA) were selected as the method of choice for relative quantification, and high resolution mapping of mRNA. RPAs are advantageous because aqueous hybridisation in conjunction with polyacrylamide gel electrophoresis offers sensitivity and resolution not available with Northern blots, and the use of a body labelled probe allows greater sensitivity than obtained with end labelled probes used in S1 and primer extension analysis.

Of the independent transfections presented in Table 4.1, six were analysed for luciferase transcripts by ribonuclease protection assay, four of which are presented in Figure 4.2. Luciferase mRNA makes up less than 0.0005% of total RNA isolated from transfected protoplasts, as determined by comparing the density of each band against a standard curve (not shown). A direct comparison between *lux* transcript abundance, and luciferase activity cannot be made, however a correlation is expected (*i. e.*, high levels of luciferase activity are expected to correspond with abundant transcripts) (Ayre, *et al.*, 1993). Such a correlation does exist for pPCV701R-*fab*, in that *lux* mRNA abundance is lower with this vector, than with pPCV701-*lux*-FM1 when luciferase activity is also lower. If the reduction in luciferase activity were the result of a point mutation, as discussed above, the level of transcript would not be reduced, unless the mutation were in the promoter region, or mRNA stability were compromised. No bands corresponding to cleavage products are visible.

Analysing *lux* transcript levels, relative to *npt*II transcripts levels, standardises transcript levels between cultures, and controls for transfection efficiency, since the *npt*II gene is transcribed from the same plasmid (Figure 4.3). Probing for ribozymes gives a direct measure of ribozyme abundance relative to *lux* transcript abundance. The density ratios of bands corresponding to luciferase RNA probe fragments protected by *lux* mRNA, and *npt*II mRNA-protected probe fragments obtained from cultures transfected with pPCV701R1-*fab* and pPCV701R4-*fab* are 8% less than, and 4% greater than those

obtained with pPCV701-*lux*-FM1 (all are within 6% of the mean), suggesting that *lux* mRNA levels are not reduced relative to *npt*II mRNA. This correlation strengthens the use of *npt*II transcript levels as an internal control, since luciferase enzyme activity is also not reduced in pPCV701R1-*fab* and pPCV701R4-*fab*, relative to pPCV701-*lux*-FM1 transfected protoplasts. Similar analysis with pPCV701R-*fab* transfected protoplasts, and protoplasts co-transfected with pPCV701-R and pPCV701-*lux*-FM1, do not demonstrate a reduction in luciferase mRNA abundance relative to *npt*II mRNA abundance. These results with *npt*II transcript levels as an internal standard support the possibility that the observed average reduction in luciferase enzyme activity in protoplasts transfected with pPCV701R-*fab* (Table 4.1), relative to controls, as determined by luminometry, is not due to ribozyme-mediated transcript elimination.

4.4 Discussion

The ability of hammerhead ribozymes to limit the expression of a reporter gene *in vivo* was tested via transient transfection in plant protoplasts. This method proved to be very rapid and reliable in comparison to analysis in stably transformed plant tissues, discussed in the following chapter. The activity of a particular ribozyme against its target is analysed within 48 hours of transfection, whereas stable integration requires a minimum of two weeks for analysis of callus tissue, and a minimum of 6 weeks for the analysis of defined plant tissues. Fluctuation between samples resulting from position effects or copy number effects are eliminated, because the plasmid DNA is not integrated into the chromosome (apart from rare recombination events), and DNA is delivered to several million cells at a time. As well, gene expression can be modulated through appropriate incubation conditions, and RNA isolation is facilitated since the protoplasts have not developed a cell wall with sufficient strength to resist immediate lysis by guanidinium *iso*-thiocyanate solutions. Delivery of target and ribozyme genes on the same plasmid is advantageous because every cell that receives one gene also recieves the other in a 1:1 ratio. However, a potential disadvantage of delivering the target and ribozyme genes on the same plasmid is that the target gene delivered to different cultures is not derived from a common stock, and creates a source of variability between samples.

The majority of transfections herein were performed by permeabilising the outer membrane with a Ca-PEG solution, followed by what is presumably passive diffusion of the DNA into the cells, and to the nucleus. Recently, an electroporation protocol was adapted, which appears to work as well, if not better than Ca-PEG transfection, in terms of reporter gene expression. The electroporation procedure involves less centrifugation and mixing, and no timed incubations in specialised solutions, each of which can introduce variability between samples. The electric pulse delivered by capacitor discharge subjects all samples to identical conditions (Fromm, *et al.*, 1987), and enables more samples to be conveniently manipulated by an individual researcher. In combination, these factors should reduce experimental variability between transfected cultures.

Choice of suspension cultures was crucial to these experiments. Two cell lines found commonly in the literature, BY-2, and BMS, failed to generate reproducible results. An alfalfa cell line performed well with Ca-PEG transfection and electroporation. Why the alfalfa line is more suited to protoplasting and transfection is unknown. The choice of cell line is not expected to affect the activity of ribozymes in transient expression studies, since all cultures are in an undifferentiated state, and exposed to the same conditions. However, in whole plant tissues, the different tissue types may have different activities as a result of the differentiated environment.

Ribozyme-mediated target gene repression was not observed for ribozymes ribo1 or ribo4 at the enzyme activity level, or the mRNA level. Likewise, antisense-mediated repression was not seen for the corresponding control constructs. However, repression of luciferase activity was observed in cultures transfected with pPCV701R-*fab*, with a corresponding reduction in *lux* mRNA. The reduction in luciferase activity observed in 14 independent transfections is statistically significant, and cannot be attributed to reduced transfection efficiency. However, it can be attributed to the quantity of covalently closed circular plasmid transfected, or mutations within the luciferase expression unit. That the repression is not the result of ribozyme-mediated transcript elimination is suported by 1) an apparent derepression of activity following isolation of fresh plasmid, 2) failure to repress activity in co-transfection assays with pPCV701-*lux*-FM1 and pPCV701R, and 3) identical ratios of *lux* mRNA to *npt*II mRNA in cultures transfected with pPCV701R-*fab*, and those transfected with pPCV701-*lux*-FM1, or pPCV701RC-*fab*.

Curiously, transcripts containing *npt*II sequences are more prevalent in pPCV701-*lux*-FP2 transfected cultures than in pPCV701-*lux*-FM1 transfected cultures. It is doubtful that increased transfection efficiency can account for the increase in *npt*II transcript levels, since there is no precedence for more efficient uptake of pPCV701-*lux*-FP2. The increase in *npt*II mRNA abundance may be attributable to differences in the upstream transcription unit of pPCV701-*lux*-FP2, and pPCV701-*lux*-FM1 and the 701-fab series. The 701-*fab* series produce a relatively short transcript (<200 nt) originating from the P2 promoter, whereas pPCV701-*lux*-FP2 results in a relatively long transcript (>2000 nt). Evidence is available that RNA polymerase II

processivity is altered during the transcription of a gene as a result of the addition, or loss of elongation factors, or phosphorylation. For example, attenuators are recognised more efficiently the closer they are to the promoter (Roberts and Bentley, 1992), and although attenuatation and termination probably do not share a common mechanism, RNA polymerase II may be more inclined to dissociate from the DNA following transcription of a short gene, than a long gene. Therefore the precedence is set for increased *npt*II transcription by either direct read through, or enhanced initiation at the *nos* promoter driving the *npt*II gene due to an increased concentration of "transcription ready" polymerases from the *lux* gene. However, this issue is not of particular importance to this study, since the *npt*II probe is primarily an internal control for standardising mRNA levels originating from the same promoter between cultures transfected with different pPCV701 based vectors.

Steinecke *et al.*, (1992) and Perriman *et al.*, (1995) report ribozyme-mediated gene repression in *Nicotiana tabacum* cultivar petit Havana SRI protoplasts and *Nicotiana tabacum* cultivar Xanthi protoplasts respectively. The first study (Steinecke *et al.*, 1992) reports a reduction in the levels of a targeted neomycin phosphotransferase transcript in protoplasts carrying a functional ribozyme, when compared to control transfections. Both genes were delivered independently, or together, on separate plasmids, and both utilised the cauliflower mosaic virus (CaMV) 35s promoter, and the CaMV 35s terminator. A mutant ribozyme was used as a negative control, which differed from the active ribozyme by a single nucleotide change in the sequence GAAAC -> GAGAC (A14G).

Target transcripts from the *npt*II gene in protoplasts co-transfected with a target vector and a four fold molar excess of ribozyme vector were analysed by ribonuclease protection assays. A protected *npt*II probe fragment corresponding to the expected 118 nt 5' cleavage product was detected from cells co-transfected with an active ribozyme gene, whereas cells co-transfected with the control ribozyme gene had the full length protected fragment only. The 3' cleavage product was not identified, presumably due to endogenous RNase activity. This is the only published report of a cleavage product being identified *in vivo* in a higher eukaryotic organism. Enzymatic activity of the *npt*II reporter gene product was monitored in similar co-transfection studies. Increasing ratios of ribozyme to

target resulted in increased repression. A 100 fold molar excess of ribozyme-containing plasmid completely abolished *npt*II activity, whereas a 10 fold molar excess, which is in the range of the molar excess of ribozyme obtained herein, reduced activity to 42%. 46% and 70% activity remained with the same molar excesses of control ribozyme, relative to independently transfected controls. The authors speculate that the antisense effect of the mutant overestimates the antisense effect of the active complex, based on minimal energy analysis of the the active, and control sequences. No *in vitro* data was presented, but it would be interesting to compare the catalytic activity of the Steinecke *et al.*, construct with other *in vitro* work.

Perriman *et al.*, (1995) have recently reported selective repression of a chloramphenicol acetyl transferase transcript by a hammerhead ribozyme, and incorporated several interesting modifications in the vector design for delivery, and into the ribozyme expression cassette. The CAT target, the active ribozyme, and the various controls were subcloned into an autonomously replicating vector derived form the African cassava mosaic geminivirus (ACMG), such that the vector is localised in the nucleus, where it replicates to high levels. The ribozyme and antisense control were subcloned into the ACMV vector in one of two configurations: 1) the ribozyme and antisense control were subcloned into a multiple cloning site (MCS) downstream of the ACMV coat protein promoter and 2) the ribozyme and antisense control were embedded into a tyrosine tRNA cassette which was subcloned in to the MCS. The MCS also contained a T7 promoter, such that the same vector was suitable for *in vivo* and *in vitro* analysis.

CAT enzyme assays performed on protoplasts co-transfected with tRNA-embedded ribozyme vectors demonstrated repression to less than 20% of the activity in protoplasts transfected with CAT vector alone. Ribozymes genes subcloned directly into the MCS reduced CAT activity to 40% of controls, and antisense RNA corresponding to the ribozyme guide sequences reduced CAT activity to 60-70% of controls. The ratio of ribozyme plasmid to CAT plasmid in each case was 3. The tRNA cassette was more efficient presumably because RNA polymerase III transcription led to higher levels of ribozyme transcription, and because the secondary structure of the tRNA cassette increased the half-life of ribozyme message - allowing it to accumulate to higher

levels. 5' or 3' cleavage products were not directly demonstrated, however a reverse PCR approach was utilised to suggest that 3' cleavage products were 3.3 fold more prevalent than full length CAT mRNA in total RNA isolated from protoplasts transfected with a tRNA-embedded ribozyme. It is worth noting that in this study, the 3' fragment was detected, whereas the other group detected the 5' product.

A third group published the failure of a ribozyme to inhibit target gene activity in *Arabidopsis thaliana* (var. Columbia) protoplasts (Massolini *et al*, 1992). The target for cleavage was transcripts from the β–glucuronidase (GUS) gene inserted downstream of the translation elongation factor A1 (EF-1α A1) promoter, and upstram of a CaMV polyA signal. A ribozyme, antisense oligo, or antisense GUS sequences were inserted downstream of a CaMV 35s promoter, and upstream of a nopaline synthase (*nos*) polyA signal in each of the respective test plasmids. Co-transfection experiments did not result in GUS repression for either the ribozyme or the antisense oligo constructs, even when very high (>4000:1) ratios of ribozyme vector to target vector were used. The ribozymes were estimated to comprise 0.25% of the total mRNA. The antisense GUS construct reduced GUS activity to 2% of controls. The activity of the ribozyme was further tested by a *cis*-acting ribozyme, in which the ribozyme was sub-cloned into the 3' untranslated region of the GUS construct, 1340 nt downstream of the target site. Slight repression of GUS activity was seen with this ribozyme (13.5%) over an antisense control (7%), relative to GUS expression in protoplasts transfected with the GUS construct alone. *In vitro* cleavage assays utilising targets and ribozymes which had nearly identical sequences to the *in vivo* counterparts, except for the 5' cap structure and 3' poly A tail, were shown to cleave *in vitro* at 50°C, with reduced activity at 20°C. Ribozyme activity was however minimal *in vitro*, explaining why the ribozymes did not work *in vivo*.

Figure 4.1

Construction of plasmids for delivery of ribozyme genes, and luciferase fusion genes to plant cell suspension cultures, and for stable insertion of genes into plant genome (Chapter 5).

A. Ribozyme catalytic domain, derived from the satellite RNA of tobacco ringspot virus, and the A to T mutation in the control domain, inserted into the BamHI site of pPCV701 (Koncz, *et al.*, 1987), to create the 701-*fab* series of ribozyme vectors.

B. Region of pPCV701-*lux*-FM1 between the left and right T-DNA borders. Please see Figure 1.2 for explanation of labels. Restriction sites are H, HindIII; E, EcoRI; P, PstI; S, SalI; B, BamHI. pPCV701 is equivalent to pPCV701-*lux*-FM1, without the *lux* fusion gene: the 701 series of ribozyme vectors is pPCV701 with the ribozymes (and controls) inserted into the BamHI site downstream of the P2 promoter.

C. Region of pPCV701-*lux*-FP2 between the left and right T-DNA borders. Please see Figure 1.2 for explanation of labels. Restriction sites are H, HindIII; E, EcoRI; P, PstI; S, SalI; B, BamHI. pPCV701-*lux*-FP2 is used as a control for estimation of ribozyme transcript levels in transfected cultures.

A

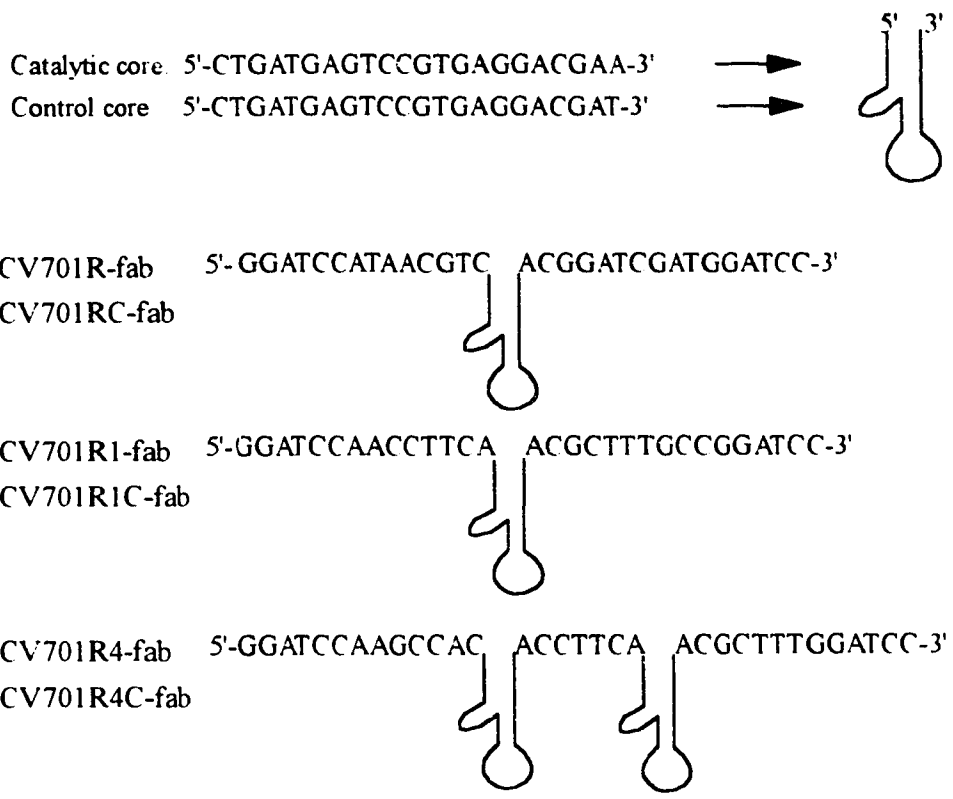
Catalytic core 5'-CTGATGAGTCCGTGAGGACGAA-3'
Control core 5'-CTGATGAGTCCGTGAGGACGAT-3'
5'
3'
pPCV701R-fab 5'-GGATCCATAACGTC ACGGATCGATGGATCC-3'
pPCV701RC-fab
pPCV701R1-fab 5'-GGATCCAACCTTCA ACGCTTTGCCGGATCC-3'
pPCV701R1C-fab
pPCV701R4-fab 5'-GGATCCAAGCCAC ACCTTCA ACGCTTTGGATCC-3'
pPCV701R4C-fab

B

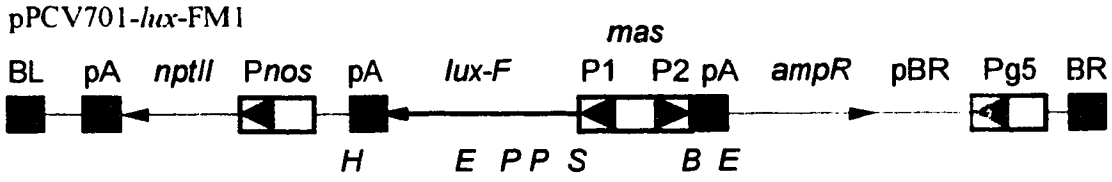
pPCV701-lux-FM1
mas
BL pA nptII Pnos pA lux-F P1 P2 pA ampR pBR Pg5 BR
H E P P S B E

C

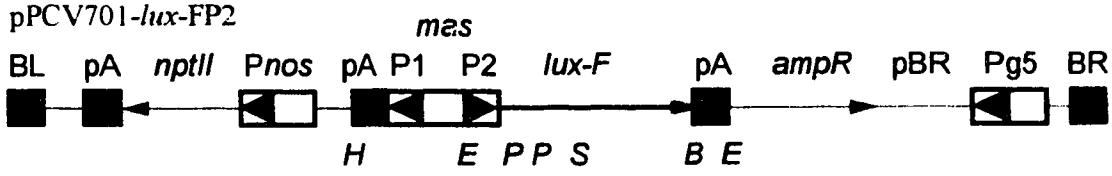
pPCV701-lux-FP2
mas
BL pA nptII Pnos pA P1 P2 lux-F pA ampR pBR Pg5 BR
H E P P S B E

Table 4.1

Luciferase activity in transiently transfected alfalfa suspension cultures. Results of each experiment are listed according to the date of the transfection. Plasmid DNA used in the transfections are listed across the top. All values are luciferase activity ratios relative to the activity of cultures transfected with pPCV701-*lux*-FM1. Reps is the number of independent transfections carried out with the respective plasmid, or combination of plasmids. Average is the average ratio relative to pPCV701-*lux*-FM1. Std Err is the sample standard error. Underlined dates were also analysed by RNase protection assay, and those marked with an asterisk are represented in Figure 4.2.

Transfection Date	Control (no vector)	pPCV701-lux-FP2	pPCV701-lux-FM1	pPCV701 R-fab	pPCV701 RC-fab	pPCV701 R1-fab	pPCV701 R1C-fab	pPCV701 R4-fab	pPCV701 R4C-fab	pPCV701-lux-FM1 +pPCV701 R	pPCV701-lux-FM1 +pPCV701 RC
24/11/91	0.02	13.25	1.00								
27/11/91	0.09	4.51	1.00			1.07	1.19	0.83	0.63		
2/12/91	0.07	6.44	1.00	0.07	0.91			2.13	1.28		
3/12/91		11.93	1.00	0.23	1.46			1.47	1.26		
10/12/91	0.01	4.24	1.00	0.20	1.31						
01/02/92	0.12	9.20	1.00	0.28	2.45	1.86					
12/02/92	0.01	8.14	1.00			1.27	1.35	0.89	0.34		
21/03/92	0.08	3.43	1.00	0.13	1.29					0.66	
*24/03/92	0.01	5.46	1.00	0.20	1.03					0.69	1.12
22/4/92	0.00	3.11	1.00	0.64	0.97					0.49	0.54
22/05/92	0.05	3.76	1.00	0.47	0.35					1.84	1.99
*23/05/92	0.07	6.70	1.00	1.09	2.35					3.85	5.23
*19/02/93a		3.11	1.00	0.80	0.73						
*19/02/93b		1.43	1.00	0.54	0.41						
8/04/93	0.00	7.88	1.00	0.58	0.93						
10/04/93	0.00	4.88	1.00							1.08	0.86
18/04/93	0.00	2.53	1.00	1.07	0.96					1.32	1.04
04/06/94	0.00	4.51	1.00	0.49	0.28	0.72	0.51				
10/06/95		6.08	1.00	1.71	0.78	1.17	0.45				
15/6/95		5.58	1.00							1.53	1.17
Reps	15	20	20	15	15	5	4	4	4	8	7
Average	0.04	5.81	1.00	0.57	1.08	1.22	0.87	1.33	0.88	1.43	1.71
Std Err	0.01	0.68	0.00	0.11	0.16	0.18	0.23	0.30	0.23	0.38	0.61

Figure 4.2

Ribonuclease protection assay results; total RNA isolated from transfections summarised in Table 4.1. The probe used was synthesised with T7 RNA polymerase from pP1*lux*BS linearised with EcoRI. The top arrow in each figure corresponds to protected probe fragments resulting from luciferase mRNA transcribed from the *mas* P1 promoter, and the bottom arrow corresponds to protected probe fragments resulting from luciferase mRNA transcribed from the *mas* P2 promoter. Size markers (pBR322 digested with HinfI) are indicated

A. Transfection of 23/05/92, 10 µg of total RNA isolated from cultures transfected with the vector indicated: Lane 1, pPCV701-*lux*-FP2; Lane 2, identical to Lane 1, using ten fold less RNase solution; Lane 3, no vector DNA; Lane 4, pPCV701-*lux*-FM1; Lane 5, pPCV701R-*fab*; Lane 6, pPCV701RC-*fab*.

B. Transfection of 19/02/93a, and 19/02/93b, 20 µg of total RNA isolated from cultures transfected with the vector indicated: Lane 1, no vector DNA; Lane 2 and 3, pPCV701-*lux*-FP2 (19/02/93a and 19/02/93b, respectively); Lane 4 and 5, pPCV701-*lux*-FM1; Lane 6 and 7, pPCV701R-*fab*; Lane 8 and 9, pPCV701RC-*fab*.

C. Transfection of 24/03/92, 20 µg of total RNA isolated from cultures transfected with the vector indicated: Lane 1, Size standard; Lane 2, pPCV701-*lux*-FP2; Lane 3, pPCV701R-*fab*; Lane 4, pPCV701RC-*fab*; Lane 5, pPCV701-*lux*-FM1; Lane 6, pPCV701-*lux*-FM1, co-transfected with pPCV701R; Lane 7, pPCV701-*lux*-FM1, co-transfected with pPCV701RC.

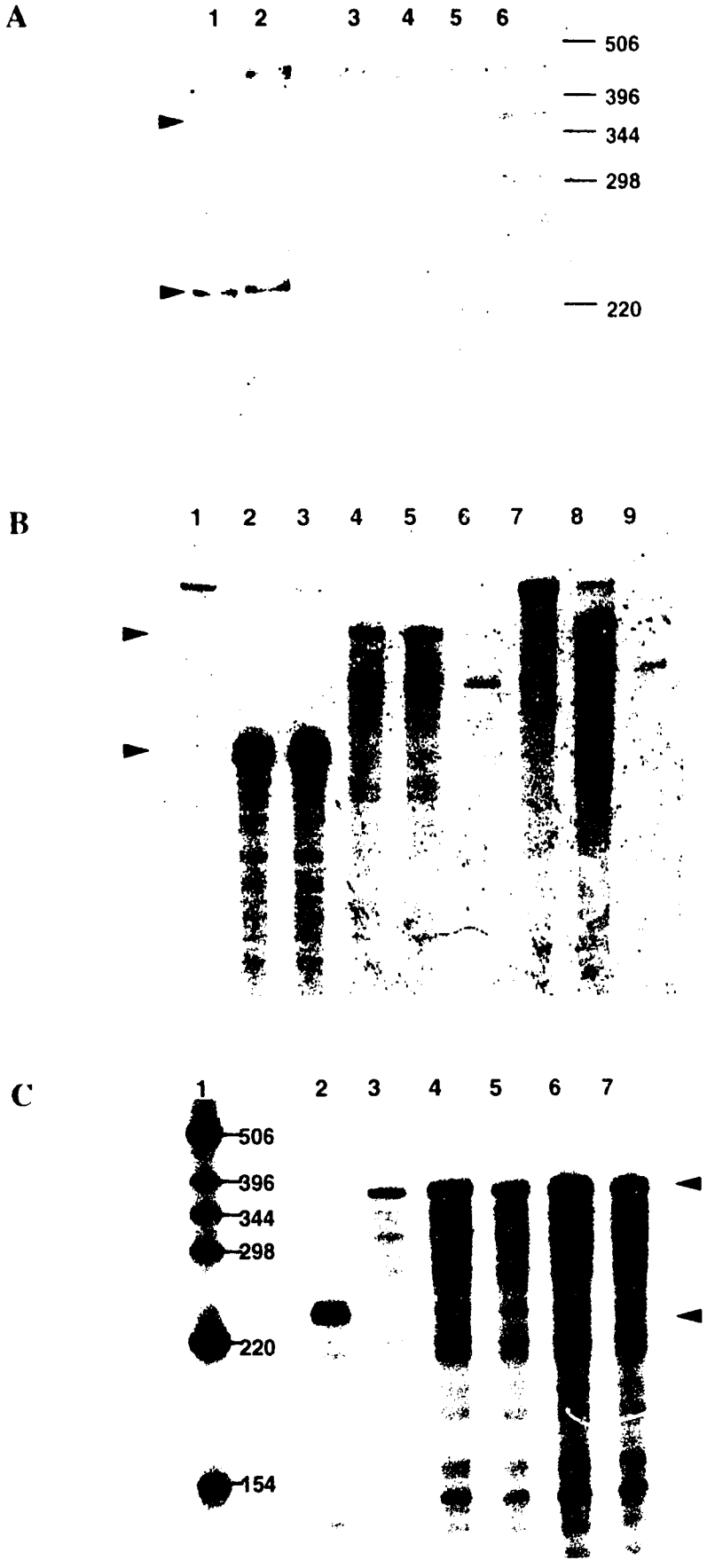
A
1 2 3 4 5 6
506
396
344
298
220
B
1 2 3 4 5 6 7 8 9
C
1 2 3 4 5 6 7
506
396
344
298
220
154

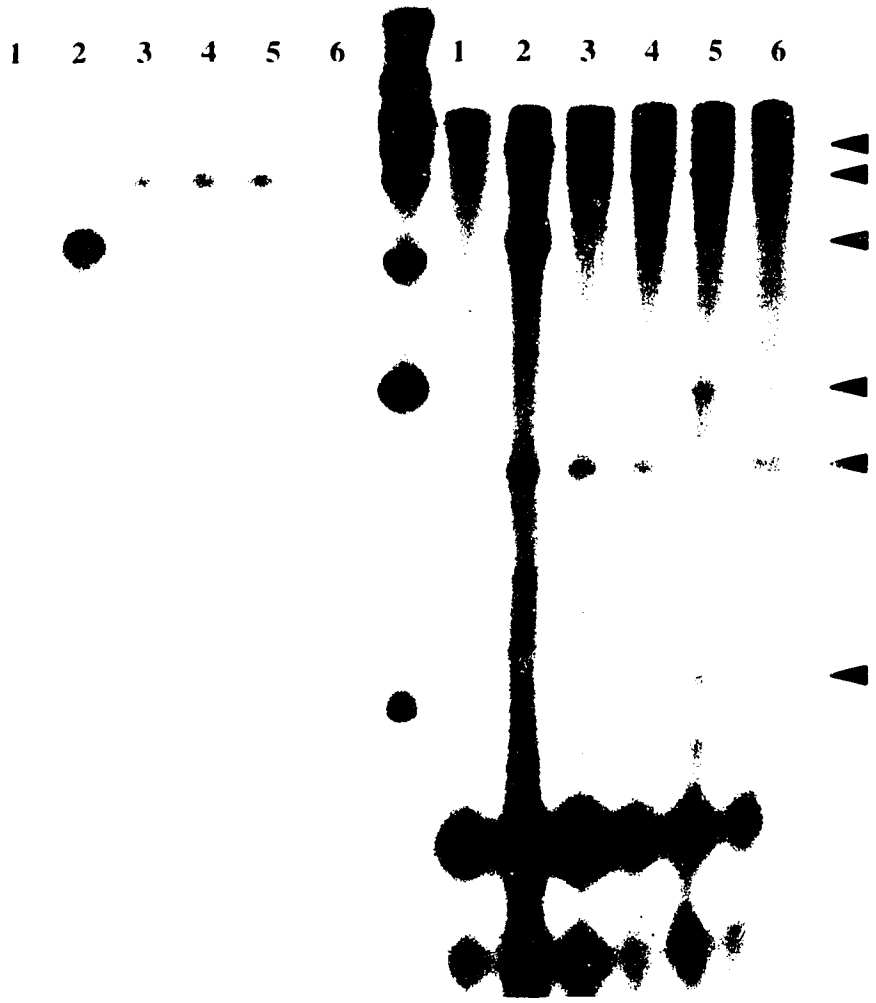

Figure 4.3

Ribonuclease protection assay results from transiently transfected alfalfa protoplasts. Left: 20 µg of total RNA with *lux* probe. Lane 1, untransfected control; Lane 2, transfected with pPCV701-*lux*-FP2; Lane 3, transfected with pPCV701-*lux*-FM1; Lane 4, transfected with pPCV701R1-*fab*; Lane 5, transfected with pPCV701R4-*fab*; Lane 6, 20 µg yeast RNA. Right: Identical to the left, with *npt*II probe, *lux* probe, and *ribo*1 probe, except Lane 5, which uses a *ribo*4 probe. Size marker is pBR322 digested with HinfI. Arrows on the right correspond to, from top to bottom: *npt*II probe fragment protected by *npt*II mRNA, *lux* probe fragment protected by full length *lux* mRNA from the *mas* P1 promoter, *lux* probe fragment protected by full length *lux* mRNA from the *mas* P2 promoter, undigested ribo4 probe, undigested ribo1 probe, and ribo4 probe fragment protected by ribo4 ribozyme RNA. Ribo1 probe fragments protected by ribo1 RNA are obscured by background.

4.5 Bibliography

An, G. (1985). High-efficiency transformation of cultured tobacco cells *Plant Physiol.* **79**, 568-570.

Ayre, B. G., Escher, A., Szalay, A. A. (1993). Bioluminescence as a measure of ribozyme activity in vivo. In: *Bioluminescence and Chemiluminescence Status Report: Proceedings of the VII International Symposium on Bioluminescence and Chemiluminescence.* Eds: Szalay, A. A., Kricka, L. J., and Stanley, P. John Wiley, and Sons., New York.

Berger, S., L., Chirgwin, J., M. (1989). Isolation of RNA. *Methods in Enzymology* **180**, 3-13.

Bird, R. C. (1986). Selective loss of small RNAs during isolation by the guanidinium thiocyanate/cesium chloride gradient method. *BioTechniques* **4**, 202-204.

Bogre, L., Olah, Z., Dudits, D. (1988). Ca^{2+}-dependent protein kinase from alfalfa (*Medicago varia*): partial purification and autophosphorylation. *Plant Science* **58**, 135-144.

Chomczynski, P., Sacchi, N. (1987). Single-step method of RNA isolation by acid guanidinium thiocyanate phenol chloroform extraction. *Analytical Biochemistry* **162**, 156-159.

Ecker, J. R., Davis, R. W. (1986). Inhibition of gene expression in plant cells by expression of antisense RNA. *Proc. Natl. Acad. Sci. USA.* **83**, 5372-5376.

Fromm, M. E., Callis, J., Taylor, L. P., Walbot, V. (1987). Electroporation of DNA and RNA into plant protoplasts. *Methods Enzymol.* **153**, 351-366.

Jiang, C., Escher, A., Szalay, A. A. (1993). Alteration of a luciferase-based binary plant transformation vector for simultaneous expression of desired gene products and bacterial luciferase in transgenic plants. In: *Bioluminescence and Chemiluminescence Status Report: Proceedings of the VII International Symposium on Bioluminescence and Chemiluminescence.* Eds.: Szalay, A. A., Kricka, L. J., and Stanley, P. John Wiley, and Sons, New York.

Koncz, C., Olsson, O., Langridge, W. H. R., Schell, J., Szalay, A. A. (1987) Expression and assembly of functional bacterial luciferase in plants. *Proc. Natl. Acad. Sci.* USA. **84**, 131-135.

Langridge, W. H. R., Li, B. J., Szalay, A A. (1985). Electric field mediated stable transformation of carrot protoplasts with naked DNA. *Plant Cell Reports*, **4**, 355-359.

Langridge, W. H. R., Fitzgerald, K. J., Koncz, C., Schell, J., Szalay, A. A. (1989). Dual promoter of *Agrobacterium tumefaciens* mannopine synthase genes is regulated by plant growth hormones. *Proc. Natl. Acad. Sci. USA*. **86**, 3219-3223.

Langridge, W. H. R., Escher, A., Szalay, A. A. (1991). Measurement of bacterial luciferase as a reporter enzyme *in vivo* in transformed bacteria, yeast, plant cells, and in transgenic plants. *Technique* **3**, 99-108.

Maas, C., and Werr, W. (1989). Mechanism and optimised conditions for PEG mediated DNA transfection into plant protoplasts. *Plant Cell Reports* **8**, 148-151.

Mazzolini, L., Axelos, M., Lescure, N., Yot, P. (1992). Assaying synthetic ribozymes in plants: high-level expression of a functional hammerhead structure fails to inhibit target gene activity in transiently transformed protoplasts. *Plant Molecular Biology* **20**, 715-731.

Murashige, T., Skoog, F. (1962). A revised medium for rapid growth and bioassays with tobacco tissue cultures. *Physiol. Plant* **15**, 473-497.

Perriman, R., Bruening, G., Dennis, E. S., Peacock, W. J. (1995). Effective ribozyme delivery in plant cells. *Proc. Natl. Acad. Sci. USA*. **92**, 6175-6179.

Steinecke, P., Herget, T., Schreier, P. H. (1992). Expression of a chimeric ribozyme gene results in endonucleotytic cleavage of target mRNA and a concomitant reduction of gene expression *in vivo*. *EMBO J.* **11**, 1525-1530.

Sullenger, B. A., Cech, T. R. (1993). Tethering ribozymes to a retroviral packaging signal for destruction of viral RNA. *Science* **262**, 1566-1569.

5. WHOLE PLANT SYSTEMS

5.1 Introduction

In order for hammerhead ribozymes to be effective agents for controlling gene expression in plants, they must be stably integrated into the plant genome. The most frequently employed method for stable insertion of genes into the plant genome is *Agrobacterium tumefaciens* mediated gene transfer. In nature, *Agrobacterium* induces crown gall disease in numerous dicotyledonous species by transferring hormone biosynthetic genes on a specific portion of DNA, known as the T-DNA (transfer DNA) from the Ti plasmid (tumour inducing) to the plant genome (Zambryski, 1988; 1992). Genetic manipulation of the T-DNA and the Ti plasmid has enabled researchers to delete the natural biosynthetic genes, and replace them with useful genes of interest (Herrera-Estrella, *et al.*, 1983; Koncz and Schell, 1986).

Using *Agrobacterium*-mediated gene transfer techniques, endogenous genes of interest have been specifically repressed by transferred genes encoding RNA complementary (antisense) to the mRNA of the gene of interest. Antisense RNA has emerged as a reliable method for gene repression in higher plants, primarily due to limitations in other gene knock-out techniques in plant systems (section 1.6). The catalytic properties of ribozymes make ribozymes potentially advantageous to antisense RNA. Direct comparisons between ribozymes and antisense controls in plant cell protoplasts support this premise (Steincke, *et al.*, 1992; Perriman, *et al.*, 1995), however a direct comparison in transgenic, regenerated plants is not presently available. Ribozymes are demonstrated to significantly reduce reporter gene transcript levels (60% reduction relative to mRNA transcript levels found in parent plants lacking the ribozyme gene), with a two fold steady state excess of ribozyme transcripts (Wegener, *et al.*, 1994).

In this chapter, experiments are described which assess the feasibility of using ribozymes to control gene expression in transformed plants. Ribozyme genes encoding ribozymes targeted to luciferase mRNA, fused to the *mas* P2 promoter, were inserted into the genome of *Nicotiana tabacum* cultivar SR1 in one of two fashions: 1) ribozyme genes

were transformed in conjunction with the luciferase gene, on the 701-*fab* series of vectors (Figure 4.1), or 2) ribozyme genes were transformed independently with the 701 series of vectors into a transgenic tobacco line expressing the luciferase gene from an endogenous promoter. In the latter case, the pattern of luciferase expression in the plants prior to insertion of the ribozyme construct is characterised (Jiang, 1994), such that any observed changes in luciferase expression may be attributed to effects imparted by the second T-DNA insert. Characterisation of luciferase activity, and transcript levels in *Arabidopsis thaliana* is also discussed.

5.2 Materials and Methods

5.2.1 Plasmids, strains and media

The 701 and 701-*fab* series of vectors, pPCV701-*lux*-FP2 and pPCV701-*lux*-FM1 were used in this study, and are described in Chapter 4. *E. coli* strain DH5α was used for plasmid amplification, and strain S17-1 (RP 4-2 (Tc::Mu), (Km::T7), Tp, Sm, Pro, *res*-, *mod*+, *rec*A-) (Simon, *et al.*, 1983) was used for conjugal transfer of the above vectors to *Agrobacterium tumefaciens*. *Agrobacterium tumefaciens* strain GV3101(pMP90RK) (Koncz and Shell, 1986) was used for transfer and integration of the T-DNA of the above vectors into the plant genomes. *E. coli* strains were grown as previously described. *Agrobacterium* was grown in either liquid or on solid (1.5% agar) YEB media (Gibco beef extract (5 g/L), Bacto yeast extract (1 g/L), Bacto peptone (1 g/L), sucrose (5 g/L)). YEB + Mg^{2+} was YEB media supplemented with 10 mM $MgCl_2$. Antibiotics were ampicillin (Ap), 100 mg/L; carbenicillin (Cb), 100 mg/L; kanamycin (Km), 100 mg/L; rifampicin (Rif), 100 mg/L; and gentamycin (Gm), 25 mg/L.

Plant tissues utilised were *Nicotiana tabacum* cv. SR1, obtained from Dr. W. Langridge, *N. tabacum* cv SR1, transgenic line 12-1, obtained from Dr. C. Jiang, and *Arabidopsis thaliana* ecotype Columbia, obtained from Dr. G. Redei. Media for all plant tissue culture was MS minimal organic media, solidified with either 0.8% agar, or 0.22% Gel Rite gellan gum (Scott Laboratories, Inc., West Warwick, R. I.) supplemented with thiamine (1 mg/L), myo-inositol (100 mg/L), KH_2PO_4 (180 mg/L), 3% sucrose for tobacco, and 2% sucrose for *Arabidopsis*. Antibiotics were cefotaxim (Claforan (Cl) Roussel), 400 mg/L, and kanamycin (Km), 100 mg/L. Plant hormones (obtained from Sigma) for tobacco shoot formation were naphthalene acetic acid (NAA), and benzylaminopurine (BAP). Seeds were generally germinated on sterile media, supplemented with appropriate antibiotics for transgenic material. Plants were either maintained on sterile media with 12 hours of artificial light at 25°C, or transferred to Metro Mix (Grace Horticultural Products, Ajax, ON.) and grown under greenhouse conditions.

5.2.2 Bacterial conjugation

The 701 series, the 701-*fab* series, pPCV701-*lux*-FM1 and pPCV701-*lux*-FP2 vectors were isolated by CsCl gradient centrifugation, and transformed into *E. coli* strain S17-1 for conjugal transfer into *Agrobacterium tumefaciens* strain GV3101(pMP90RK). Each S17-1 culture harbouring the respective plasmids were plated to LB + Ap and grown overnight. GV3101(pMP90RK) was streaked on YEB + Km + Rif + Gm. Several loops of each S17-1 culture were resuspended in YEB + Mg^{2+} broth, washed, and resuspended to a concentration of $6x10^8$ cells/150 µl (as determined by spectrophotometry, OD=600), and the GV3101(pMP90RK) was resuspended to $2x10^8$ cells/100 µl. The dilutions were mixed, and plated to YEB + Mg^{2+} (w/o selection) for overnight growth.

Several loops of the co-cultivated cells were resuspended in YEB + Mg^{2+} and adjusted to a concentration of $1x10^8$ cells per 100 µl. One hundred and fifty µl, and 50 µl of each mixture was plated to YEB + Mg^{2+} + Gm + Km + Rif + Cb media and grown for 2-3 days at 29°C. Colonies of each of the *Agrobacterium trans*-conjugants were streaked on fresh media to obtain single colonies, and subsequently plated to master plates.

5.2.3 Analysis of trans-conjugants

Master plates with *trans*-conjugant colonies were screened for the presence of either a 701 series vector, or a 701-*fab* series vector, by colony hybridisation (Ausubel, *et al.*, 1994) with a random-primed probe labelled with digoxigenin dUTP (Boehringer Mannheim). The template for probe synthesis was a 700 bp EcoRI-PstI fragment isolated from pBR322, corresponding to a portion of the gene encoding ampicillin resistance (*bla*). Colonies were also screened by low light video imaging. Colonies detected by hybridisation, and demonstrating high levels of luciferase activity, were selected for further analysis.

Plasmid DNA was isolated from 5 ml *Agrobacterium* cultures by a standard alkaline lysis miniprep, double digested with EcoRI and PstI, and analysed by EtBr

staining of agarose gels, and Southern blotting using a ^{32}P labelled probe synthesised from pPCV701-*lux*-FM1 by random primed labelling.

Ribozyme inserts were amplified by PCR in preparation for Taq cycle sequencing. The 5' forward primer was the P2 sequencing primer (section 4.2.2), and the 3' reverse primer was g7pA-M13 (TGT AAA ACG ACG GCC AGT GAC TGA GTG CGA TAT TAT G) which contains 18 nt of universal primer at its 5' end, such that amplified sequences would contain a universal primer binding site. Approximately 100 ng of DNA isolated from *Agrobacterium* was mixed with 50 pmoles of both g7pA-M13 and P2 sequencing primer, in a standard 50 µl PCR reaction mixture. Initial denaturation was for five minutes at 94°C, and amplification was carried out for 30 cycles of 1) 1 minute at 94°C, 2) 1 minute at 55°C, and 3) 2 minutes at 72°C. PCR products were extracted with phenol/chloroform, precipitated with ethanol, and resuspended in 25 µl of ddH_2O. PCR products were resolved on either 8% non-denaturing polyacrylamide gels, or 1.2% agarose gels stained with EtBr, as well as quantitated by spectrophotometry.

100 ng of double stranded PCR product was sequenced by Taq cycle sequencing, using the ABI labelled universal primer as per the manufacture's instructions.

5.2.4 Plant transformation

Tobacco leaf disk transformation and culture conditions were essentially as described (Horsch, *et al.*, 1985; Koncz and Schell, 1986). *Trans*-conjugant *Agrobacterium* cultures were grown overnight in 10 ml YEB + Gm + Km + Rif + Cb broth at 25°C on a rotary shaker. Cultures were concentrated by centrifugation, and resuspended in 10 ml of YEB broth without antibiotics. Leaf disks, 1 cm in diameter, were excised from sterile *N. tabacum* cultivar SR1 plants grown on MS + 3% sucrose solid media and submersed in the *Agrobacterium* suspension for approximately 5 minutes. Wild-type SR1 leaf disks were submersed in cultures harbouring the 701-*fab* series, while leaf disks from the 12-1 transgenic line were submersed in cultures carrying the 701 series. Leaf disk explants were briefly placed on sterile filter paper to remove excess *Agrobacterium*, and subsequently transferred to MS + 3% sucrose solid media. After 2 days co-cultivation, explants were transferred to shooting media (MS media + 3%

sucrose, 0.1 mg/L NAA, and 0.5 mg/L BAP) + Cl + Km to prevent further *Agrobacterium* propagation, and for selective growth of transformed plant cells. Media for 12-1 leaf disks was supplemented with hygromycin (Hm), 20 mg/L (the original T-DNA insert in 12-1 plants contains a hygromycin resistance gene). Explants were sub-cultured every one to two weeks to fresh media. Shoots approximately 3 cm in size were excised and transferred to MS + 3% sucrose + Cl (+ Hm for 12-1) media in sterile jars to initiate root formation. Plantlets 5 cm is size with good root formation were transferred to Metro Mix in 6 inch pots, and grown to maturity in the greenhouse for RNA or luciferase analysis, and for seed collection.

Transformation of *Arabidopsis* was as described (Marton and Browse, 1991), and transgenic plants were grown to seed in foam-plugged test tubes (20 mm x 150 mm) (Redei, *et al.*, 1988).

5.2.5 Seed collection and seed sterilisation

For seed collection, tobacco plants were self-fertilised by covering the flower buds with porous plastic bags (Cryovac Crispy-wrap bags, RAP-ID Paper and Packaging, Inc., Edmonton, AB.) to prevent contact with neighbouring plants under crowded greenhouse conditions, and to minimise the possibility of pollen transfer. Seeds were collected from mature seed pods, and stored in small plastic bottles (25 ml), or 2 ml glass vials. No extra precautions were used for *Arabidopsis*, since *Arabidopsis* typically self fertilises (Meyerowitz and Pruitt, 1985). Tobacco seeds were sterilised in 1.5 ml Eppendorf tubes by immersion in 20% commercial bleach for 7 minutes, followed by a brief wash (<2 minutes) in 70% ethanol, and several washes in sterile distilled H_2O. *Arabidopsis* seeds were sterilised by immersion in 70% ethanol for 5 minutes. Seeds were air dried overnight in a laminar flow hood.

5.2.6 Tissue collection and analysis

For RNA isolation, or luciferase activity assays via luminometry, desired tissue (*i. e.*, whole leaves or portions of flowers) were harvested and placed in polypropylene bags in the greenhouse, and stored on ice. Detailed excision of tissues suitable for analysis

was carried out at the lab bench. RNA isolation was as described (section 4.2.7), from fresh tissue homogenised in solution D solution. Fresh tissue was also used for luminometry, as described (section 4.2.6; Langridge *et al.*, 1991). Analysis of tobacco tissues was performed on the T1 generation (transgenic plants regenerated from the original explant), or the T2 generation (self-fertilised offspring of the T1 generation). For *Arabidopsis*, RNA and luciferase analyses were carried out on tissue derived from T2, or T3 generation plants.

5.3 Results

5.3.1 Plant cell transformation

Agrobacterium-mediated transformation of tobacco leaf explants generated more kanamycin resistant shoots than could be conveniently manipulated. The number of plants regenerated and grown to seed was therefore limited by required time commitment and space.

Agrobacterium-mediated transformation of *Arabidopsis* root explants (Marton and Browse, 1991) was, however, relatively recalcitrant to *Agrobacterium* infection. The number of kanamycin-resistant calli on each root explant was variable between infections, possibly as a function of differential virulence between *Agrobacterium* cultures harbouring the individual 701-*fab* vectors. *Arabidopsis* calli eventually became embryogenic, resulting in clumps of small plantlets, each of which were not independently transformed. Obtaining second generation (T2) seeds from the transformed (T1) generation was necessary, since not enough T1 tissue was generated for analysis, and the stress of growing on synthetic media would bias the results in comparison to plants grown under natural soil conditions. Obtaining T2 seeds was hampered primarily by two co-operative factors: 1) *Arabidopsis* regenerated from root explants do not readily develop roots, and therefore were grown to maturity in sterile media, and 2) *Arabidopsis* does not set seed under the high humidy conditions intrinsic to aseptic cultures. Growing the transgenic *Arabidopsis* plantlets on synthetic media in test tubes sealed with foam plugs allowed enough aeration to partially overcome the latter problem, but viable seeds were not obtained from many plants which matured to flowering. Therefore, *Arabidopsis* transformed with the vectors pPCV701R1-*fab*, and pPCV701R4-*fab* are not presently available, preventing analysis of ribozyme activity.

5.3.2 Luciferase analysis - whole plant systems

Plant tissues from transgenic tobacco, and *Arabidopsis*, at several stages of development were analysed for luciferase activity by luminometry to determine which tissue was most suitable for RNA isolation and analysis. The assumption was made that

enhanced levels of enzyme activity would correlate with enhanced transcript levels, based on experiments carried out with alfalfa protoplasts (Ayre, *et al.*, 1993)

Most of the luciferase enzyme activity analysis was carried out relative to fresh weight, estimating the amount of tissue utilised between samples. In general, one 20 mm diameter tobacco leaf disk, or approximately 200 mg of flower buds, meristematic tissue, or the upper portion of mature flowers (including petal tips, anthers, and stigma), was ground for each assay. The fresh weight quantities of *Arabidopsis* tissue analysed for luciferase activity was less than that used for tobacco, but equivalent amounts were estimated between individual transformants. In instances where luciferase activity levels were measured as a function of light units per mg protein, the protein concentrations in the homogenate fluctuated within a factor of three, well within the accuracy required for these estimations of tissue activity.

Generally, transgenic leaf tissue carrying the *lux* gene cassette downstream of the mannopine synthase P1 promoter (pPCV701-*lux*-FM1, and the 701-*fab* series) did not demonstrate activity significantly above that of negative controls. Young tissue near the top of the plants, *i. e.*, flowers, buds, meristems and immature leaves, exhibited the highest levels of luciferase activity, in both tobacco and *Arabidopsis* (results not shown). This is most likely the results of the high concentrations of young dividing and expanding cells, as well as the effect of increased hormone concentrations in these tissues. pPCV701-*lux*-FP2 plants were approximately 10 fold more active than pPCV701-*lux*-FM1 and 701-*fab* plants in all tissues analysed, consistent with the results obtained with protoplasts (section 4.3.2). Transgenic *Arabidopsis* tissue gave strong luciferase enzyme activity relative to the equivalent tissues excised from transgenic tobacco, presumably because the *mas* promoter is more active in *Arabidopsis* (results not shown).

Luciferase levels fluctuated between individual transformants transformed with the same construct due to position effects and/or transgene copy number effects. Position effects are the result of genes encoded by the T-DNA being influenced by the chromatin surrounding the site of insert. Genes on T-DNA inserted into a region of the chromosome which is actively transcribed will be expressed to higher levels than the same genes, fused to the same promoters, incorporated into a region which is not actively transcribed (Peach

and Velten, 1991; Breyne, *et al.*, 1992; Allen, *et al.*, 1993). It was noted that mature flower tissue from pPCV701-*lux*-FM1 transgenic tobacco, particularly those grown in close proximity to plants transformed with pPCV701-*lux*-FP2, demonstrated uncharacteristically high luciferase activity (results not shown). This effect was attributed to pollen from adjacent pPCV701-*lux*-FP2 tobacco plants landing on the stigmas of the less active transformants. Pollen tube growth is associated with high levels of auxin, such that luciferase activity from pPCV701-*lux*-FP2 pollen probably biased the results obtained from pPCV701-*lux*-FM1 plants. Therefore, only tissues from unopened, or very recently opened, self-fertilised tobacco flowers were considered for analysis, and Cryovac bags were used to ensure self-fertilisation for seed collection. The same phenomenon was not observed in transgenic *Arabidopsis* due to the low frequency of cross-fertilisation. As a result of copy number, and position effects, meaningful conclusions from statistical analysis were not obtained due to the small sample size of transgenic plants produced (<10 individual transformants per construct).

Recognising the problems of position effects and transgene copy number associated with independent transformants, seeds for a transgenic SR1 tobacco line, 12-1, were obtained from Dr. Chao Jiang (Jiang, 1994). 12-1 was transformed with vector pPCVG-*lux*-A+B, which consists of a promoterless *luxA* gene adjacent to the *Agrobacterium* T-DNA right border. Therefore, *lux* gene expression in plants transformed with pPCVG-*lux*-A+B is dependent on downstream promoters endogenous to the plant (Koncz, *et al.*, 1989). 12-1 demonstrates high levels of luciferase activity predominantly in petals and stamens, which corresponds to tissues in which the *mas* promoter activity is highest (Langridge, *et al.*, 1989).

Double trangenic tobacco lines were generated by *Agrobacterium* mediated transformation of 12-1 with the 701 series of vectors (pPCVG-*lux*-A+B carries a hygromycin phosphotransferase gene, while the 701 series carries the neomycin phosphotransferase gene, allowing differential antibiotic selection). The T1 generation of 12-1 plants transformed with the 701 series of vectors were grown to maturity. Young flowers, either not fully opened, or open for less than 24 hours, were collected for analysis of luciferase activity via luminometry. Tissue consisting of petal tips, anthers, and stigma

was excised by cutting the flower perpendicular to the axis of radial symmetry, and luciferase activity was measured as light units per mg of protein (L.U./mg). The results were averaged, and are presented in Table 5.1; luciferase activity in similar tissues from 12-1 was previously determined as approximately 475 L.U./mg (Jiang, 1994). Analysis of the results by several tests of similarity, available with the SAS for Windows statistical software package (Student-Newman-Keuls Test, Tukey's Studentised Range Test, and Scheffe's Test), suggest that the differences in luciferase activity obtained among 12-1 plants transformed with different ribozyme vectors are not significant.

Although the levels of luciferase enzyme activity are much higher in 12-1 plants than in SR1 plants transformed with pPCV701-*lux*-FM1, pPCV701-*lux*-FP2, or the 701-*fab* series of vectors, ribonuclease protection assay quantification of transcript levels suggests that luciferase mRNA is not more prevalent. Therefore, that no reduction in luciferase activity was observed is not the result of *lux* mRNA levels exceeding the effectiveness of the ribozymes. The high level of light emission in 12-1 plants is potentially the result of translational control, or could be attributed to the increased activity of the LuxALuxB heterodimer (*i. e.*, the wild-type luciferase enzyme, section 1.7) relative to the fusion protein (Escher, *et al.*, 1989).

5.3.3 In vivo cleavage - whole plant systems

T1 generation tobacco plants transformed with pPCV701-*lux*-FP2, pPCV701-*lux*-FM1, and the 701-*fab* series were self fertilised as described in section 5.2.5. Seeds from at least two of each independent transformants were germinated on MS + 3% sucrose + Km to select for plants homozygous, or heterozygous for the transgene, and grown to 5 cm in size under aseptic conditions. RNA was isolated from approximately 500 mg of immature T2 tissue - mostly meristematic tissue, young stem, and immature leaves. RNase protection assays were performed on these samples to quantify the levels of luciferase mRNA, neomycin phosphotransferase mRNA, and ribozyme, as well as to detect luciferase cleavage products, should cleavage occurred. Tissue was also collected for luciferase analysis via luminometry. With the exception of the pPCV701-*lux*-FP2 plants, luciferase enzyme activity in this tissue was below the level

of detection for both control and ribozyme containing plants, as expected based on luminometry performed on the T1 generation.

The autoradiogram resulting from RNase protection assays performed on transgenic tobacco mRNA is represented in Figure 5.1. Bands appearing on the autoradiogram were identified by comparing the relative mobility of each against a double stranded DNA standard (pBR322 digested with HinfI). Table 5.2a lists the size of the respective bands appearing on the autoradiogram. Table 5.2b lists the size of the protected fragments expected for luciferase mRNA cleavage products. Protected *npt*II, luciferase, and ribo4 probe fragments are labelled (Figure 5.1). Bands corresponding to protected ribo, and ribo1 probe fragments are not visible in the image since the expected bands (52 nt) co-migrate with the non-specific background bands (note that this background is present in total SR1 mRNA and total yeast mRNA control lanes). Ribo, riboC, ribo1, and ribo1C mRNA could potentially be detected and quantified by primer extension, however it is unlikely that the respective quantities, relative to luciferase or *npt*II mRNA, would be different from those seen with ribo4, and ribo4C. Based on band intensity, the steady state levels of ribozyme RNA is estimated to be approximately 6 times that of *lux* mRNA levels in transgenic tobacco.

The intensity of the bands resulting from protected luciferase probe fragments were measured relative to the intensities of the corresponding bands resulting from protected *npt*II probe fragments, in order to compare luciferase mRNA levels between independent transformants. The ratio of luciferase mRNA levels to *npt*II mRNA levels should be less susceptible to fluctuations resulting from copy number and position effects, since the two genes are part of the same T-DNA insert. However, the legitimacy of this assumption is questionable, since it is demonstrated by Peach and Veltens (1991), that expression ratios from promoters within the same T-DNA insert can fluctuate between independent transformants. In the above study, reporter gene activity was determined by quantifying protein levels rather than transcript abundance, and callus tissue was utilised rather than whole plant tissues. Nonetheless, visual analysis of Figure 5.1 does suggest a relationship in the abundance of the two transcripts, as none of the samples tested display deviations of the magnitude reported by Peach and Veltens. Statistical analysis using the

Student-Newman-Keuls Test, Tukey's Studentised Range Test, and Scheffe's Test suggest that there is no significant reduction in the level of full length luciferase mRNA in plants transformed with ribozymes active *in vitro*, and ribozyme controls, or pPCV701-*lux*-FM1 controls.

Analysis of ribozyme activity in *Arabidopsis* was not performed, since transgenic lines with the pPCV701R1-fab, and pPCV701R4-fab vectors were not obtained. However, ribonuclease protection assays performed on transgenic *Arabidopsis* plants which are available demonstrate increased luciferase mRNA levels per μg of total RNA, relative to equivalent tissues excised from transgenic tobacco, presumably because the *mas* promoter is more active in *Arabidopsis* (results not shown). This, in conjunction with increased levels of luciferase enzyme activity in *Arabidopsis* relative to tobacco, as determined by luminometry (section 5.3.2), and because of the small size of the mature plant, the use of *Arabidopsis* would facilitate similar molecular genetic studies, if transformation and regeneration efficiencies were improved.

5.4 Discussion

The results herein indicate that ribozymes are not significantly reducing the levels of the *lux* mRNA target in transgenic plants. Comparisons between individual transformants is severly hampered by position effects, and transgene copy numbers. Transformation of ribozyme genes into plant tissue previously transformed with a luciferase gene construct, and characterised with respect to luciferase activity, helped to overcome these problems, however the levels of ribozyme produced in individual transgenics would still fluctuate. A more effective approach would be to transform the luciferase gene, and ribozyme genes separately, followed by crossing to produce T2 progeny heterozygous for both genes. In this manner, both genes could be analysed with respect to mRNA levels in the respective parents, and compared directly to mRNA levels in the progeny. Seed stock for such an experiment was produced during the course of this project for both tobacco, and *Arabidopsis*.

Wegener *et. al.*, (1994) have recently demonstrated ribozyme-mediated repression of a reporter gene in a similar fashion. A ribozyme construct was trasformed into tobacco plants previously transformed with an *npt*II target gene. A single transformant with reduced *npt*II activity relative to the *npt*II-containing parent plant was selected for further study. This plant was crossed with wild-type tobacco, to allow for the segregation of the ribozyme gene away from the *npt*II gene. Ribozyme RNA levels in one of the resulting progeny plants was characterised, and this plant was crossed with a second trangenic line, expressing the *npt*II gene from the same promoter as the ribozyme (CaMV 35s). Ribozyme steady state levels in the parent containing the ribozyme gene was estimated to be twice that of the *npt*II mRNA levels in the parent plant containing the *npt*II gene. The progeny of this cross displayed an 80% reduction in *npt*II enzyme activity, and a 60% reduction in *npt*II mRNA levels.

It is significant that ribozyme levels were only 2 fold greater than *npt*II mRNA levels in the above study, since ribozyme levels from the *mas* P2 promoter are estimated to be 5 fold more prevalent than *lux* mRNA levels from the *mas* P1 promoter. Comparison of *lux* mRNA levels by RPA analysis suggests that *lux* mRNA is less prevalent in 12-1

plants than in plants expressing *lux* from the *mas* P1 promoter. In spite of the greater ribozyme to target ratios herein, target gene expression is not reduced.

Two interesting issues which are not addressed by Wegener *et al.*, are co-suppression, and the antisense effects of the ribozymes. Co-suppression is a poorly understood phenomenon in which a sense strand transgene can reduce the expression of a homologous endogenous gene (Napoli, *et. al.*, 1990; van der Krol, *et. al.*, 1990). The fact that both the ribozyme gene and the *npt*II gene were driven by the CaMV 35s promoter may have resulted in a co-suppression effect, rather than repression by cleavage. The authors of this report admit that they cannot excluded the possibility that the reduction in target gene activity is mainly due to an antisense effect.

Table 5.1

Comparison of luciferase activity in *N. tabacum* cv. SR1, trangenic line 12-1, which expresses the luciferase gene in a flower specific manner, transformed independently with the 701 series of ribozyme vectors. Values are expressed as light units per mg protein, and were obtained from nearly, or newly opened flower tissue. Average luciferase expression is given, and error is expressed as sample standard error.

Transforming Vector	Plant Number 1	2	3	4	5	6	7	8	9	10	Average	Std. Err
pPCV701R-fab	324	300	471	466							390	46
pPCV701RC-fab	245	184	305	404	545	483	338	389	501		377	40
pPCV701R1-fab	362	362	505	310	309	344	631	441	390	407	411	33
pPCV701R1C-fab	333	671	393	485	510	557	532	474			494	36
pPCV701R4-fab	307	341	291	536	338	345	309	341			351	27
pPCV701R4C-fab	368	136	339	435	281	347	337				321	35

Figure 5.1

Ribonuclease protection assay results from RNA isolated from *N. tabacum* cv. SR1 plants transformed with the 701-*fab* series of vectors. Each lane represents an RPA performed on 20 μg of total tobacco RNA isolated from selfed progeny of an independently transformed parent plant. In the following list, samples are indicated by the transforming vector, followed by a number assigned to the parent plant. All samples were probed with *lux* and *npt*II RNA probes, and a ribozyme specific probe. Samples represented in lanes 6-12 were probed with a ribo specific probe, samples in lanes 13-17 were probed with a ribo1 probe, and samples in lanes 18-23 were probed with a ribo4 probe.

Lanes 1, and 2: pPCV701-*lux*-FP2, transgenics 2, and 4.

Lanes 3, 4, and 5: pPCV701-*lux*-FP1, transgenics 1, 2 and 4,

Lanes 6, 7, 8, and 9: pPCV701R-*fab*, transgenics 1, 2, 3, and 4.

Lanes 10, 11, and 12, pPCV701RC-*fab*, transgenics 1, 1A, and 3.

Lanes 13, 14, and 15: pPCV701R1-*fab*, transgenics 1, 2, and 3.

Lanes 16, and 17: pPCV701R1C-*fab*, transgenics 1, and 2.

Lanes 18, 19, and 20: pPCV701R4-*fab*, transgenics 1, 3, and 4.

Lanes 21, 22, and 23: pPCV701R4C-*fab*, transgenics 1, 2, and

Lane 24, pPCV702-*lux*F (luciferase fusion downstream of the CaMV 35s promoter).

Lane 25, SR1 RNA; Lane 26, pPCV701-*lux*-FP2-2 (10 μg); Lane 27, pPCV701-*lux*-FP2-2 (40 μg); Lane 28, 20 μg yeast RNA.

For clarification, the bands appearing on the gel are represented in the centre: blue represents undigested probe, and from top to bottom are *lux*, *npt*II, ribo4, and ribo1. Red markers correspond to full length protected probe fragments, and from top to bottom are *npt*II, *lux* (from *mas* P1 promoter), *lux* (from *mas* P2, or CaMV 35s promoter), ribo4, and ribo, and ribo1. Size standards are indicated on both sides of the figure.

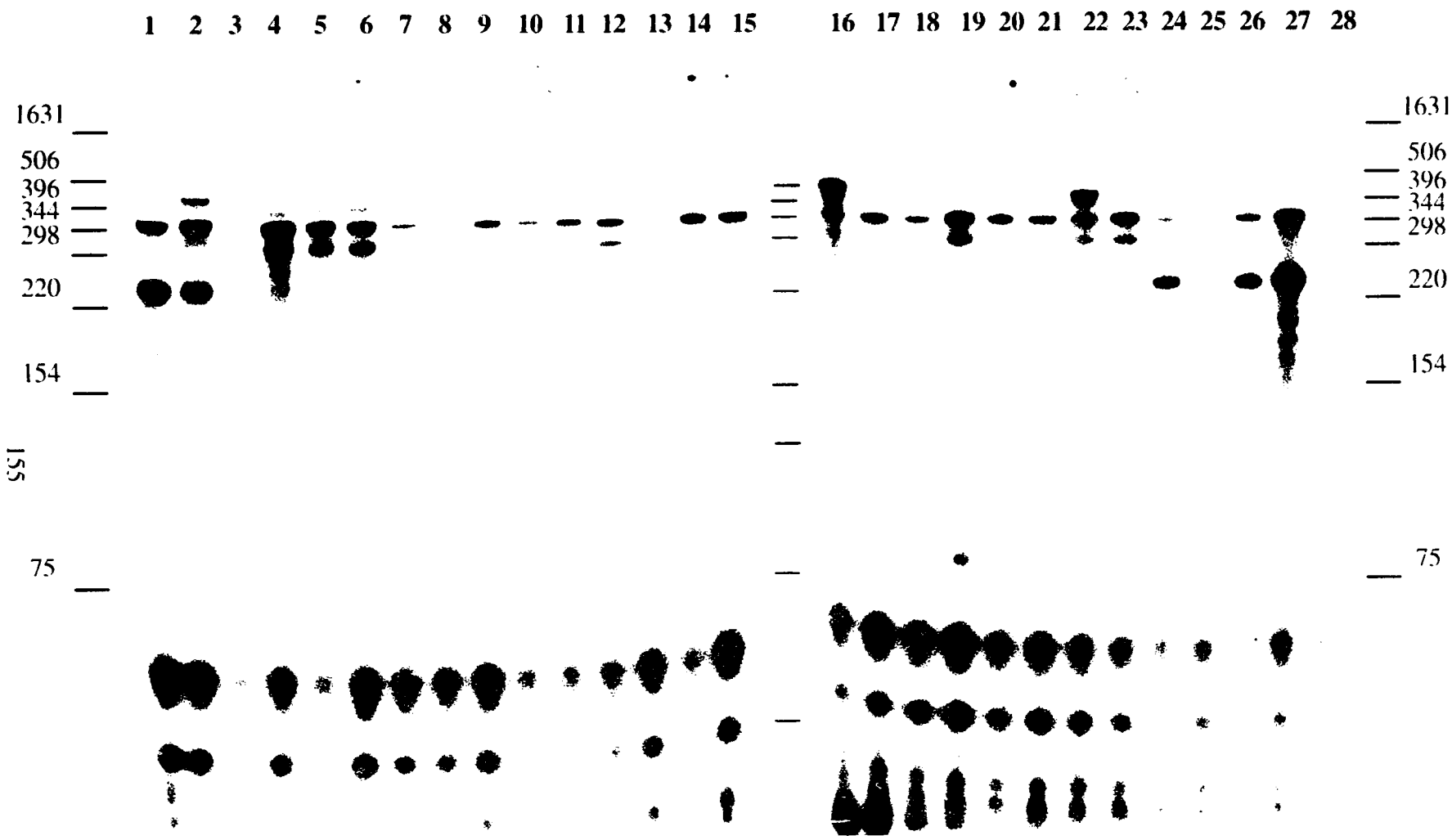
1 2 3 4 5 6 7 8 9 10 11 12 13 14 15 16 17 18 19 20 21 22 23 24 25 26 27 28
1631
506
396
344
298
220
154
75
155

Table 5.2a Size of bands expected for each full length, undigested RPA probe, and the size expected for probe fragments protected by the corresponding complementary mRNA.

Probe	Probe Length	Protected Length
nptII	419	350
P1lux	432	308
Ribo	126	52
Ribo1	126	52
Ribo4	151	77

Table 5.2b Size of bands expected for *lux* probe protected by *lux* mRNA cleavage products generated by each ribozyme.

Ribozyme	5' Protected Fragment	3' Protected Fragment
Ribo	230	78
Ribo1	132	176
Ribo4	126	176

5.5 Bibliography

Allen, G. C., Hall, G. E. Jr., Childs, L. C., Weissinger, A. K., Spiker, S., Thompson, W. F. (1993). Scaffold attatchment regions increase reporter gene expression in stably transformed plant cells. *The Plant Cell*, **5**, 603-613.

Ausubel, F. M., Brent, R., Kingston, R. E., Moore, D. D., Seidman, J. G., Smith, J. A., Struhl, K., (eds.) (1994) *Currect Protocols in Molecular Biology*. John Wiley and Sons, Inc., New York.

Ayre, B. G., Escher, A., Szalay, A. A. (1993). Bioluminescence as a measure of ribozyme activity *in vivo*. In: *Bioluminescence and Chemiluminescence Status Report: Proceedings of the VII International Symposium on Bioluminescence and Chemiluminescence*. Eds., Szalay, A. A., Kricka, L. J., and Stanley, P. John Wiley and Sons, Inc., New York.

Breyne, P., Van Montagu, M., Depicker, A., Gheysen, G. (1992). Characterisation of a plant scaffold attatchment region in a DNA fragment that normalises transgene expression in tobacco. *The Plant Cell*, **4**, 463-471.

Escher, A., O'Kane, D. J., Lee, J., Szalay, A. A. (1989). Bacterial luciferase αβ fusion protein is fully active as a monomer and highly sensitive *in vivo* to elevated temperature. *Proc. Natl. Acad. Sci. USA*. **86**, 6528-6532.

Herrera-Estrella, L., Depicker, A., Van Montagu. M., Schell, J. (1983). Expression of chimaeric genes transferred into plant cells using a Ti-plasmid derived vector. *Nature* **303**, 209-213.

Horsch, R. B., Fry, J. E., Hoffmann, N. L., Eichholtz, D., Rogers, S. G., Fraley, R. T. (1985). A simple and general method for transferring genes into plants. *Science* **227**, 1229-1231.

Jiang, C. (1994). T-DNA tagging *in vivo*: Isolation and characterisation of a putative plant promoter mediating gene espression in tobacco flowers. Ph. D. Thesis, University of Alberta.

Jiang, C., Langridge, W. H. R., Szalay, A. A. (1992). Identification of plant genes *in vivo* by tagging with T-DNA border linked luciferase genes followed by inverse polymerase chain reaction amplification. *Plant Mol. Biol. Rep.* **10**, 345-361.

Koncz, C., Schell, J. (1986). The promoter of TL-DNA gene 5 controls the tissue specific expression of chimaeric genes carried by a novel type of *Agrobacterium* binary vector. *Mol Gen Genet.* **204**, 383-396.

Koncz, C., Martini, N., Mayerhofer, R., Koncz-Kalman, Z., Korber, H., Redei, G., Schell, J. (1989). High-frequency T-DNA-mediated gene tagging in plants. *Proc. Natl. Acad. Sci. USA*. **86**, 8467-8471.

van der Krol, A. R., Mur, L. A., Beld, M., Mol, J. N. M., Stuitje, A. R. (1990). Flavonoid genes in petunia: addition of a limited number of gene copies may lead to a suppression of gene expression. *The Plant Cell* **2**, 291-299.

Langridge, W. H. R., Escher, A., Szalay, A. A. (1991). Measurement of bacterial luciferase as a reporter enzyme *in vivo* in transformed bacteria, yeast, plant cells, and in transgenic plants. *Technique* **3**, 99-108.

Langridge, W. H. R., Fitzgerald, K. J., Koncz, C., Schell, J., Szalay, A. A. (1989). Dual promoter of *Agrobacterium tumefaciens* mannopine synthase genes is regulated by plant growth hormones. *Proc. Natl. Acad. Sci. USA*. **86**, 3219-3223.

Marton, L., Browse, J. (1991). Facile transformation of *Arabidopsis*. *Plant Cell Reports* **10**, 235-239.

Meyerowitz, E. M., Pruitt, R. E. (1985). *Arabidopsis thaliana* and plant molecular genetics. *Science* **229**, 1214-1218.

Napoli, C., Lemieux, C., Jorgensen, R. (1990). Introduction of a chimeric chalcone synthase gene into petunia results in reversible co-suppression of homologous genes *in trans*. *The Plant Cell* **2**, 279-289.

Peach, C., Velten, J. (1991). Transgene expression variability (position effect) of CAT and GUS reporter genes driven by linked divergent T-DNA promoters. *Plant Mol. Biol.* **17**, 49-60.

Perriman, R., Bruening, G., Dennis, E. S., Peacock, W. J. (1995). Effective ribozyme delivery in plant cells. *Proc. Natl. Acad. Sci. USA*. **92**, 6175-6179.

Redei, G. P., Koncz, C., Schell, J. (1988). Transgenic *Arabidopsis*. In: *Chromosome Structure and Function*. Eds. Gustafson, J. P., Appels, R. 175-200.

Simon, R., Priefer, U., Puhler, A. (1983). A broad host range mobilisation system for *in vivo* genetic engineering: Transposon mutagenesis in gram negative bacteria. *Bio/technology* **1**, 784-791.

Steinecke, P., Herget, T., Schreier, P. H. (1992). Expression of a chimeric ribozyme gene results in endonucleotytic cleavage of target mRNA and a concomitant reduction of gene expression *in vivo*. *EMBO J.* **11**, 1525-1530.

Wegener, D., Steinecke, P., Herget, T., Petereit, I., Philipp, C., Schreier, P. H. (1994). Expression of a reporter gene is reduced by a ribozyme in transgenic plants. *Mol. Gen. Genet.* **245**, 465-470.

Zambryski, P. C. (1988). Basic processes underlying *Agrobacterium*-mediated DNA transfer to plant cells. *Annu. Rev. Genet.* **22**,1-30

Zambryski, P. C. (1992). Chronicles from the *Agrobacterium*-plant cell DNA transfer story. *Annu. Rev. Plant Physiol. Plant Mol. Biol.* **43**, 465-490.

6. DISCUSSION

6.1 General Conclusions

The goal of this research was to measure the ability of hammerhead ribozymes to cleave a targeted substrate molecule, to the end of using ribozymes to control gene expression in higher plants. From the literature on ribozyme activity, three general characteristics of ribozyme design, in relation to activity, are established. 1) Minimal ribozymes, acting against minimal targets (i. e., with no single stranded sequences beyond the duplexed guide sequences) have activities approaching the rate of chemical cleavage, k_2, in single turnover reactions. 2) For ribozymes with duplexed guide arms greater than 12 base pairs in length, product dissociation is rate-limiting, and the ribozyme loses the ability to differentiate between closely related targets. 3) Ribozyme and target pairs with single-stranded sequences flanking the duplexed guide arms have substrate association as the rate-limiting step in single turnover reactions, due to the requirement for helix-coil transitions.

These general rules of ribozymes are supported by the findings presented in Chapter 2. All of the ribozymes tested had extensive single stranded sequences flanking the guide arms, and displayed k_{cat} values significantly below the theoretical k_2 value of 1 min^{-1}, due to low substrate association rates, k_1, as evident from the slow appearance of bands corresponding to substrate/ribozyme complexes over time on non-denaturing gels (section 2.3.6, and 2.4.4). Presumably for the same reason, short, single ribozymes (ribo1BS and CTribo1) were more effective than longer, double ribozymes (ribo4BS and CTribo4). Increasing the length of the target sequence from 449 nt, as used for *in vitro* cleavage assays, to 2.3 kb, as would be formed by transcription of the *lux* fusion gene *in vivo*, eliminated observable cleavage activity, possibly due to a further reduction in k_1. In multiple turnover experiments, (Figure 2.7) an initial rate was observed, followed by a slower steady state. The initial rate was observed until the amount of product formed was one half of the amount of ribozyme in the reaction, indicating that the rate-limiting step of the initial phase was substrate association, followed by product dissociation in the

rate-limiting step of the second phase, and that appproximately 50% of the ribozyme, or ribozyme/substrate complex was trapped in an inactive conformation. Attempts to overcome, or reduce, these rate-limiting steps with the addition of protein factors which may facilitate RNA-RNA interactions, and to simulate the conditions that ribozymes and targets may be exposed to *in vivo*, were performed by the addition of nuclear extracts to the *in vitro* reactions. However, contrary to published reports, hnRNPs in the nuclear extracts failed to enhance ribozyme activity to discernible levels (section 2.4.5).

In vivo, ribozyme activity against the chosen target was not observed in *E. coli*, even though ribozyme transcripts were estimated to be present in a greater than 20 fold excess, which was sufficient for significant target cleavage *in vitro*. It was considered that the coupled transcription-translation system of prokaryotes may prevent active ribozyme-substrate interactions, but the addition of streptomycin to inhibit ribosome initiation did not alter the results obtained (section 3.4). Likewise, ribozyme activity against a target mRNA was not observed in transfected and transformed plant tissues under conditions similar to those in which ribozyme activity is reported *in vivo* (section 4.4, and 5.4).

Isolated RNA, exposed to conditions known to result in cleavage *in vitro*, also resulted in the failure to detect cleavage products (section 3.3.6). In conjunction with *in vitro* cleavage assays utilising *in vitro* transcribed ribozymes and full length target (section 2.3.6), it is concluded that the full length target is a poor substrate, even though the ribozymes produced *in vivo* are active (section 3.3.3).

Despite the results herein, ribozymes do have potential to control gene expression in plants (Wegener *et al.*, 1994; Perriman, *et al.*, 1993) and other organisms (Cantor, *et al.*, 1993; Sullenger and Cech, 1993; Zhou, *et al.*, 1994). However, as evident from the sparse literature on this topic relative to the number of laboratories working with ribozymes (the most recent ribozyme meeting at Breckenridge Colorado, had 180 participants, and at least 30 laboratories are studying hammerhead ribozymes in plants; J. Rossi, personal communication), it is evident that ribozymes have not lived up to their theoretical potential.

6.2 Effective Ribozyme Expression in Plant Cells

What follows is a series of steps which should be employed for effective target site selection, and ribozyme design, with emphasis on hammerhead ribozymes applications in plants. Although these recommended steps may seem laborious, the results herein, and those in published reports (Saxena and Ackerman, 1990; Mazzolini, *et al.*, 1992) emphasise the need for preliminary testing to achieve the desired results. It should be noted that techniques for effective target site selection and ribozyme design are generally applicable to all organisms, and can be applied to any of the known catalytic RNA motifs. Larson *et al.*, (1993) have published a similar outline, with emphasis on ribozymes as anti-HIV agents.

Target site selection is perhaps the most significant, and the most easily controlled factor leading to productive ribozyme/substrate interactions, since selection of an inappropriate target may result in poor, or even deleterious, cleavage activity. The initial choice of transcript to target for cleavage is important, but not always flexible. Clearly, whether targeting an endogenous mRNA, or a viral transcript, the selection made must most efficiently lead to the desired results. However, targets with the following characteristics will be more susceptible to specific ribozyme-mediated degradation than others. First, transcripts for regulatory genes may be better targets than those of structural genes, since incomplete elimination of the transcript can reduce protein levels sufficiently to eliminate the gene product's effect. Structural genes however, are frequently produced in excess, and a decrease in transcript may have no discernible result. Second, the half-life of the prospective target should be considered, since ribozymes will presumably be ineffective against very short lived transcripts. For example, ribozyme ribo1BS, used herein, has a k_{cat} of approximately 0.02 to 0.03 min^{-1}, and would, under saturating conditions, be most effective against transcripts with a half-life exceeding 50 minutes. Third, sequences which are not likely to mutate to a resistant state should be selected, such as those conserved among related species, regulatory sequences, or sequences with non-degenerate codons. Fourth, steps should be taken to reduce the number of possible homologous sequences which could be inadvertently targeted, such as

conserved domains in a family of genes. Fifth, although detailed analysis of ribozyme effectiveness should be carried out at the RNA level, choosing a target with an easily assayable phenotype could be a consideration, in order to quantify ribozyme efficiency.

After choosing an appropriate target transcript, one or more target sites must be selected. In naturally occurring hammerhead reactions, the sequence GUC most frequently occurs 5' to the cleavage site. Although other sequences can be utilised, the GUC sequence is the most efficient, and if possible, should be maintained. GUC sequences can be rapidly identified in a known gene by computer analysis. Following identification of potential sites, RNA folding algorithms may be employed to predict the secondary structure surrounding, or involving each of the proposed sites. As well, the probability of active ribozyme/substrate complex formation can be predicted using the technique of Denman (1993). Computer analysis has limitations, however, and target sites predicted to contain extensive stable structures, or inactive ribozyme/substrate complexes, should be eliminated with discretion. Lessons learned from well-studied, naturally occurring antisense RNA interactions, such as those involved in Tn10 transposon regulation and the regulation of *Col*E1 DNA replication, indicate that stem-loop structures can facilitate RNA-RNA interactions (Eguchi, *et al.*, 1991). The presence, or absence of competing secondary structure in the target can be determined experimentally by two simple methods: 1) limited RNase digestion of the target transcript *in vitro* with RNase H and RNase A/RNase T1, to obtain a foot print of double stranded regions and single stranded regions, respectively, and 2) hybridisation of labelled oligonucleotides corresponding to the ribozyme guide sequences to the target, followed by native gel electrophoresis. Oligonucleotides which can access and hybridise to their respective targets will be retarded in the gel.

Likewise, it is important to consider ribozyme design, which the researcher has more control over, but it is emphasised that the ribozymes will be ineffective if a poor target is chosen. The basic ribozyme should follow the Haseloff and Gerlach design, with a catalytic domain sequence of those found in nature, such as the satellite RNA of the tobacco ringspot virus. Sequences in stem loop-structure II can be modified, if necessary, to avoid potentially inactive secondary structures. Indeed, it is reported that reducing the

length of stem loop structure II has a minimal effect on cleavage activity, providing at least two base pairs are maintained (Tuschl and Eckstein, 1993). An antisense control ribozyme, containing a debilitating point mutation in the conserved domain should be incorporated into the experimental design. The absense of competing secondary structure within the ribozyme expression cassette should be analysed as described above for the target molecule. The optimal length of the guide arm sequences is determined to be 13 (total) for one system *in vivo* (Bertrand, *et al.*, 1994), although this variable has not been extensively tested, and should be determined empirically. Longer sequences would be advantageous, to take advantage of the intrinsic antisense effects of ribozymes (Homann, *et al.*, 1993), but specificity may be lost, emphasising the the requirement to choose a target sequence with a minimal number of possible homologs.

A suitable expression cassette must also be considered, as the researcher will want to strive for maximal ribozyme expression, and half-life, to saturate the system as much as possible, and ensure that the half-life of the ribozyme is greater than the catalytic turnover rate. However, with increasing concentrations of catalyst, the probability of non-specific cleavage also increases, as active complexes between excess ribozyme and non-target sequences are more likely to occur. (The specificity of a ribozyme for two potential targets is determined from the respective k_{cat}/K_M values.) The cassette utilised for efficient ribozyme gene expression is usually a RNA polymerase II cassette, containing a suitable promoter and poly-adenylation signal flanking the ribozyme, or a RNA polymerase III cassette. In a pol II expression system, the m7G cap structure, and the poly A tail contribute to RNA stability, and transport to the cytoplasm, but, these flanking sequences will also presumably reduce activity by lowering the association rate. Alternating *trans*-acting, and self-cleaving ribozymes can be utilised to minimise the length of single stranded RNA flanking the ribozyme guide arms (*i. e.*, the self-cleaving ribozymes dissect extraneous sequences from the *trans*-acting ribozymes), with improved activity *in vitro* (Ventura, *et al.*, 1993; Ohkawa, *et al.*, 1993); although, the loss of the m7G cap structure, and the poly A tail would drastically reduce the half-life of these ribozymes *in vivo*. The 40S ribosomal subunit binding at the m7G cap structure, and scanning along the transcript will disrupt secondary structure less stable than -50 kcal/M, such that ribozymes in

association with target transcripts will be dissociated by the ribosome (Hershey, 1991). Translation can also prevent productive associations in prokaryotes (Inokuchi, *et al.*, 1994). Further, the addition of an intron to the ribozyme and target to ensure routing of the transcripts through the normal splicing machinery in the nucleus may be advantageous, as such routing may provide an enhanced localisation effect - or may just as likely isolate the two transcripts from each other (discussed below; Rosbash and Singer, 1993).

Utilisation of an RNA polymerase III expression system has several advantages over the RNA polymerase II system: gene expression occurs in all tissues, and at an order of magnitude higher (Cotten and Birnstiel, 1989; Bertrand, *et al.*, 1994; Perriman, *et al.*, 1995). Pol III transcripts, such as tRNA, frequently contain extensive secondary structures, which contribute to long transcript half-life, and may limit the formation of inactive secondary structure between the ribozyme, and flanking sequences. It is the opinion of the author, that an RNA polymerase III transcript is best suited for the expression of ribozymes in higher eucaryotes.

Notwithstanding, the RNA polymerase II mannopine synthase P1/P2 promoter system of vector pPCV701, utilised in this study, is advantageous for initial tests of ribozyme activity against a target, for several reasons. Firstly, it is relatively well characterised (Velten, *et al.*, 1984). Secondly, it is inducible by auxin, and wounding (Langridge, *et al.*, 1989). Thirdly, the close proximity of the transcriptional start sites (<400 nucleotides; Velten *et al.*, 1984) may impart an advantageous co-localisation of the ribozyme and target at the site of transcription (Sullenger and Cech, 1993), although this issue was not addressed in detail in this dissertation. Fourthly, since the P2 promoter is approximately 5-10 times more active than the P1 promoter, placing the ribozyme downstream of P2, and the target downstream of P1, will result in a known ratio of ribozyme excess. Alternatively, switching the locations of the genes will result in target excess to test for ribozyme turnover *in vivo*. Finally, this vector system allows delivery of the target and the ribozyme genes on a single vector, ensuring a 1:1 co-transfection ratio.

However, the *mas* promoter has disadvantages, as well. As was discussed in section 4.3.2, the target used for comparing different ribozymes is essentially derived from different pools, resulting in potential ambiguities. As well, expression in plant tissues is

highly tissue, and developmentally dependent: in the case of this research, very sensitive RNA detection methods (ribonuclease protection assays), with high specific activity probes, and lengthy exposure times, had to be used in order to get appreciable signal. Transcription from the *mas* promoter, as with transcription from any RNA polymerase II expression cassette, results in the incorporation of untranslated promoter sequences, and a polyA tail, which presumably reduces activity. These sequences could be minimised by reducing the distance between the cloning site, and the transcriptional start site and the poly A signal.

Once a target sequence(s) lacking potential secondary structure is (are) identified, and a suitable ribozyme expression cassette is chosen, ribozyme activity can be analysed *in vitro* with either chemically synthesised ribozymes, or with ribozymes transcribed from a DNA template. Several rapid techniques are available for *in vitro* transcription from PCR products, or hemi-duplexes, eliminating the need for subcloning, and vector linearisation (Mullis and Faloona, 1987; Milligan, *et al.*, 1987). Depending on the number, and nature of target sites available, a single RNA, or DNA oligonucleotide may be synthesised with degenerate bases throughout the flanking arms, such that a single synthesis would produce a pool of potential ribozymes which can be analysed *en masse*. The efficiency of each ribozyme is determined by gel electrophoresis, and autoradiography of the cleavage products, in a manner analogous to DNase, or RNase foot printing (Larson, *et al.*, 1993). An alternative to equation 2.2 (section 2.3.5),

$$d[P_r]/dt = k_{cat}/K_M[R_r][S], \qquad (6.1)$$

where $d[P_r]$ is the change in product formation resulting from an individual ribozyme in the mixture $[R_r]$, relative to time (t), with substrate concentration, [S], allows the specificity of each ribozyme for the target to be analysed in a single reaction, providing each cleavage product can be attributed to a single ribozyme, and one of the reagents (usually S) is in large excess over the other (Fersht, 1977).

The *in vivo* effect of the ribozyme(s) should be assessed in a suitable model system, once effective target site/ribozyme combinations are identified, prior to final delivery to the organism of interest. In the case of plants, transient transfection into protoplasts derived from a suspension culture is the system of choice for *in vivo* testing.

Testing in protoplasts is highly recommended, since the generation of transformed plants is a lengthy (minimum two weeks for callus, and six weeks for juvenile plants), and laborious process, and incorporates several sources of ambiguity, such as position, and copy number effects (Peach and Velten, 1991). In instances where the gene of interest is not naturally expressed in a suspension culture line, protoplasts may be obtained from tissue in which the gene is expressed, or the gene of interest may be expressed from an heterologous promoter. In the hands of the author, the A2 alfalfa suspension culture line was drastically more amenable to transfection by both Ca-PEG precipitation, and electroporation, than either BY-2 tobacco and BMS maize lines - both of which are frequently used in other laboratories.

Upon identifying a ribozyme substrate pair which results in significant target transcript elimination *in vivo*, as determined by transient expression assays, ribozyme-mediated regulation of transcript levels can be tested in transgenic plants. *Agrobacterium tumefaciens* infection with a suitable binary vector system is most frequently utilised for production of transgenic plants, however other techniques are available. The genes to be transferred to the plant chromatin, regardless of the expression cassette utilised, are sub-cloned between the left and right T-DNA borders, and transferred to plant cells in manner analogous to a combination of bacterial conjugation, and viral infection (Zambryski, 1992). If a reporter gene is targeted for basic ribozyme analysis, as in this study, it is recommended that the target and ribozyme be transformed independently, followed by characterisation of each gene separately (Wegener, *et al.*, 1994). Homozygous parent plants are then crossed to produce heterozygous progeny expressing both genes at predetermined levels. If an endogenous transcript, or a viral transcript is targeted, then ribozymes are transferred directly, with the generation of several independent transformants, and ribozyme activity is measured against appropriate controls.

6.3 Improvement of Ribozyme Activity *In Vivo*

To date, ribozymes have not lived up to their theoretical potential, and the advantage of catalytic RNA over standard antisense RNA technologies has been called into question (Bertrand, *et al.*, 1994). However, evidence is available that incorporation of a catalytic domain into an antisense construct can enhance the repressive properties of the molecule (Homann, *et al.*, 1993). To date, there are no published reports of ribozymes acting in a truly catalytic fashion, with multiple turnovers, *in vivo*.

Continued research into ribozyme-mediated gene regulation will indubitably lead to improved activity, as our understanding of RNA-RNA, and RNA-protein interactions within the cell improves. Improved cleavage activity, particularly by enhancing substrate association and product dissociation, may be obtained through improved ribozyme and vector design, and target site selection. Increases in our knowledge of the role of secondary structures in RNA-RNA interactions will also be a benefit (Eguchi, *et al.*, 1991). Discoveries in the roles that proteins play, particularly the heterogeneous ribonucleoproteins, in RNA interactions and processing will be essential (Munroe and Dong, 1992; Portman and Dreyfuss, 1994), to answer whether heterologous proteins, or polypeptides, may enhance ribozyme activity (section 2.1.6; Muller, *et al.*, 1994). Specific protein-RNA interactions which could enhance hammerhead ribozyme activity may be found, analogous to the enhancement of group I intron splicing by CYT-18 (Mohr, *et al.*, 1992). The chemical cleavage rate, k_2, could potentially be enhanced by the powerful, yet still emerging techniques of "*in vitro* evolution" (Beaudry and Joyce, 1992; Szostak, 1992).

Enhancements will also be obtained by increasing the effective concentration of the ribozyme in the vicinity of the target. Increasing the effective concentration throughout the cell would be accomplished by increasing both transcription, and the half-life of the ribozyme, by utilising an RNA polymerase III expression cassette. Alternatively, the local concentration of the ribozyme can be increased by compartmentalisation. Sullenger and Cech (1993) demonstrated efficient elimination of a targeted viral transcript by packaging a ribozyme into the viral particle. Evidence presented for the migration of transcripts

through defined "tracks" during maturation and export of the RNA to the cytoplasm suggest that the insertion of specific sequences could result in compartmentalisation, or at least localisation of a ribozyme with its respective target during processing (Xing, *et al.*, 1993; Robash and Singer, 1993). As well, 3' untranslated sequences are shown to traffic RNA transcripts to specific regions of the cell (Kislauskis, *et al.*, 1993), such that incorporating the 3' untranslated region of the target gene into the ribozyme expression cassette could target the ribozyme to the substrate (N. Lee, personal communication). Direct analysis of the effects of co-localisation at the site of transcription, as hypothesised for the *mas* P1/P2 promoter, would be very interesting, indeed.

Considering the above list of potential means for increasing ribozyme activity *in vivo* which are already suggested in the literature, it is evident that continued ribozyme research will not only enhance the potential of using ribozymes to control gene expression, but will also advance our knowledge of the inner workings of the eucaryotic cell. Therefore, despite the inability to demonstrate ribozyme-mediated transcript elimination *in vivo* herein, and the limited success of ribozymes in the literature in general, it is the opinion of the author that ribozymes are generating, and will continue to generate, extensive critical thought and experimentation in the roles of RNA in the regulation of gene expression.

6.4 Bibliography

Beaudry, A. A., Joyce, G. F. (1992). Directed evolution of an RNA enzyme. *Science* **257**, 635-641.

Bertrand, E., Pictet, R., Grange, T. (1994). Can hammerhead ribozymes be efficient tools to inactivate gene function? *Nucleic Acids. Res.* **22**, 293-300.

Cantor, G. H., McElwain, T. F., Birkebak, T. A., and Palmer, G. H. (1993). Ribozyme cleaves *rex/tax* mRNA and inhibits bovine leukaemia virus expression. *Proc. NAtl. Acad. Sci. USA* **90**, 10932-10936.

Cotten, M., Birnstiel, M. L. (1989). Ribozyme-mediated destruction of RNA *in vivo*. *EMBO J.* **8**, 3861-3866.

Denman, R. B. (1993). Using RNAFOLD to predict the activity of small catalytic RNAs. *BioTechniques*, **15**, 1090-1094.

Eguchi, Y., Itoh, T., Tomizawa, J. (1991). Antisense RNA. *Annu. Rev. Biochem.* **60**, 631-652.

Fersht, A. (1977). In: *Enzyme Structure and Mechanism*. W. H. Freeman and Company, San Fransisco CA.

Hershey, J. W. B. (1991). Translational control in mammalian cells. *Annu. Rev. Biochem.* **60**, 717-755.

Homann, M., Tzortzakaki, S., Rittner, K., Sczakiel, G., Tabler, M. (1993). Incorporation of the catalytic domain of a hammerhead ribozyme into antisense RNA enhances its inhibitory effect on the replication of human immunodeficiency virus type 1. *Nucleic Acids Res.* **21**, 2809-2814.

Inokuchi, Y., Yuyama, N., Hirashima, A., Nishikawa, S., Ohkawa, J., Taira, K. (1994). A hammerhead ribozyme inhibits the proliferation of an RNA Coliphage SP in *Escherichia coli*. *J. Biol. Chem.* **269**, 11361-11366.

Kislauskis, E. H., Li, Z., Singer, R. H., Taneja, K. L. Isoform-specific 3'-untranslated sequences sort α-cardiac and β-cytoplasmic actin messenger RNAs to different cytoplasmic compartments. *J. Cell Biol.* **123**, 165-172.

Langridge, W. H. R., Fitzgerald, K. J., Koncz, C., Schell, J., Szalay, A. A. (1989). Dual promoter of *Agrobacterium tumefaciens* mannopine synthase genes is regulated by plant growth hormones. *Proc. Natl. Acad. Sci. USA*. **86**, 3219-3223.

Larson, G. P., Bertrand, E., Rossi, J. J. (1993). Designing and testing of ribozymes as therapeutic agents. *Methods: A Companion to Methods in Enzymology* **5**, 19-27.

Mazzolini, L., Axelos, M., Lescure, N., Yot, P. (1992). Assaying synthetic ribozymes in plants: high-level expression of a functional hammerhead structure fails to inhibit target gene activity in transiently transformed protoplasts. *Plant Mol. Biol.* **20**, 715-731.

Milligan , J. F., Groebe, D. R., Witherell, G. W., Uhlenbeck, O. C. (1987). Oligoribonucleotide synthesis using T7 RNA polymerase and synthetic DNA template. *Nucleic Acids. Res.* **15**, 8783-8798.

Mohr, G., Zhang, A., Gianelos, J. A., Belfort, M., Lambowitz, A. M. (1992). The *Neurospora* CYT-18 protein supresses defects in the phage T4 td intron by stabilising the catalytically active structure of the intron core. *Cell* **69**, 483-494.

Muller, G., Strack, B., Dannull, J., Sproat, B. S., Surovoy, A., Jung, G., Moelling, K. (1994) Amino acid requirements of the nucleocapsid protein of HIV-1 for increasing catalytic activity of a *Ki-ras* ribozyme *in vitro*. *J. Mol. Biol.* **242**, 422-429.

Mullis, K. B., Faloona, F. (1987). Specific synthesis of DNA *in vitro* via a polymerase catalyzed chain reaction. *Methods Enzymol.* **155**, 335-350.

Munroe, S. H., Dong, X. (1992). Heterogeneous nuclear ribonucleoprotein A1 catalyzes RNA-RNA annealing. *Proc. Natl. Acad. Sci. USA.* **89**, 895-899.

Ohkawa, J., Yuyama, N., Takebe, Y., Nishikawa, S., Taira, K. (1993). Importance of independence in ribozyme reactions: kinetic behavior of trimmed and of simply connected multiple ribozymes with potential activity against human immunodeficiency virus. *Proc. Natl. Acad. Sci. USA.* **90**, 11302-11306.

Peach, C., Velten, J. (1991). Transgene expression variability (position effects) of CAT and GUS reporter genes driven by linked divergent T-DNA promoters. *Plant Mol. Biol.* **17**, 46-60.

Perriman, R., Bruening, G., Dennis, E. S., Peacock, W. J. (1995). Effective ribozyme delivery in plant cells. *Proc. Natl. Acad. Sci. USA.* **92**, 6175-6179.

Portman, D. S., Dreyfuss, G. (1994). RNA annealing activities in HeLa nuclei. *EMBO J.* **13**, 213-221.

Rosbash, M., Singer, R. H. (1993). RNA travel: tracks from DNA to cytoplasm. *Cell* **75**, 399-401.

Saxena, S. K., Ackerman, E. J. (1990). Ribozymes correctly cleave a model substrate and endogenous RNA *in vivo*. *J. Biol. Chem.* **265**, 17106-17109.

Sullenger, B. A., Cech, T. R. (1993). Tethering ribozymes to a retroviral packaging signal for destruction of viral RNA. *Science* **262**, 1566-1569.

Szostak, J. W. (1992). *In vitro* genetics. *Trends Biochem. Sci.* **17**, 89-93.

Tuschl, T., Eckstein, F. (1993). Hammerhead ribozymes: importance of stem-loop II for activity. *Proc. Natl. Acad. Sci. USA*. **90**, 6991-6994.

Velten, J., Velten, L., Schell, J. (1984). Isolation of a dual plant promoter fragment from the Ti plasmid of *Agrobacterium tumefaciens*. *EMBO J.* **3**, 2723-2730.

Ventura, M., Wang, P., Ragot, T., Perricaudet, M., Saragosti, S. (1993). Activation of HIV-specific ribozyme activity by self-cleavage. *Nucleic Acids Res.* **21**, 3249-3255.

Wegener, D., Steinecke, P., Herget, T., Petereit, I., Philipp, C., Schreier, P. H. (1994). Expression of a reporter gene is reduced by a ribozyme in transgenic plants. *Mol. Gen. Genet.* **245**, 465-470.

Xing, Y., Johnson, C. V., Dobner, R. P., Lawrence, J. B. (1993). Higher level organisation of individual gene transcription and RNA splicing. *Science* **259**, 1326-1330.

Zambryski, P. C. (1992). Chronicles from the *Agrobacterium*-plant cell DNA transfer story. *Annu. Rev. Plant Physiol. Plant Mol. Biol.* **43**, 465-490.

Zhou, C., Bahner, I. C., Larson, G. P., Zaia, J. A., Rossi, J. J., Kohn, D. B. (1994). Inhibition of HIV-1 in human T-lymphocytes by retrovirally transduced anti-*tat* and *rev* hammerhead ribozymes. *Gene* **149**, 33-39.